3 Stability and Dispersion Characterization of Nanofluid

3.1 Introduction

Hopefully, the application of nanofluid will save energy as well as reduce emissions, global warming potential, and the greenhouse-gas effect. The performance of nanofluids depends on their stability, which is related to the proper dispersion of nanoparticles. Fig. 3-1 shows an example of stable and unstable nanofluids.

Therefore, the following scientific questions need to be considered:

1. How are nanoparticles aggregated and sediment?
2. What are the factors that could determine whether a nanofluid is stable or not?
3. How to control a nanofluid in the dispersed state, and stable?

The above questions are the main concerns of many industries, including chemical manufacturing, food, energy, and many others. The preparation of stable colloids is necessary for the industrial applications of paints, inks, pharmaceutical and cosmetic products, biological activities, drilling muds, agricultural chemicals, and firefighting foams (Mahbubul, Saidur, Hepbasli, & Amalina, 2016).

Aggregated particles rapidly sediment due to the gravitational effect. The knowledge to destruct the unwanted colloid is required for water purification, fining of wines and beer, sewage disposal, breaking of oil emulsions and foams, dewatering of sludge, dispersal of aerosol and fog, disposal of radioactive waste, etc. (Everett, 1988). The microstructure analyses are necessary to study the colloidal dispersion characteristics such as particle size, shape, aggregation, and polydispersity. The stability of nanofluids is an important phenomenon that needs to be characterized. Zeta potential study gives the idea of the stability of a suspension.

Duangthongsuk and Wongwises (2009) suggest that there are three effective methods available to achieve stability of suspension, which are: (1) control of the pH value of suspensions; (2) addition of surface activators or surfactants; and (3) use of ultrasonic vibration. All these techniques aim to change the surface properties of suspended nanoparticles to avoid the formation of the cluster of particles in order to achieve a stable suspension (Duangthongsuk & Wongwises, 2009). It should be noted that whether or not pH control and/or surfactant are used to enhance stability, ultrasonication (or this kind of treatment) must be done to prepare a stable and well-dispersed nanofluid (specifically, in the two-step method). Therefore, ultrasonication is the main factor in the preparation and stability of nanofluids. For this reason, this chapter will emphasize more on the effect of ultrasonication on colloidal dispersion properties of nanofluids. Moreover, the effects of surfactant and pH

Preparation, Characterization, Properties, and Application of Nanofluid. DOI: https://doi.org/10.1016/B978-0-12-813245-6.00003-4

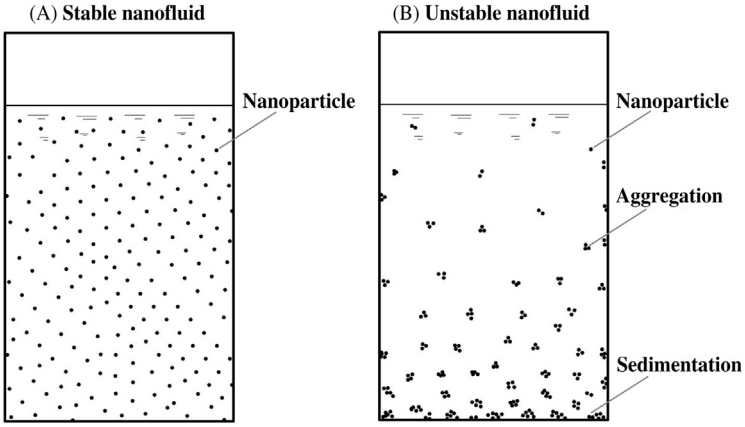

FIGURE 3-1 Example of stable and unstable colloidal suspension: (A) well dispersed and stable nanofluid, and (B) aggregated, sedimented, and unstable nanofluid.

control are also included at the end of this chapter. Some contents of this chapter are collected from the studies of Ghadimi, Saidur, and Metselaar (2011), Mahbubul et al. (2014), Mahbubul, Elcioglu, Saidur, and Amalina (2017), and Mahbubul, Saidur, Amalina, Elcioglu, and Okutucu-Ozyurt (2015a).

3.2 Ultrasonication

Due to the surface energy of nanoparticles, they do not want to disperse in fluids, rather they want to aggregate. The ultrasonication process can break the agglomeration and disperse nanoparticles in suspensions. However, for proper dispersion of nanoparticles, it is necessary to know the required amount of sonication time that can overcome the surface energy of particles. The available literature about the effect of ultrasonication on stability and dispersion properties of different nanofluids is given in brief in Table 3-1.

When the literature is overviewed in Table 3-1, it can be seen that the general idea of the need for longer ultrasonication of nanofluids for better nanoparticle dispersion may not be valid, since many recent research report that there may be an optimum duration for better dispersion stability, which may not necessarily be the longest ultrasonication duration tested. Therefore, the stability of nanofluids and required ultrasonication duration should be carefully investigated in order to get better performances from these fluids in applications. [This paragraph is adapted from Mahbubul et al. (2017), copyright (2017), with permission from Elsevier.]

More details of the research on this topic are discussed here. Based on the dispersion criteria (microstructures, cluster size, zeta potential, and others), some researchers point out that the highest ultrasonication duration is better. Yang et al. (2006) studied the effect of ultrasonication on agglomeration size for nanotube-in-oil dispersions. They characterized by TEM and found that cluster size decreased with increasing sonication time/energy.

Table 3-1 Summary of the Available Literature on the Effect of Ultrasonication

Investigators	Nanofluid	Sonication Period	Investigation	Findings
Kwak and Kim (2005)	CuO–EG	0–30 h	Cluster size, zeta potential	9 h period is best
Yang, Grulke, Zhang, and Wu (2006)	CNT–oil	5–30 min	TEM, thermal conductivity, viscosity	Highest period is best
Chen, Ding, and Tan (2007)	TiO_2–EG	0–40 h	Cluster size	20 h period is optimum
Yu, Grossiord, Koning, and Loos (2007)	MWCNT–DW	0–120 min	UV-vis, TEM	Highest period is best
Lee et al. (2008)	Al_2O_3–water	0–30 h	TEM, zeta potential	~ 5 h period is best
Amrollahi, Hamidi, and Rashidi (2008)	CNT–EG	15–1200 min	TEM, thermal conductivity	Highest period is best
Chung et al. (2009)	ZnO–water	0–60 min	Cluster size	Highest period is best
Garg et al. (2009)	MWCNT–DIW	20–80 min	TEM, thermal conductivity, viscosity, HTC	No optimum result
Zhu, Li, Wu, Zhang, and Yin (2010)	$CaCO_3$–DW	1–45 min	Cluster size	20–30 min period is better
Nguyen, Rouxel, Hadji, Vincent, and Fort (2011)	Al_2O_3–water	0–600 s	Cluster size	Highest period is best
Rashmi et al. (2011)	MWCNT–DW	1–24 h	UV-vis	4 h is optimum period
Kole and Dey (2012)	ZnO–EG	4–100 h	DLS, TEM, thermal conductivity	60 h is optimum period
Yu et al. (2012)	SWCNT–DIW	10–120 min	UV-vis, AFM	Highest period is best
Ruan and Jacobi (2012)	MWCNT–EG	5–1355 min	TEM, thermal conductivity, viscosity	Highest period is best
Ghadimi and Metselaar (2013)	TiO_2–DW	0–15 min	UV-vis, TEM	Highest period is best
Sadeghi, Etemad, Keshavarzi, and Haghshenasfard (2015)	Al_2O_3–water	0–180 min	PSD, zeta potential, UV-vis, thermal conductivity	Highest period is best
Mahbubul et al. (2014)	Al_2O_3–water	0–180 min	TEM, PSD, zeta potential, photo capturing, viscosity	Highest period is best
Mahbubul et al. (2015a)	Al_2O_3–water	0–5 h	TEM, PSD, zeta potential	The optimum duration was found to be ~3 and ~5 h, respectively, for 50% and 25% amplitudes
Mahbubul et al. (2015b)	Al_2O_3–water	0–5 h	TEM, PSD, zeta potential, thermal conductivity, viscosity, density	Highest period is best
Mahbubul et al. (2017)	TiO_2–water	0–180 min	TEM, PSD, zeta potential, pH	150 min is the optimum period

PSD, DLS, HTC, UV-vis, and TEM refer to particle size distribution, dynamic light scattering, heat transfer coefficient, ultraviolet visible spectroscopy, and transmission electron microscopy, respectively.

Amrollahi et al. (2008) applied ultrasonication for 20 h to homogenize CNT in EG. They analyzed the microstructure by TEM and settling time by the naked eye. The precipitation measured by the human eye is not a precise method, even though the author claimed that the precision was ± 10 min. The author reported that at lower ultrasonication, nanofluids with higher particle concentrations were rapidly sedimented because of strong closely packed clusters that existed in the suspension, which were not broken by the limited sonication period. However, with the increase of ultrasonication duration, these clusters became loose and further prolonged ultrasonication; they become very small clusters and then become individual particles, therefore, the sedimentation rate decreases. The authors also observed the above-stated phenomena with TEM microstructure even though they analyzed TEM only after three durations as 15 min, 5 h, and 20 h of ultrasonication and for only 2.5 vol.% concentration of particles.

Ruan and Jacobi (2012) applied 5, 40, 140, 520, and 1355 min of ultrasonication duration to homogenize multiwalled carbon nanotubes (MWCNTs) in EG. The nanofluids were prepared using both continuous and pulse modes of ultrasonication. Microstructure, agglomerate size, and nanotube length and aspect ratio were determined by TEM to study the effect of ultrasonication. They observed that the average cluster size, nanotube length, and aspect ratio of nanotubes decreased with increasing sonication time or energy. [This paragraph is adapted from Mahbubul et al. (2015a), copyright (2015), with permission from Elsevier.]

Also, Yu et al. (2012) conducted a set of experiments to find out the effect of the ultrasonication parameters with a sonicator having maximum power of 120 W and frequency of 20 kHz. They conducted the research for single-walled carbon nanotubes (SWCNTs) with deionized water (DIW) and ultrasonicated for 10−120 min with 10 min intervals. They set five different powers (20, 40, 60, 80, 100, and 120 W) of the homogenizer and characterized with a UV-visible spectrophotometer and atomic force microscopy (AFM). They found that nanotube length was decreased with an increase of sonication duration. They recommended that sonication power is a more influential parameter compared to sonication time and larger sonicator tip diameter performed better. However, they collected 1.5 mL (3 vol.% of initial solution) of sample after every 10 min of ultrasonication that had two types of effect. One is the sonication process is interrupted and the other, which is more important, is that the specific power per volume/gram is geometrically increased as volume decreases and power increases. However, during the calculation and comparison only the linear relation was considered as time and power increased, decreasing volume was not considered. Again, after collecting the sample the solutions were centrifuged for 2 h and, finally, the supernatant (upper 60% of the volume) was used for the analysis. Therefore, the actual effect of colloid could not be achieved after centrifuge because most of the particles precipitating by this method, and so were not considered for analysis.

Another study concerned with the dispersion stability of alumina−water nanofluids, which were 1-year-old, was performed by Elcioglu and Okutucu-Ozyurt (2014). PSD of the nanofluids was analyzed in a weekly manner to monitor for any changes. On the other hand, the nanoparticles formed aggregates over 1 year. The authors ultrasonicated the nanofluids via an ultrasonic bath, for up to 5 h. A reduction in the aggregate size was observed, to some

extent, in almost every week compared to before ultrasonication values; but the after-ultrasonication particle size approached the 1-week before value within a short period of time. The study was indicative of the requirement of performing such measurements in a frequent and periodic manner. Sadeghi et al. (2015) studied the effect of ultrasonication duration up to 180 min for alumina−water nanofluid with an ultrasonic vibrator (200 W and 24 kHz). They analyzed the zeta potential, cluster size, and polydispersity index (PDI). They observed that the zeta potential was increased with an increase of ultrasonication. They also found that PDI and cluster size decreased with increasing ultrasonication duration and reported that during the first 30 min PDI and cluster size rapidly decreased and after that slowly decreased.

However, some other investigators noticed that there are particular ideal ultrasonication durations existing, depending on various parameters of nanofluids, for example, particle concentration and type, and quantity of base fluid (Kabir, Saha, & Jeelani, 2007). Kwak and Kim (2005) studied the optimum ultrasonication duration for CuO−EG nanofluid. They ultrasonicated the mixture for between 1 and 30 h and characterized the nanofluid by dynamic light scattering (DLS) and zeta potential measurements. They found that 9 h of sonication was optimum and that, after longer sonication, the particles coalesced again (Mahbubul et al., 2014). Furthermore, they found the highest zeta potential value for 9 h of ultrasonication. Nevertheless, they could not describe any specific reason behind this phenomenon. Lam, Lau, Cheung, and Ling (2005) studied the effect of ultrasonication durations in nanoclay/epoxy composites. The samples were first mixed by hand-stirring and then ultrasonicated for 5, 10, 15, 30, and 60 min and characterized by scanning electron microscopy (SEM). They report that cluster sizes were decreased with the increase of ultrasonication duration. The authors reported that due to insufficient energy, the nanoclay platelets were unable to escape from the clusters. Again, they urged that the effect of too much energy would create a larger cluster as the collision of every single platelet would increase and they would tangle up and react. Chen et al. (2007) ultrasonicated a TiO_2−EG suspension for up to 40 h for the same objective of discovering the optimum sonication duration. Their characterization by light scattering to find out the aggregated size shows that 20 h of ultrasonication is best and corresponding cluster size was 140 nm. After which a further size reduction could not be achieved.

Yu et al. (2007) studied the dispersion behavior of MWCNTs under varying sonication times. They prepared nanofluid with 0.1 wt.% MWCNTs in distilled water with 0.15 wt.% of sodium dodecyl sulfate (SDS) as the surfactant. A continuous power of 20 W was used for sonication with various durations of 0, 5, 15, 30, 40, 50, and 120 min. They characterized the colloid with a UV-visible spectrophotometer and TEM and reported that maximum achievable dispersion of MWCNTs was reached after certain sonication energy (sonication time) (Mahbubul et al., 2014). Kabir et al. (2007) analyzed the influence of ultrasonication on nanofibers/polyurethane foam composite and reported that there is an optimum ultrasonication duration for a specific nanoparticle concentration; a lower sonication period is required for higher amplitudes and vice versa; and higher ultrasonication duration is essential for higher concentration also for a higher amount of base fluids. Lee et al. (2008) ultrasonicated Al_2O_3 nanoparticles in water for durations of 0, 5, 20, and 30 h. TEM and zeta potential

measurements were used to characterize the nanofluid. It was found that a sonication duration of ~5 h gave the best results (this paragraph is adapted with permission from Mahbubul et al. (2014). Copyright (2014) American Chemical Society).

Garg et al. (2009) investigated the effect of sonication time of nanofluid on dispersion behaviors. They prepared four samples of 1 wt.% MWCNTs in DIW with GA as additives and subjected the samples to ultrasonication for 20, 40, 60, and 80 min. They analyzed TEM and found that the optimum ultrasonication time for homogenization was 40 min, using a 130 W and 20 kHz ultrasonicator. Zhu et al. (2010) determined the influence of ultrasonication time on average cluster size. They analyzed solutions of $CaCO_3$−water, which were ultrasonicated for 1−45 min and found that the cluster size rapidly decreased within 20 min of ultrasonication and then slightly increased with ultrasonication duration. As their primary substance was in paste form, therefore, most of the aggregates were soft and broken up rapidly within 20 min. Nguyen et al. (2011) studied the effect of ultrasonication duration, power, and pulsed mode on de-agglomeration of alumina nanoparticles in water where the maximum input power of the machine was 400 W with a frequency of 20 kHz. They used 10%, 30%, and 60% of vibration amplitude with different pulsed mode and the optimal break-up of agglomeration was for 30% amplitude. In the case of 60% amplitude, cluster size again increased after 300 s of ultrasonication; therefore, the author's pointed out that higher power of ultrasonication could reagglomerate the particles. Nevertheless, for 10% and 30% amplitudes, the aggregate sizes were continuously decreased with an increase of sonication time. They used different modes (continuous and pulsed) with long and short duration; however, no difference and similar outcomes were observed. Chakraborty et al. (2012) analyzed the influence of ultrasonication durations on TiO_2 nanofluid. They added 0.1, 0.2, and 0.4 wt.% of silver (Ag) nanoparticles and ultrasonicated for 10, 20, and 30 min. They observed the settling time and reported that for a lower concentration of particles, ultrasonication did not have a significant role. Kole and Dey (2012) ultrasonicated ZnO nanoparticles in EG for up to 100 h and characterized the PSD and microstructure. They reported that the lowest cluster size was obtained for 60 h of sonication and after that cluster size again increased. [This paragraph is adapted from Mahbubul et al. (2015a), copyright (2015), with permission from Elsevier.]

Rashmi et al. (2011) analyzed the effect of ultrasonication duration on stability of 0.01 and 0.1 wt.% CNT−water−GA nanofluid with the aid of a UV-visible spectrophotometer. They homogenized the mixtures for 1, 4, 8, 16, and 20 h using an ultrasonic bath and reported 4 h to be the optimum duration for both concentrations. The authors focused that the structure of CNTs was damaged as bending, buckling, and dislocations, which were the reasons for lower stability after prolonged ultrasonication. LotfizadehDehkordi, Ghadimi, and Metselaar (2013) studied (with an ultrasonic disruptor) the effective ultrasonication period for TiO_2−water nanofluids through analysis with a Box-Behnken design to investigate the influence of ultrasonication power (20%−80%), ultrasonication time (2−20 min), and volume concentration (0.1−1.0 vol.%); and the significance of the models was tested by analysis of variance (ANOVA). The experiments were performed using a UV-visible spectrophotometer for after 1-week and 1-month intervals. Their results showed that longer duration of sonication and high power decreased the stability of nanofluid.

Furthermore, two different trends have also been observed by the same study. Chung et al. (2009) dispersed two types (A and B) of ZnO nanopowder in water and ultrasonicated the dispersions for 60 min. They characterized the effects of various sonication times using TEM and photon correlation spectroscopy (PCS). The PCS results showed that ultrasonication reduced the mean cluster size to 100 nm within 60 min for powder A and within 20 min for powder B, whereas further ultrasonication of up to 60 min did not reduce the cluster size. Nevertheless, the TEM results showed that aggregates still existed in the suspension (this paragraph is adapted with permission from Mahbubul et al. (2014). Copyright (2014) American Chemical Society).

From the above studies, no notable conclusions could be drawn. Some of the researchers recommended that a higher sonication time is better. However, others found the minimum agglomeration was after a certain duration of ultrasonication. Nevertheless, there is no specific or common duration of ultrasonication suggested by the researchers that could be followed for better solution (Mahbubul et al., 2015a). Moreover, among the available studies, most are related only to a few items. However, to get a good conclusion, different evaluation techniques simultaneously need to be carried out (Ghadimi et al., 2011) because ultrasonication may affect many parameters, as shown in Fig. 3-2.

3.2.1 Microstructure

In many cases, the microstructure of nanoparticles is observed first, before they were mixed with a base fluid such as the microstructures of Al_2O_3 nanoparticles taken by FESEM without any treatment (as received), as shown in Fig. 3-3. The microstructure and composition of the nanoparticles were characterized by FESEM (Model AURIGA, Zeiss, Germany). As-received nanoparticles were characterized by FESEM at 1 kV accelerating voltage without any treatment. Magnification scales on 1000× and 10,000× were used to capture the image within

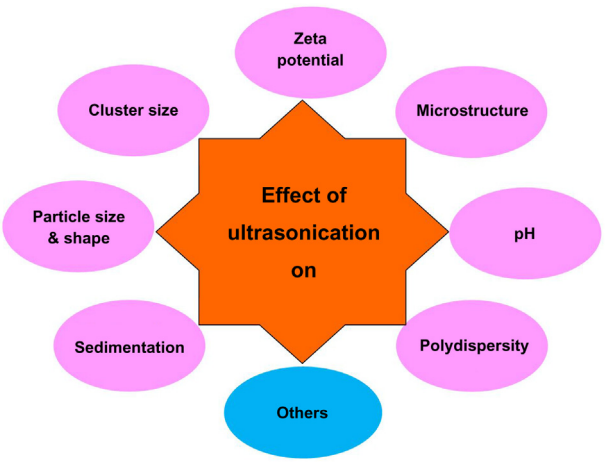

FIGURE 3-2 Effect of ultrasonication on different parameters.

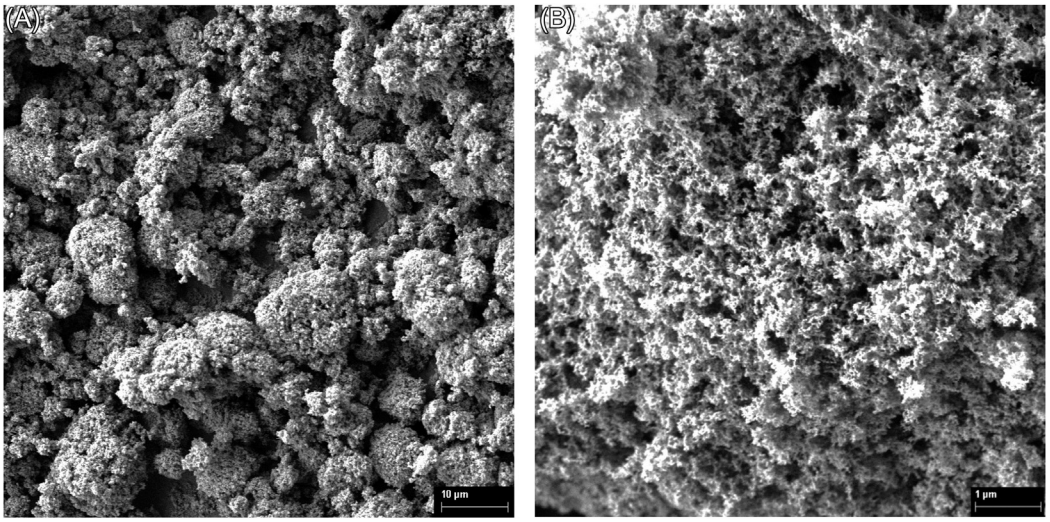

FIGURE 3-3 FESEM images of Al_2O_3 nanoparticles (A) in 10- and (B) 1-μm scales. *Reprinted with permission from Mahbubul, I.M., Chong, T.H., Khaleduzzaman, S.S., Shahrul, I.M., Saidur, R., Long, B.D., and Amalina, M.A. (2014). Effect of ultrasonication duration on colloidal structure and viscosity of alumina–water nanofluid.* Industrial & Engineering Chemistry Research 53*, 6677–6684. Copyright (2014) American Chemical Society.*

Table 3-2 Elemental Composition of Al_2O_3 Nanoparticles by EDAX Analysis for the Red Marking Rectangular Area of Fig. 3-5

Element	Wt.%	At%
O K	44.72	57.71
Al K	55.28	42.29
Matrix	Correction	ZAF

Source: Reprinted with permission from Mahbubul, I.M. (2015). *Investigation of fundamental properties of nanorefrigerants,* LAP Lambert Academic Publishing, Saarbrücken (Mahbubul, 2015), copyright (2015) OmniScriptum GmbH & Co. KG.

10- and 1-μm plots, respectively. In Fig. 3-3A, in the 10-μm range, high agglomeration of nanoparticles is observed. Fig. 3-3B shows the particles in the smaller range of 1 μm, in which the nanoparticles are found in loose clustered form and spherical shape. Therefore, it could be predicted that the nanoparticles will be easily dispersed in liquid with the vibration of ultrasonication. [This paragraph is adapted with permission from Mahbubul et al. (2014). Copyright (2014) American Chemical Society.]

The elemental compositions of the nanoparticles have also been checked by SEM-EDAX analysis, which confirms the composition of Al_2O_3 nanoparticles (as shown in Table 3-2 and Fig. 3-4 for the corresponding red marked rectangular area in Fig. 3-5).

First, four volume concentrations (0.01, 0.1, 0.5, and 1 vol.%) of Al_2O_3–water nanofluids were prepared by 1 h of ultrasonication using 50% ultrasonication amplitude with 2 s ON

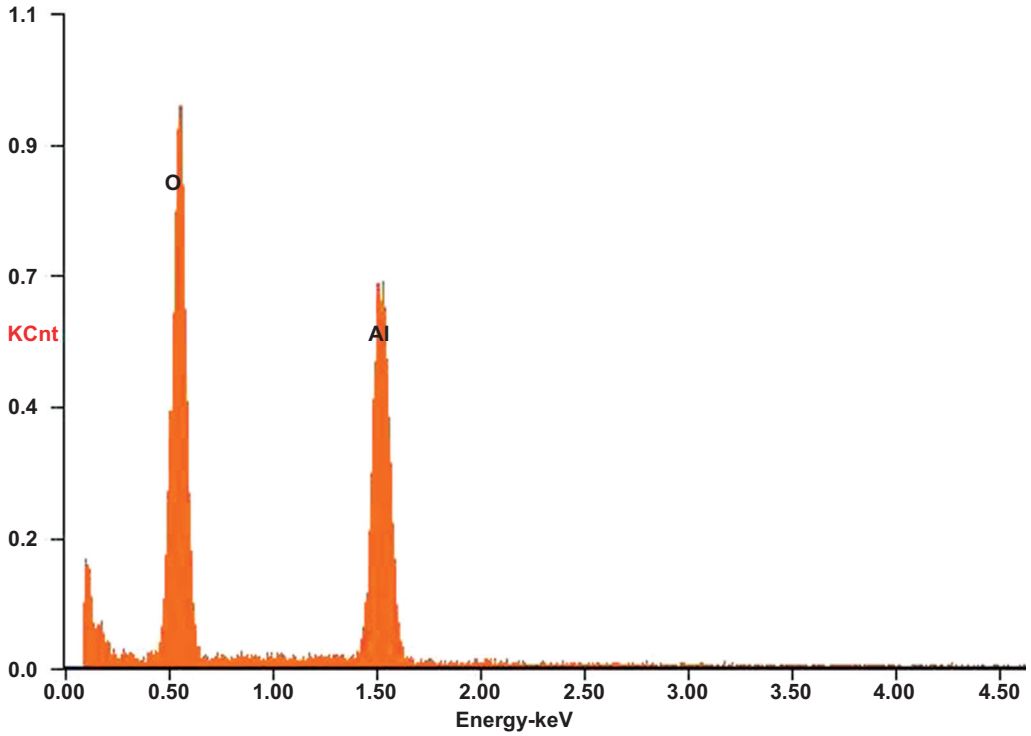

FIGURE 3-4 EDAX analysis of Al_2O_3 nanoparticles for the red marked rectangular area of Fig. 3-5. *Reprinted with permission from Mahbubul, I.M. (2015).* Investigation of fundamental properties of nanorefrigerants, *LAP Lambert Academic Publishing, Saarbrücken, copyright (2015) OmniScriptum GmbH & Co. KG.*

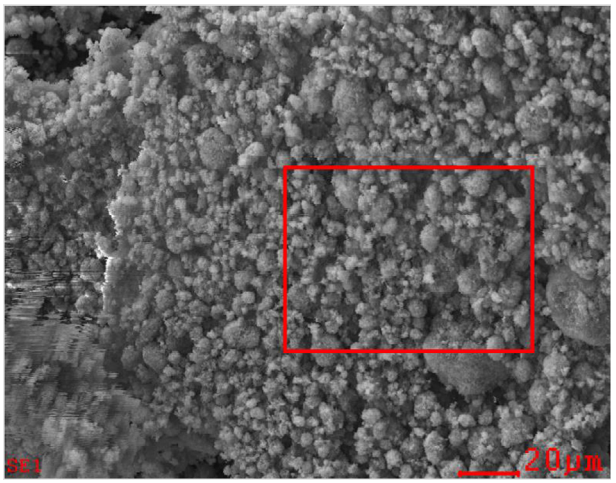

FIGURE 3-5 FESEM image of Al_2O_3 nanoparticles during EDAX analysis with the red marked rectangular area. *Reprinted with permission from Mahbubul, I.M. (2015).* Investigation of fundamental properties of nanorefrigerants, *LAP Lambert Academic Publishing, Saarbrücken, copyright (2015) OmniScriptum GmbH & Co. KG.*

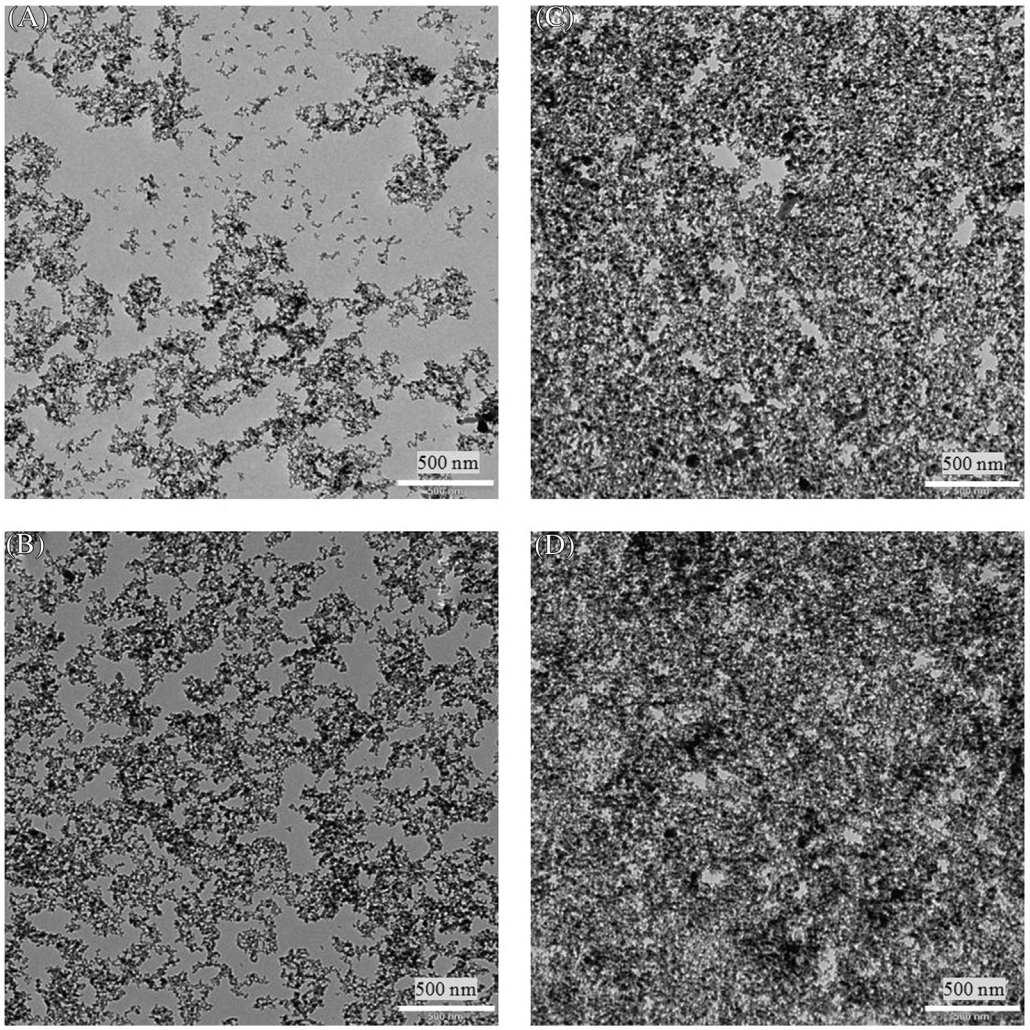

FIGURE 3-6 TEM images showing the microstructure of 1 h ultrasonicated Al_2O_3–water nanofluids of (A) 0.01, (B) 0.1, (C) 0.5, and (D) 1 vol.% concentrations. *Reprinted from Mahbubul, I. M., Saidur, R., Amalina, M. A., Elcioglu, E. B., and Okutucu-Ozyurt, T. (2015). Effective ultrasonication process for better colloidal dispersion of nanofluid.* Ultrasonics Sonochemistry 26, *361–369, copyright (2015), with permission from Elsevier.*

and 2 s OFF pulses. Then the microstructures of these four samples were analyzed by a TEM (Model LIBRA 120, Zeiss, Germany) and the results are provided in Fig. 3-6. Based on the TEM analyses, the dispersion characteristics of the samples with varying nanoparticle concentrations can be observed in Fig. 3-6. It is revealed from the TEM micrographs that the particles were in a rather involved and overlapping condition for 1 vol.% nanofluid compared to the 0.01, 0.1, and 0.5 vol.% samples. Such an observation of the sample microstructure can give preliminary conclusions on the nanoparticle-clustering tendency, which is

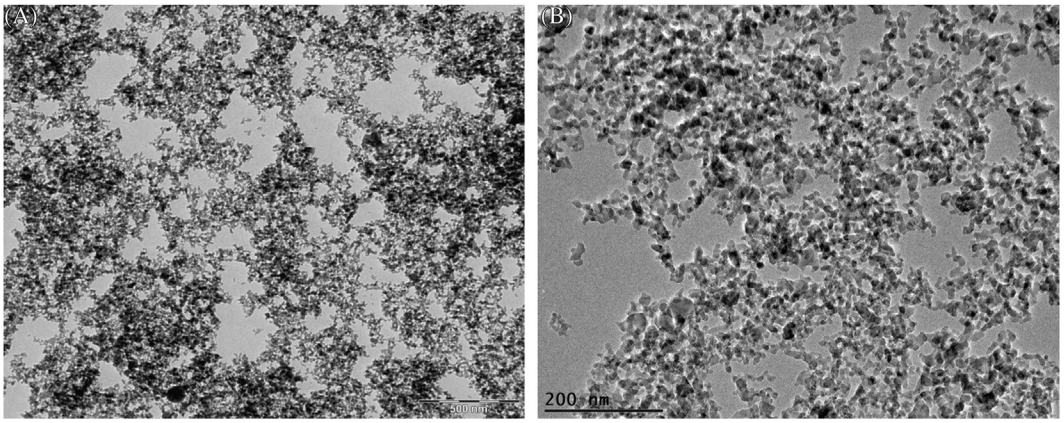

FIGURE 3-7 Microstructure of Al_2O_3−water nanofluid prepared without ultrasonication (0 h); (A) and (B) are 6300× and 12,500× magnifications and the corresponding scale bars are 500 nm and 200 nm, respectively.

inevitable in the long term. In order not to render the possible improvements in thermophysical properties coming with the increased nanoparticle concentration, 0.5 vol.% nanofluid is selected for further investigation as it appeared to be the preferable one among the concentrations studied, in terms of the nanoparticle dispersion. The sample of 1 vol.% was found to be the most concentrated nanofluid. However, 0.01 vol.% was observed to have the most diluted concentration. Hence, 0.5 vol.% of Al_2O_3−H_2O nanofluids have been further investigated for the effective ultrasonication parameters. [This paragraph is adapted from Mahbubul et al. (2015a), copyright (2015), with permission from Elsevier.]

To observe the effect of ultrasonication duration, the microstructure is analyzed by TEM after the nanoparticles are suspended in a fluid. The TEM image of Al_2O_3−water nanofluid after being suspended in water by stirring and without sonication is shown in Fig. 3-7. To obtain a better understanding of the microstructure, the images are portrayed with 500 nm and 200 nm scale bars. From Fig. 3-7, it is clear that the nanoparticles were not properly dispersed and there was strong clustering among the nanoparticles (Mahbubul et al., 2014). This aggregate occurs when the nanoparticles were agglomerated in dry powder form and even after mixing with water they still exist. Therefore, ultrasound energy is necessary to break down such aggregates. Some locations that are empty in Fig. 3-7 imply the presence of no particles, whereas some places are darker indicating high aggregation of nanoparticles (Mahbubul et al., 2014).

The TEM images of Al_2O_3−water nanofluid after 1 h ultrasonication with two different amplitudes (25% and 50%) are shown in Fig. 3-8. Fig. 3-8 shows that 1 h of ultrasonication is not enough for good dispersion of nanoparticles. The left-hand side figures (Fig. 3-8A and B) are micrographs of 25% amplitude, which show that there are still a lot of aggregates of particles. The right-hand side figures (Fig. 3-8C and D) are micrographs of 50% amplitude and these microstructures show a better colloidal dispersion compared to that of 25% amplitude.

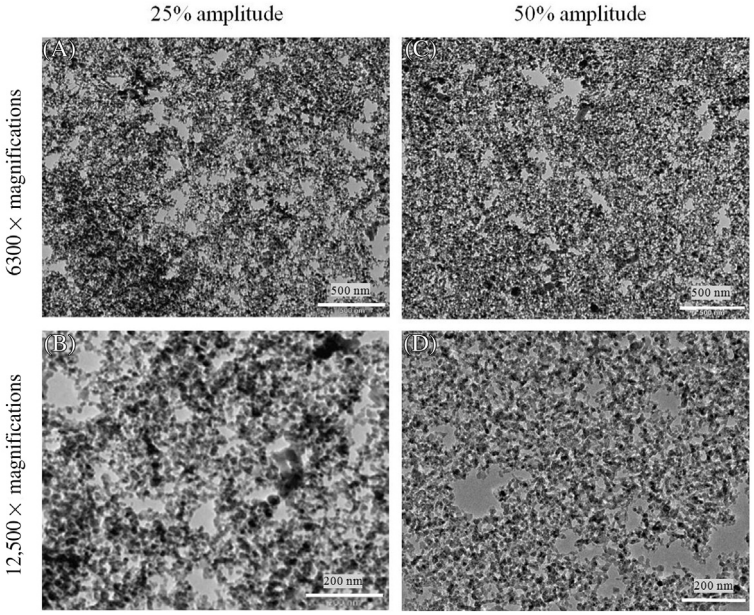

FIGURE 3-8 Microstructure of Al_2O_3–water nanofluid prepared by 1 h of ultrasonication duration. *Reprinted from Mahbubul, I. M., Saidur, R., Amalina, M. A., Elcioglu, E. B., and Okutucu-Ozyurt, T. (2015). Effective ultrasonication process for better colloidal dispersion of nanofluid.* Ultrasonics Sonochemistry 26, *361–369, copyright (2015), with permission from Elsevier.*

Nevertheless, there are some clusters of particles visible in Fig. 3-8C. Fig. 3-8 shows that better dispersion of nanoparticles is found for higher power (amplitude) of sonicator even for the same duration. Lam et al. (2005) reported that through lack of enough energy, nanoparticles would not be able to escape from the clusters, and, as a result, large aggregation will be observed. The higher aggregation was seen in the case of nanofluids prepared by 1 h of ultrasonication with 25% amplitude being the result of the above statement. [This paragraph is adapted from Mahbubul et al. (2015a), copyright (2015), with permission from Elsevier.]

Fig. 3-9 shows the microstructure of Al_2O_3 nanoparticles in water after 2 h of ultrasonication with 25% and 50% amplitude. Fig. 3-9A and B (the left-hand side figures) are micrographs of 25% amplitude at 6300 × and 12,500 × magnifications, respectively, in 500- and 200-nm scales, respectively. Similarly, the right-hand side figures (Fig. 3-9C and D) are micrographs of 50% amplitude. It is clear from Fig. 3-9 that the nanoparticles were well dispersed and similar dispersion has been observed for nanofluids prepared by 2 h of ultrasonication with 25% and 50% amplitudes. Nevertheless, there are a few small overlaps observed, which are the nanoclusters among the particles. Such nanoclusters could not be fully broken down, even after prolonged ultrasonication. It is impossible to get the initial size of particles after dispersion into fluid (Elcioglu & Okutucu-Ozyurt, 2014). Particle size distribution (PSD) analysis gives an idea of the size of the nanoclusters. Ghadimi et al. (2011) report that the cluster of nanofluids will be at least three times higher than the average particle diameter.

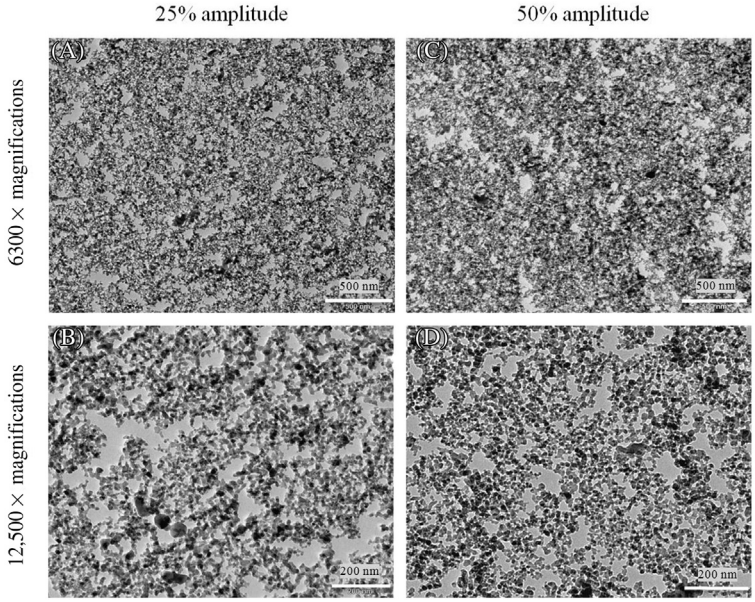

FIGURE 3-9 Microstructure of Al_2O_3−water nanofluid prepared with 2 h of ultrasonication. *Reprinted from Mahbubul, I. M., Saidur, R., Amalina, M. A., Elcioglu, E. B., and Okutucu-Ozyurt, T. (2015). Effective ultrasonication process for better colloidal dispersion of nanofluid.* Ultrasonics Sonochemistry 26*, 361−369, copyright (2015), with permission from Elsevier.*

[This paragraph is adapted from Mahbubul et al. (2015a), copyright (2015), with permission from Elsevier.]

The microstructures of Al_2O_3−water nanofluid prepared by 3 h of ultrasonication with two different amplitudes (25% and 50%) are shown in Fig. 3-10. The left-hand side figures (Fig. 3-10A and B) are micrographs of 25% amplitude and the right-hand side figures (Fig. 3-10C and D) are micrographs of 50% amplitude. More spreading (meaning better dispersion with smaller cluster size) of nanoparticles is seen in Fig. 3-10. There are only a few empty areas visible in the micrograph. Even though there is no large agglomeration observed, there are small nanoclusters of particles. Either the agglomeration of nanoparticles did not have enough energy to completely break down the clusters or the nanoparticles received more energy and started to re-agglomerate. Nevertheless, it is impossible to completely break down the clusters of particles (Ghadimi et al., 2011). It is reported in the literature (Kwak & Kim, 2005; Lam et al., 2005; Nguyen et al., 2011) that higher power of ultrasonication could re-agglomerate the particles as the collision of each particle will increase and they will tangle up. A comparatively higher dispersion of particles is observed for the nanofluids prepared by 50% amplitude in comparison to the 25% one. This indicates that using 25% amplitudes of sonicator power, even after 3 h of ultrasonication, nanoparticles do not get enough energy to completely be dispersed into water. [This paragraph is adapted from Mahbubul et al. (2015a), copyright (2015), with permission from Elsevier.]

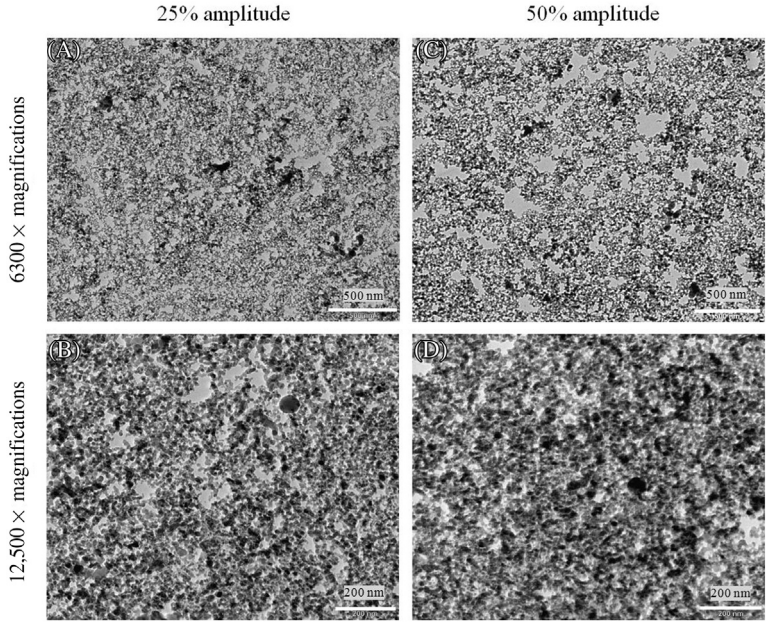

FIGURE 3-10 Microstructure of Al_2O_3—water nanofluid prepared with 3 h of ultrasonication. *Reprinted from Mahbubul, I. M., Saidur, R., Amalina, M. A., Elcioglu, E. B., and Okutucu-Ozyurt, T. (2015). Effective ultrasonication process for better colloidal dispersion of nanofluid.* Ultrasonics Sonochemistry 26*, 361—369, copyright (2015), with permission from Elsevier.*

The micrographs taken by TEM for the nanofluids prepared by 4 h ultrasonication with 25% and 50% amplitudes are shown in Fig. 3-11. Fig. 3-11A and B (the left-hand side figures) are the micrographs of 25% amplitude with 6300 × and 12,500 × magnifications, respectively, with 500- and 200-nm scales, respectively. Similarly, the right-hand side figures (Fig. 3-11C and D) are micrographs of 50% amplitude. More spreading of nanoparticles is seen in Fig. 3-11. There are no significant empty areas visible in the micrographs taken for the nanofluid prepared by 50% amplitude. However, there are some (but few) empty areas that can be seen for the nanofluids of 25% amplitude. Moreover, there are some clusters of particles. Therefore, it could be expected that further higher ultrasonication with 25% amplitude could break down the remaining aggregates and disperse more particles. Fig. 3-12 shows the microstructures of Al_2O_3—water nanofluid prepared by 5 h ultrasonication. The left-hand side figures (Fig. 3-12A and B) are micrographs of 25% amplitude and the right-hand side figures (Fig. 3-12C and D) are micrographs of 50% amplitude. More spreading of nanoparticles is seen in the figure for 5 h of ultrasonication and a similar trend was observed for the applied power of 25% and 50% sonicator amplitude. However, there are minor overlaps of nanoparticles but no empty areas can be seen in Fig. 3-12C and D for 50% amplitude. A higher particle dispersion but with few empty areas and minor overlapping of particles is observed in Fig. 3-12A and B for 25% amplitude. Therefore, nanofluids prepared

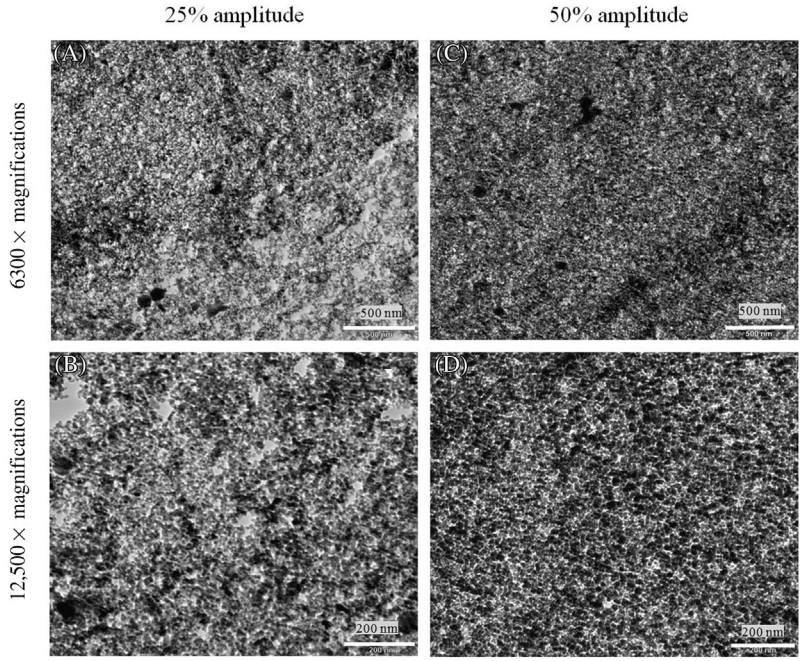

FIGURE 3-11 Microstructure of Al_2O_3–water nanofluid prepared with 4 h of ultrasonication. *Reprinted from Mahbubul, I. M., Saidur, R., Amalina, M. A., Elcioglu, E. B., and Okutucu-Ozyurt, T. (2015). Effective ultrasonication process for better colloidal dispersion of nanofluid.* Ultrasonics Sonochemistry 26*, 361–369, copyright (2015), with permission from Elsevier.*

by 25% amplitudes did not have enough ultrasound energy to have the mono-dispersed condition. The images of Fig. 3-12 are a darker black color, which is more significant in Fig. 3-12C and D for 50% amplitude. This could be due to the erosion of the sonicator tip. Mandzy, Grulke, and Druffel (2005) reported that erosion of an ultrasonic tip could be contaminated with the fluid as a result of longer ultrasonication duration. [This paragraph is adapted from Mahbubul et al. (2015a), copyright (2015), with permission from Elsevier].

Therefore, a strong morphological change in the colloid occurs with the variation of the ultrasonication duration, as nanoparticles are dispersed until 2 h of sonication, after which they start to coalesce. Kwak and Kim (2005) found a similar type of morphology, as further sonication after the optimum sonication time caused the nanoparticles to coalesce again (this paragraph is adapted with permission from Mahbubul et al. (2014). Copyright (2014) American Chemical Society).

The final particle sizes (average) of Al_2O_3–water nanofluid after each ultrasonication were measured from TEM images, and plotted as histograms of particle diameter. Fig. 3-13 presents a histogram of particle sizes of the nanofluid prepared by 0 h of ultrasonication. Although the primary particle size (average) was 13 nm, a wide range of particle sizes from 6 to 20 nm is observed in Fig. 3-13 for the nanofluid prepared by 0 h of ultrasonication. Most of the

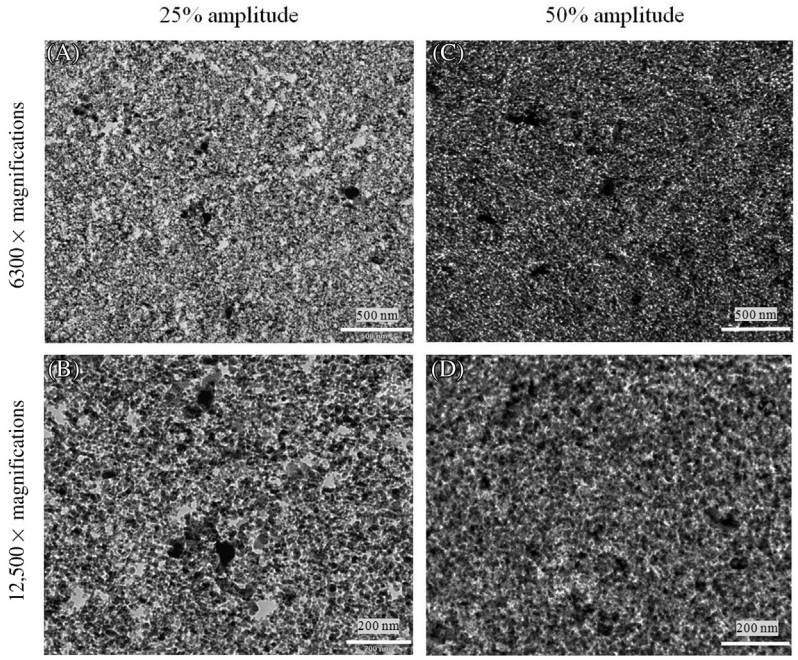

FIGURE 3-12 Microstructure of Al_2O_3–water nanofluid prepared with 5 h of ultrasonication. *Reprinted from Mahbubul, I. M., Saidur, R., Amalina, M. A., Elcioglu, E. B., and Okutucu-Ozyurt, T. (2015). Effective ultrasonication process for better colloidal dispersion of nanofluid.* Ultrasonics Sonochemistry 26*, 361–369, copyright (2015), with permission from Elsevier.*

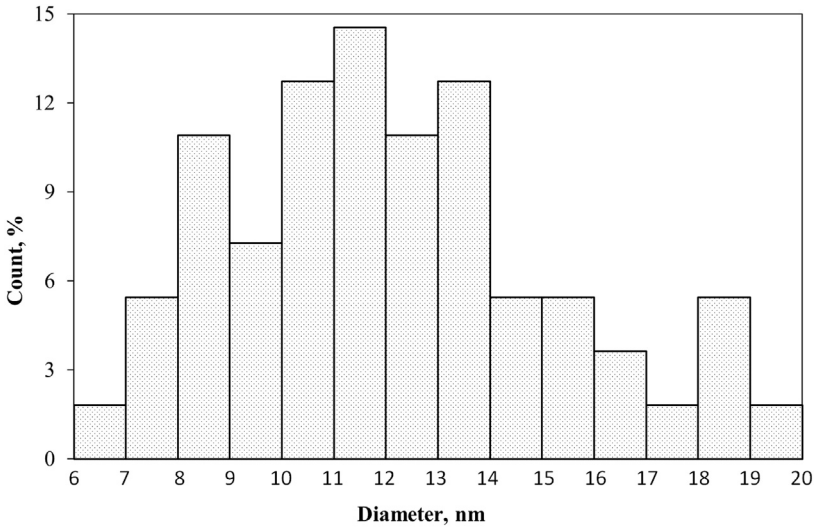

FIGURE 3-13 Histogram of the individual particle diameter of Al_2O_3–water nanofluid prepared by 0 h (without ultrasonication).

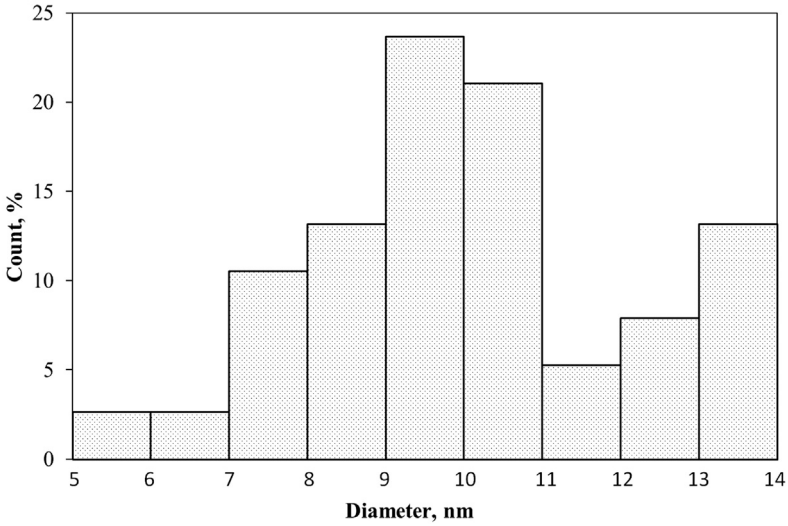

FIGURE 3-14 Histogram of the individual particle diameter of Al_2O_3–water nanofluid prepared with 1 h of ultrasonication.

nanoparticles were in the range of 10–14 nm, which is more than 50% of total population. A very few nanoparticles were found to be over 20 nm size, but are not included in the histogram.

The histogram of particle sizes of the Al_2O_3–water nanofluid prepared with 1 h of ultrasonication shows that particle sizes were within the range of 5–14 nm as reported in Fig. 3-14. Here the particle size range is smaller than that of Fig. 3-13 for 0 h of ultrasonication. Therefore, with the start of ultrasonication, nanoparticles are starting to break down and eroding was also observed (Özcan-Taşkin, Padron, & Voelkel, 2009). Particle–particle collision is also a reason for erosion. After 1 h of ultrasonication, most of the nanoparticles were found to be in the range of 9–11 nm. Almost 45% of total population was within this range.

Fig. 3-15 shows a histogram of particle sizes of the Al_2O_3–water nanofluid prepared with 2 h of ultrasonication. It can be seen in Fig. 3-15 that most of the nanoparticles were within the range of 8–11 nm, among them 10–11 nm range particles were approximately 31% of the total volume. The highest nanoparticle diameter was observed to be about 12 nm, which is less than the primary average diameter (13 nm). Therefore, most of the particles were either broken or eroded with 2 h of ultrasonication.

The histogram of particle sizes of the Al_2O_3–water nanofluid prepared with 3 h of ultrasonication is shown in Fig. 3-16. It can be seen in Fig. 3-16 that after 3 h of ultrasonication, the particle sizes were again decreased. Most of the particles (70%) were within the range of 7–10 nm. Moreover, 30% of total particles were within 8–9 nm diameter sizes.

Fig. 3-17 presents a histogram of particle sizes of the Al_2O_3–water nanofluid prepared with 4 h of ultrasonication. A similar range of particle sizes to that reported in Fig. 3-16 for

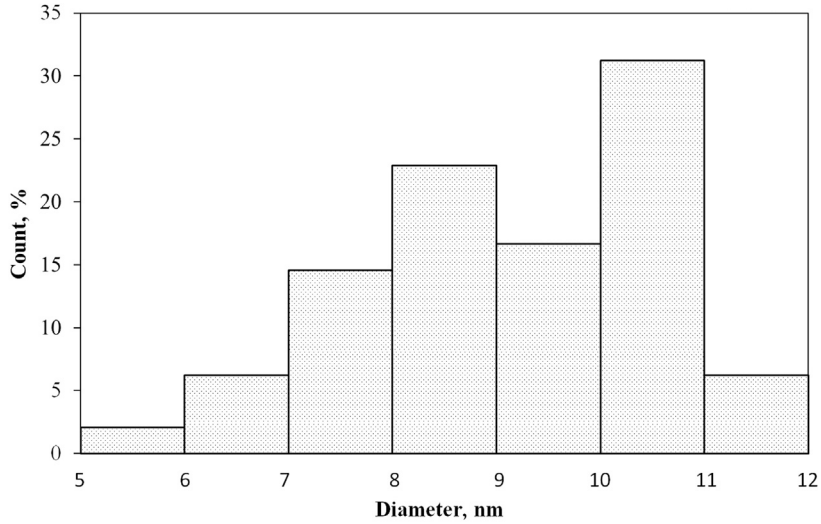

FIGURE 3-15 Histogram of the individual particle diameters of Al_2O_3−water nanofluid prepared with 2 h of ultrasonication.

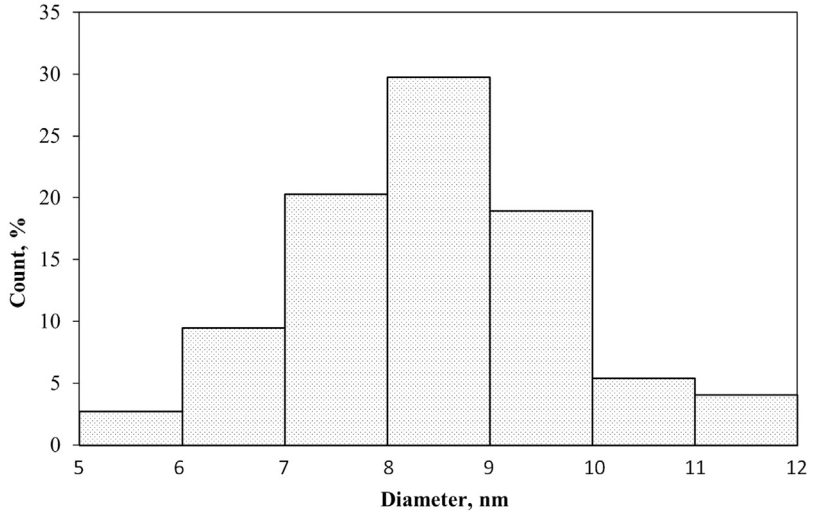

FIGURE 3-16 Histogram of the individual particle diameter of Al_2O_3−water nanofluid prepared with 3 h of ultrasonication.

3 h of ultrasonication was observed. However, here more than 75% of nanoparticles are within 7−10 nm range and about 32% of nanoparticles are in 8−9 nm range. Therefore, until 3 h of ultrasonication, nanoparticle diameters were rapidly decreased, after that no significant decrease in size is observed with further sonication.

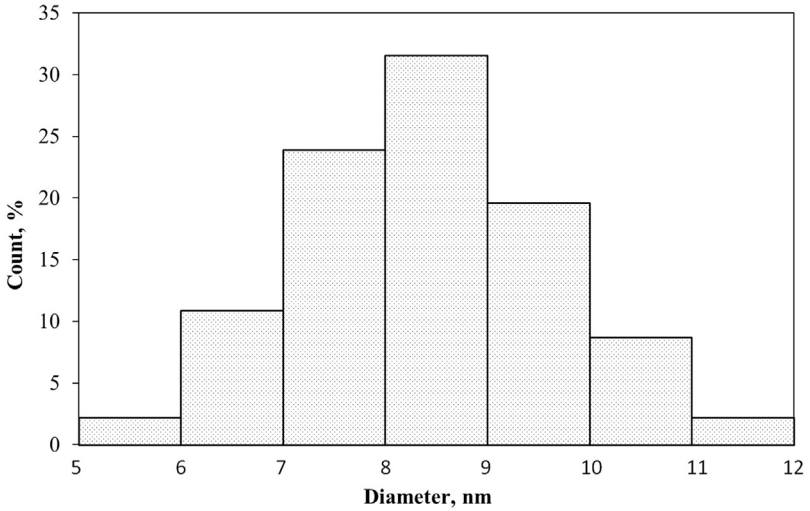

FIGURE 3-17 Histogram of the individual particle diameter of Al_2O_3–water nanofluid prepared with 4 h of ultrasonication.

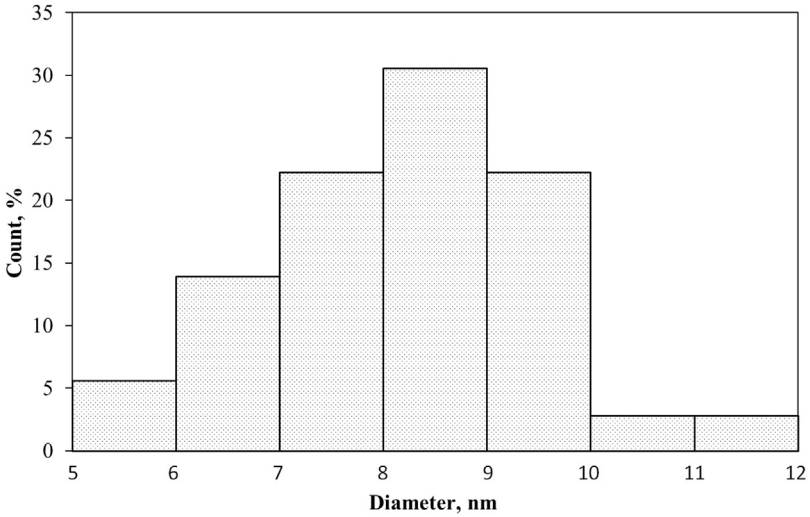

FIGURE 3-18 Histogram of the individual particle diameter of Al_2O_3–water nanofluid prepared with 5 h of ultrasonication.

A histogram of particle sizes of the Al_2O_3–water nanofluid prepared with 5 h of ultrasonication is reported in Fig. 3-18. After 5 h of ultrasonication, most of the particle diameters were within the range of 7–10 nm, and about 75% of the total population was within this range. Furthermore, the highest level of distribution (about 31% of particles) was in the

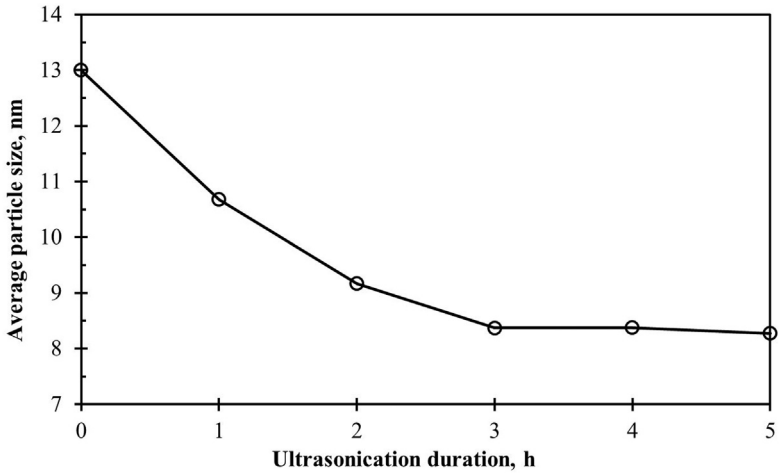

FIGURE 3-19 Average final particle sizes of Al_2O_3 nanoparticles after different durations of ultrasonication.

8−9 nm range, which is similar to that reported in Figs. 3-16 and 3-17 for 3 and 4 h of ultrasonication, respectively. Therefore, even after 5 h of ultrasonication, the particle diameters did not reduce from that of 3 h of ultrasonication. It could be assumed that 3 h of ultrasonication could be the optimum duration for the nanofluid. Nevertheless, the distribution of particles with a diameter less than 7 nm was observed to be higher and particles having a diameter over 10 nm was found to be lower after 5 h of ultrasonication in comparison to that of 3 and 4 h of ultrasonication.

The final particle sizes (average) of Al_2O_3−nanofluid for each ultrasonication period are plotted in Fig. 3-19. It can be seen in Fig. 3-19 that the average nanoparticle size was decreased with the increase of ultrasonication duration. An almost linear decreasing trend of particle size was observed up to 3 h of ultrasonication and the average final particle size was found to be 8.32 nm $\pm$ 0.05 nm for 3 h of ultrasonication. Yang et al. (2006) reported that prolonged ultrasonication time affects the size and aspect ratio of particles, which is more significant for nanotubes because of their larger particle length (Mahbubul et al., 2014). However, the average particle size was found to be the same with further ultrasonication after 3 h, as shown in Fig. 3-19. Lee et al. (2008) reported that after 5 h of ultrasonication, most particles were smaller than the initial size of 30 nm $\pm$ 5 nm. The particle size is looked to be 10 nm for their reported TEM image in the 50 nm scale (Lee et al., 2008). [This paragraph is adapted with permission from Mahbubul et al. (2014). Copyright (2014) American Chemical Society.]

For another type of sample, the morphology of the TiO_2 nanopowder was evaluated through SEM imaging. Field emission (FE) is a particular electron source that provides high resolution for the microanalysis of samples (Mahbubul et al., 2017). The FESEM analysis is conducted to characterize the morphology (as shown in Fig. 3-20, the shape of nanoparticles was near-spherical), dispersity, and compositions of nanoparticles (as shown in Table 3-3 and Fig. 3-21 for the corresponding red marked rectangular area of Fig. 3-22).

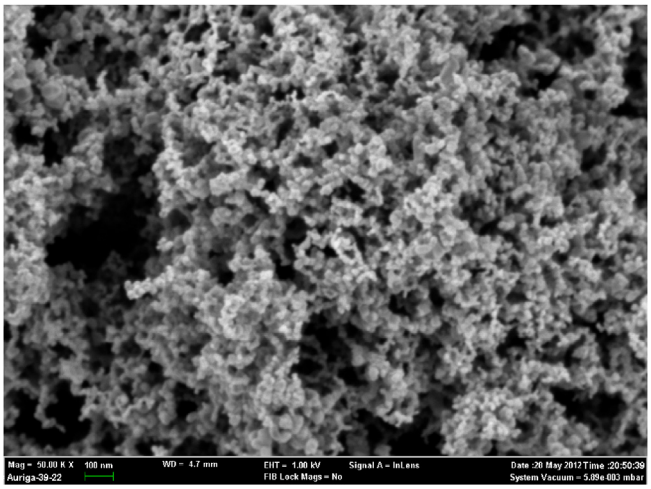

FIGURE 3-20 The FESEM image of TiO_2 nanoparticles. *Reprinted from Mahbubul, I. M., Elcioglu, E. B., Saidur, R., and Amalina, M. A. (2017). Optimization of ultrasonication period for better dispersion and stability of TiO_2–water nanofluid.* Ultrasonics Sonochemistry 37, *360–367, copyright (2017), with permission from Elsevier.*

Table 3-3 Elemental Composition of TiO_2 Nanoparticles by EDAX Analysis for the Red Marked Rectangular Area of Fig. 3-22

Element	Wt.%	At%
Ti L	60.52	33.86
O K	39.48	66.14
Matrix	Correction	ZAF

Source: Reprinted with permission from Mahbubul, I.M. (2015). Investigation of fundamental properties of nanorefrigerants, LAP Lambert Academic Publishing, Saarbrücken, copyright (2015) OmniScriptum GmbH & Co. KG.

From Fig. 3-20, it can be seen that the nanoparticles were loosely aggregated and might be dispersed relatively easily with the application of ultrasound energy, in comparison to the dispersion of a highly aggregated structure. Dispersity of the nanoparticles is gathered in Fig. 3-23, where TEM images are shown for different ultrasonication durations and different magnifications of the device. It can be inferred from Fig. 3-23 that nanoparticles were in a rather agglomerated condition before ultrasonication (see the images with the title "0 min"). According to Wen and Ding (2005), this agglomeration before dispersion could be due to the handling, storing, and/or manufacturing processes. It could be noted that most of the nanoparticles have a tendency to agglomerate and even re-agglomerate with each other due to the van der Waals attractive forces. Therefore, ultrasonication is used as a source of repulsive force, which produces resistance against interparticle attractive forces and disperses nanoparticles in the base fluid (Wen & Ding, 2005). Fig. 3-23 illustrates that with increasing ultrasonication duration of 150 min, the dispersity of nanoparticles became more even and

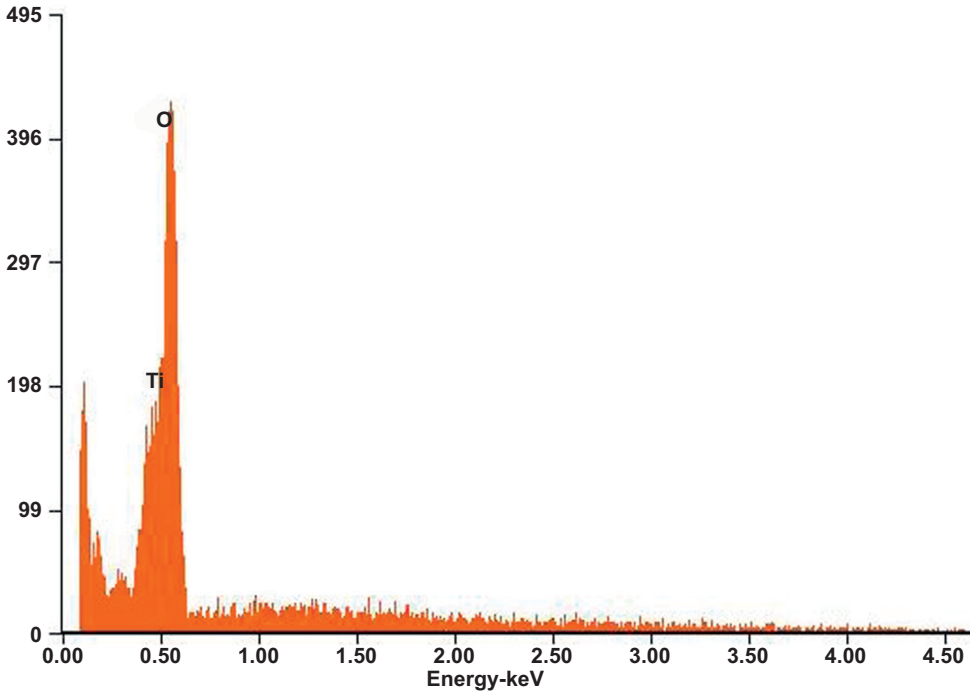

FIGURE 3-21 EDAX analysis of TiO_2 (~21 nm) nanoparticles for the red marked rectangular area of Fig. 3-22. *Reprinted with permission from Mahbubul, I.M. (2015).* Investigation of fundamental properties of nanorefrigerants, *LAP Lambert Academic Publishing, Saarbrücken, copyright (2015) OmniScriptum GmbH & Co. KG.*

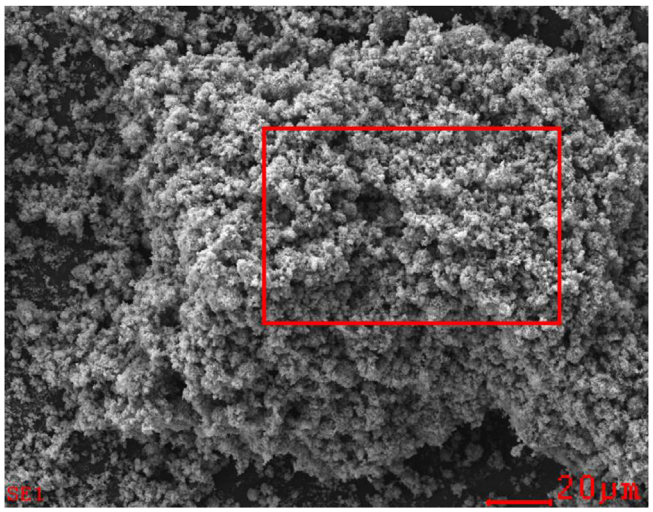

FIGURE 3-22 SEM image of TiO_2 nanoparticles during EDAX analysis with the red marked rectangular area. *Reprinted with permission from Mahbubul, I.M. (2015).* Investigation of fundamental properties of nanorefrigerants, *LAP Lambert Academic Publishing, Saarbrücken, copyright (2015) OmniScriptum GmbH & Co. KG.*

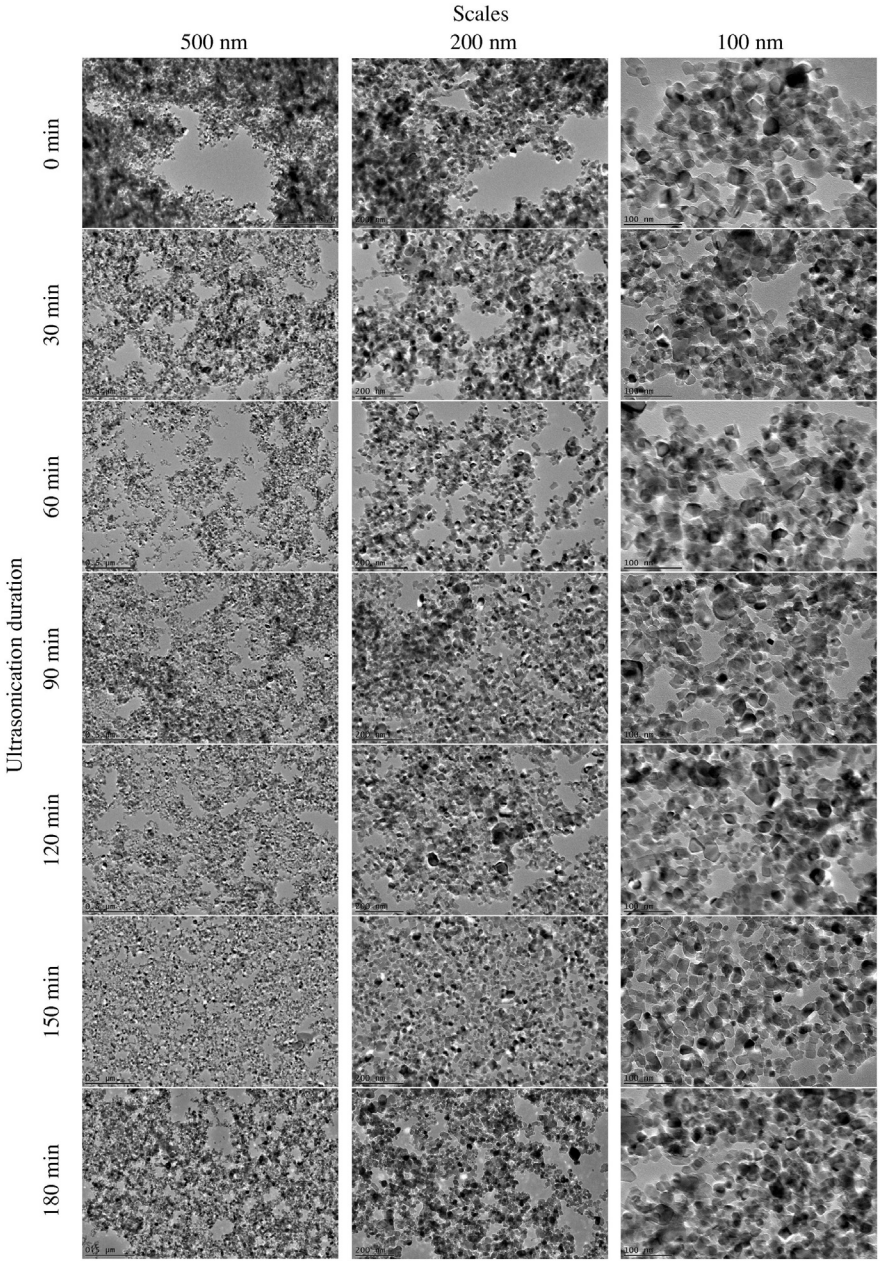

FIGURE 3-23 TEM microstructure of TiO_2-H_2O nanofluids for different periods of ultrasound treatment, with different magnifications. *Reprinted from Mahbubul, I. M., Elcioglu, E. B., Saidur, R., and Amalina, M. A. (2017). Optimization of ultrasonication period for better dispersion and stability of TiO_2–water nanofluid.* Ultrasonics Sonochemistry 37, *360–367, copyright (2017), with permission from Elsevier.*

homogeneous, and the presence of agglomerates was diminished significantly. This is attributed to the fact that ultrasonic energy broke down the nanoparticle agglomerates, and could yield a more homogeneous nanofluid sample. On the other hand, further increase of ultrasonication period resulted in a slight tendency for re-agglomeration of nanoparticles (see the images of Fig. 3-23 with the label "180 min"). By comparing the images with the labels "150 min" and "180 min" in Fig. 3-23, re-agglomeration of particles with the latter sonication period may be seen. Re-agglomeration of nanoparticles is an interesting phenomenon and from the ultrasonication point of view, it is reported in the literature (Kwak & Kim, 2005; Lam et al., 2005; Nguyen et al., 2011) that higher power of ultrasonication could re-agglomerate the particles as a result of the increased collision of particles. [This paragraph is adapted from Mahbubul et al. (2017), copyright (2017), with permission from Elsevier.]

3.2.2 Aggregate Size

There is uncertainty about the microstructure of nanofluids taken by TEM because this technique analyses a very small amount of the sample, and even the full sample could not be observed simultaneously. Therefore, a number of analytical techniques are available for evaluating the particle size of a suspension, in addition to electron microscopy; such as DLS, centrifugal liquid sedimentation, and small-angle X-ray scattering, to name a few (Rice et al., 2013). The following figures corresponding to the particle size distribution of nanofluid samples were attained by DLS measurements with a zetasizer. Although the size distribution of nanoparticles is mostly referred to as particle size distribution, in reality, aggregation of particles is most significant in the dispersion. In that case, one may talk about a cluster of particles, rather than individual particles. Fig. 1-2 (in Chapter 1) presents an idea about the clustering mechanism. In that case, the effective diameter is not the diameter of a single particle. Rather, it is the diameter of a group of aggregated particles. [This paragraph is adapted from Mahbubul et al. (2017), copyright (2017), with permission from Elsevier.]

A zetasizer instrument was used to analyze the aggregation of particles using the photon correlation spectroscopy (PCS) method. The effect of the ultrasonication process on PSD was measured for nanofluid prepared by 1, 2, 3, 4, and 5 h of ultrasonication with 25% and 50% amplitude and reported in Fig. 3-24. Fig. 3-24A–E show 1, 2, 3, 4, and 5 h of ultrasonication with 25% amplitude and Fig. 3-24F–J show 1, 2, 3, 4, and 5 h of ultrasonication with 50% amplitude. Considering the initial particle size (13 nm), the aggregated state of the nanoparticles can be observed through the PSD results presented in Fig. 3-24. The aggregation is also evident in the FESEM image shown in Fig. 3-3. According to the distributions in Fig. 3-24, the largest particle aggregate detected by the zetasizer device is approximately 200–250 nm. However, the frequency of such a large aggregate is very low compared to that of smaller aggregate within the base liquid. Based on the analyses performed for each case in Fig. 3-24, the range for the particle aggregate size has been obtained between 42–300 nm, approximately, depending on the ultrasonication duration and amplitude. In addition to the aggregate size, their distribution characteristics are also of great importance. It is realized from Fig. 3-24 that the PSDs of the samples ultrasonicated at 25% amplitude are mostly

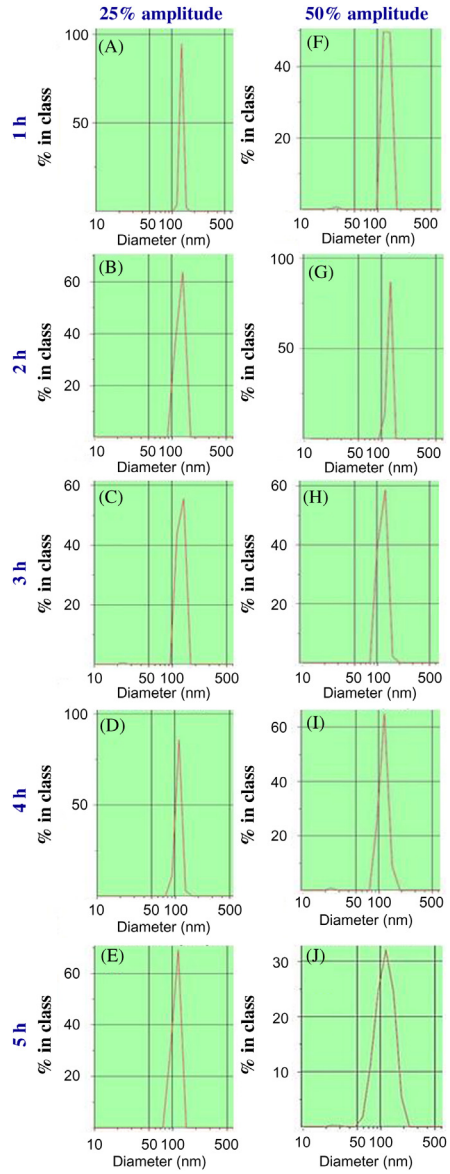

FIGURE 3-24 Particle (cluster) size distribution (based on intensity) of Al_2O_3 nanoparticles at different durations of ultrasonication with different power amplitudes. *Reprinted from Mahbubul, I. M., Saidur, R., Amalina, M. A., Elcioglu, E. B., and Okutucu-Ozyurt, T. (2015). Effective ultrasonication process for better colloidal dispersion of nanofluid.* Ultrasonics Sonochemistry 26*, 361–369, copyright (2015), with permission from Elsevier.*

narrower than those for 50% amplitude, for the same ultrasonication duration. This result becomes more pronounced for longer ultrasonication. For a given ultrasonication duration, the only variable in the comparison for the character of PSDs is the ultrasonication amplitude. Hence, it can be concluded from Fig. 3-24 that higher amplitude results in more

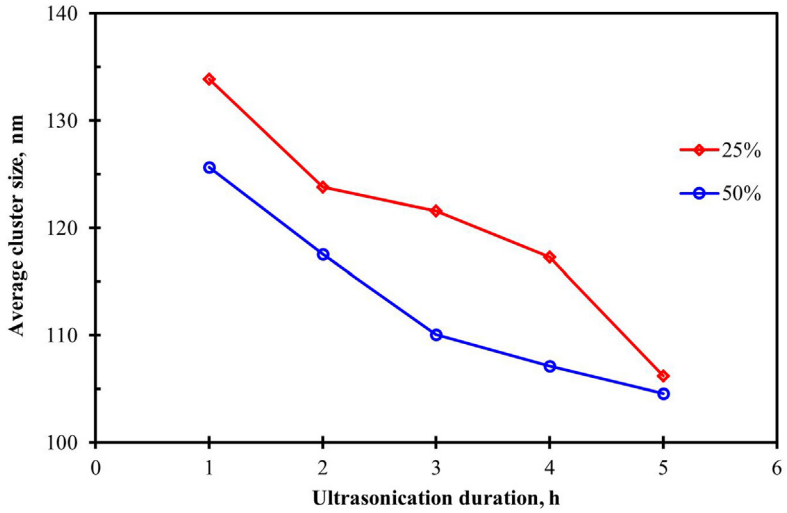

FIGURE 3-25 Average cluster sizes of Al_2O_3 nanoparticles after varying ultrasonication durations, at 25% and 50% amplitudes. *Adapted from Mahbubul, I. M., Saidur, R., Amalina, M. A., Elcioglu, E. B., and Okutucu-Ozyurt, T. (2015). Effective ultrasonication process for better colloidal dispersion of nanofluid.* Ultrasonics Sonochemistry 26, *361–369, copyright (2015), with permission from Elsevier.*

effective ultrasonication, yielding smaller particles. However, for the PSD-sensitive and narrow PSD requiring applications, smaller amplitudes may be preferred, considering the advantages and drawbacks of having a slightly larger but narrower PSD. [This paragraph is adapted from Mahbubul et al. (2015a), copyright (2015), with permission from Elsevier.]

The average aggregate size variation with ultrasonication duration at different amplitudes is provided in Fig. 3-25. As illustrated in Fig. 3-25, the average cluster size decreased with increasing ultrasonication duration. As the ultrasonication duration increases, the total amount of ultrasonication energy that the sample is subjected to increases, according to the relation $E = P \times t$, where E, P, and t stand for the total amount of energy delivered to the suspension, the applied power, and the total amount of time, respectively (Taurozzi, Hackley, & Wiesner, 2012). Having quantitatively realized the nanoparticle aggregation through PSD analyses, reduction in the average particle size can be observed for increasing ultrasonication durations from 1 to 5 h. In addition, the higher the amplitude, the lower the observed aggregate size. However, after 5 h of ultrasonication, the cluster size was almost the same as for the nanofluids prepared by 25% and 50% amplitudes. This phenomenon could be because the lowest attainable cluster size was reached after 5 h and further ultrasonication may not decrease the cluster size. Such criteria have been reported in the literature (Chen et al., 2007; Chung et al., 2009). [This paragraph is adapted from Mahbubul et al. (2015a), copyright (2015), with permission from Elsevier.]

The cluster size distributions of Al_2O_3 nanoparticles after different durations of ultrasonication with 50% amplitudes are shown in Fig. 3-26. The distribution curves are plotted in a single

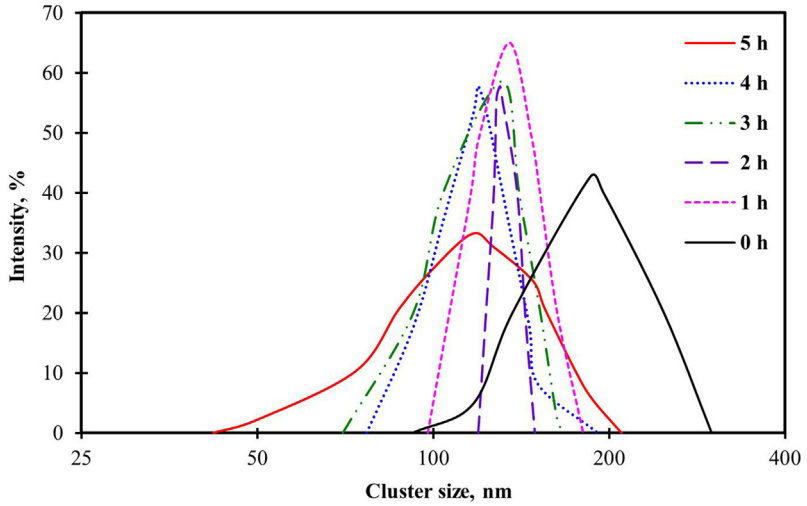

FIGURE 3-26 Distribution of cluster sizes of Al_2O_3 nanoparticles after different ultrasonication durations with 50% amplitudes. *Adapted from Mahbubul, I. M., Saidur, R., Amalina, M. A., and Niza, M. E. (2016). Influence of ultrasonication duration on rheological properties of nanofluid: An experimental study with alumina–water nanofluid.* International Communications in Heat and Mass Transfer 76, *33–40, copyright (2016), with permission from Elsevier.*

figure to understand the effect of ultrasonication duration on aggregate sizes. Only the 50% amplitude is considered here, to concentrate only on the effect of the sonication period. From Fig. 3-26, it is observed that the highest aggregates were about 300 nm but within the range of distribution from 92–300 nm for 0 h of ultrasonication. The TEM images of Fig. 3-7 were also evidence of large aggregation of particles for 0 h of ultrasonication. The narrowest distribution was observed for 2 h of ultrasonication, which was approximately 70–168 nm. Even best dispersion and very few clusters were observed for in the TEM micrograph of Fig. 3-9 for 2 h of ultrasonication. The broadest distribution range was observed for 0 h and followed by 5 h of ultrasonication, which was approximately 92–300 nm and 42–210 nm, respectively. Because of the longest duration (5 h), a wide range of aggregation is created. Most agglomerations were broken down, but some small clusters could have coalesced again with prolonged ultrasonication (Kwak & Kim, 2005). [This paragraph is adapted from Mahbubul, Saidur, Amalina, and Niza (2016), copyright (2016), with permission from Elsevier.]

The effect of ultrasonication duration (with 50% amplitudes) on the average cluster size is reported in Fig. 3-27. Some more PSD results are presented here for some of the intermediate durations (e.g., 0.5, 1.5, 2.5, 3.5, and 4.5 h). It can be seen in Fig. 3-27 that the aggregated size decreased with increasing sonication time. The average cluster size rapidly decreased with the start of sonication. The aggregation of nanoparticles started to break down with the ultrasonication vibration. Initially, the decreasing rate of aggregation size was found to be higher. After a certain duration, the rate of decrease was lower. As the ultrasonication duration increases, the total amount of ultrasonication energy that the sample is subjected to

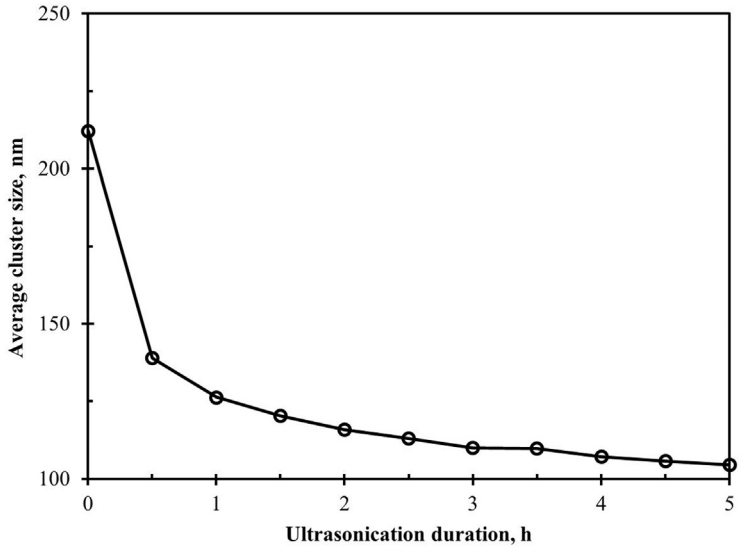

FIGURE 3-27 Average cluster sizes of Al_2O_3 nanoparticles after different durations of ultrasonication. *Adapted from Mahbubul I.M., Shahrul I.M., Khaleduzzaman S.S., Saidur R., Amalina M.A. and Turgut A. (2015). Experimental investigation on effect of ultrasonication duration on colloidal dispersion and thermophysical properties of alumina–water nanofluid,* International Journal of Heat and Mass Transfer 88, *73–81, copyright (2015), with permission from Elsevier.*

increases the total amount of energy delivered to the suspension. The average cluster size decreased from 212 nm (for 0 h, i.e., without ultrasonication) to 139 nm with 0.5 h of ultrasonication. However, with further ultrasonication, the average aggregate size was slowly decreased after 0.5 h of ultrasonication. For example, it was found to be 126 nm for 1 h of ultrasonication, yet it was 105 nm for 5 h of sonication. Therefore, during the first 1 h of ultrasonication, average cluster size decreased about 86 nm (from 212 to 126 nm) but after 1 h of ultrasonication by using 4 h of further ultrasonication (from 1 to 5 h) the aggregate size reduced only 21 nm (from 126 to 105 nm). [This paragraph is adapted from Mahbubul et al. (2015b), copyright (2015), with permission from Elsevier.]

Further, some literature results on the effect of ultrasonication duration on cluster sizes are combined and presented in Fig. 3-28. The results of Mahbubul et al. (2017), Sadeghi et al. (2015), and Mahbubul et al. (2014) are compared in Fig. 3-28. The results presented in Fig. 3-28 are indicative of a decrease of mean cluster sizes with ascending ultrasonication period. When the data are examined, it can be seen that the use of intense ultrasonic energy resulted in a more than twofold decrease in cluster size, by breaking down the nanoparticle aggregates. While an appreciable decrease of cluster sizes for ultrasonication durations up to 150 min can be seen in Fig. 3-28, no significant improvements were observed in cluster size decreases with longer ultrasonication durations (i.e., 180 min). It is also observed in Fig. 3-28 that cluster sizes sharply decreased right after the application of ultrasound energy. The tendency of the decrease in cluster size was greater in the beginning, in comparison to the latter parts of

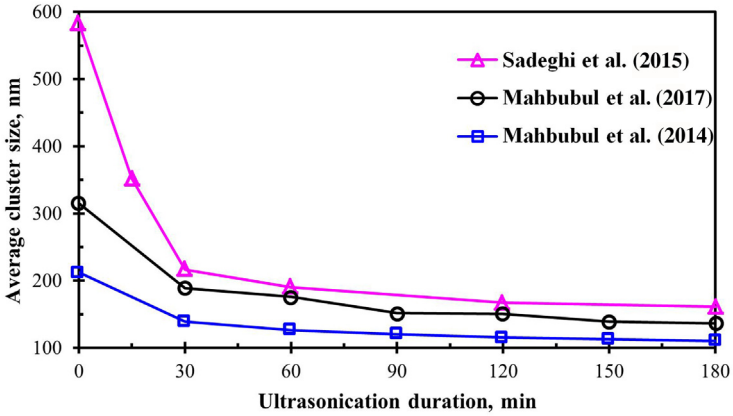

FIGURE 3-28 Average cluster sizes of nanoparticles after different periods of ultrasound treatment. *Adapted from Mahbubul, I. M., Elcioglu, E. B., Saidur, R., and Amalina, M. A. (2017). Optimization of ultrasonication period for better dispersion and stability of TiO_2–water nanofluid.* Ultrasonics Sonochemistry 37, *360–367, copyright (2017), with permission from Elsevier.*

ultrasonication period. The data of Mahbubul et al. (2017) and Mahbubul et al. (2014) had similar decreasing trends in cluster size rate with ultrasonication. However, Mahbubul et al. (2017) studied TiO_2–H_2O nanofluids and Mahbubul et al. (2014) studied Al_2O_3–H_2O nanofluids. During the first 30 min of ultrasonic treatment, the rate of decrease in average cluster size was the highest for the data in Sadeghi et al. (2015), compared to those of Mahbubul et al. (2014, 2017); in comparison to the latter parts of the ultrasonication period. The average cluster size data obtained in Sadeghi et al. (2015) were higher than those of the compared study. The reason behind this outcome is most probably due to the fact that the primary nanoparticle size in Sadeghi et al. (2015) was 25 nm, and nanoparticles might initially have a high level of agglomeration. Their achievable minimum cluster size was about 158 nm after 180 min of ultrasonication for Al_2O_3–H_2O nanofluid. Moreover, another possible reason for larger cluster sizes obtained by Sadeghi et al. (2015) could be the greater volume concentration of 1% considered, comparatively higher in comparison to 0.5 vol.% studied in Mahbubul et al. (2014, 2017). The data reported in Mahbubul et al. (2014) were the lowest sized compared to the data of Mahbubul et al. (2017) and Sadeghi et al. (2015). Mahbubul et al. (2014) reported 110 nm cluster size after 180 min of ultrasonication, while the primary nanoparticle size of their samples was 13 nm. Nevertheless, Nguyen et al. (2011) found 150 nm cluster size only after 180 s of ultrasonication and their primary size was 13 nm of the Al_2O_3 nanoparticles. It could be noted that the primary nanoparticle diameter was around 21 nm of TiO_2 nanoparticles in Mahbubul et al. (2017), according to the information provided by the manufacturer, and the cluster sizes collected were within the range of 167–315 nm after different ultrasonication durations. Chen et al. (2007) found a lowest aggregate size of $\sim$140 nm for TiO_2 nanoparticles, after 20 h of ultrasonication, where the primary particle size was 25 nm. Therefore, aggregate size depends more on initial primary size than the sonication power (Özcan-Taşkin

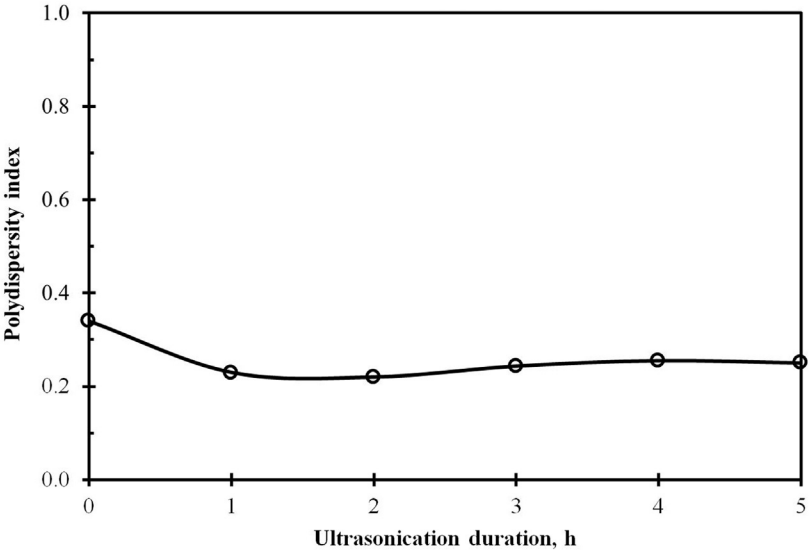

FIGURE 3-29 Polydispersity index of 0.5 vol.% of Al_2O_3−water nanofluid after varying ultrasonication durations.

et al., 2009). Also, the differences in the decreasing rates can be attributed to the effect of the nanoparticle (or cluster) material types, which may affect the tendency of the primary nanoparticles to form agglomerates, and break down to a mono-dispersed condition if previously agglomerated. [This paragraph is adapted from Mahbubul et al. (2017), copyright (2017), with permission from Elsevier.]

3.2.3 Polydispersity Index

The relation of ultrasonication durations on the polydispersity index (PDI) studied for 50% amplitude sonicator power and reported in Fig. 3-29. From Fig. 3-29, it can be seen that the highest PDI value was found to be 0.34 for the nanofluid prepared without ultrasonication (0 h). The PSD results of Fig. 3-26 also support this, as the range of cluster size for nanofluid prepared by 0 h of ultrasonication was 92−300 nm, which is the widest range among the results of Fig. 3-26. The TEM images of Fig. 3-7 also show that there were a large number of agglomerations exited in the nanofluid prepared with 0 h of ultrasonication. The results of average particle size reported in Fig. 3-13 also support this, as broad sizes (6−20 nm) of particles existed for 0 h of sonication. PDI was decreased with an increase of ultrasonication duration until 2 h and the lowest PDI value was found to be 0.22 for 2 h of ultrasonication. The distribution of cluster sizes reported in Fig. 3-26 also supports the above result. The cluster sizes of nanoparticles for 2 h of sonication were within the range of 119−150 nm, which is the smallest range of the results. The TEM images of Fig. 3-9 show that there were fewer clusters of particles in the nanofluid prepared by 2 h of ultrasonication. It could be

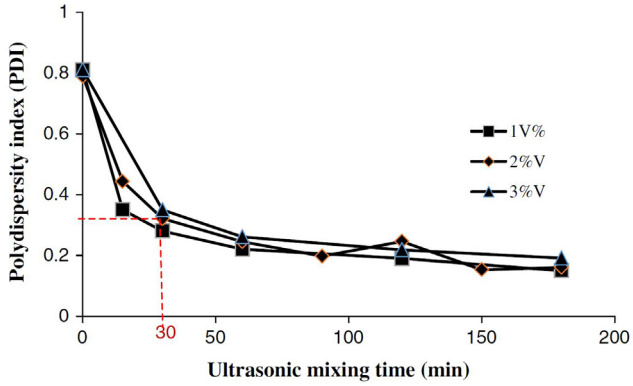

FIGURE 3-30 Effect of ultrasonication mixing on polydispersity index (PDI). *Reprinted by permission from Springer Nature, Sadeghi, R., Etemad, S. G., Keshavarzi, E., and Haghshenasfard, M. (2015). Investigation of alumina nanofluid stability by UV−vis spectrum.* Microfluidics and Nanofluidics 18*, 1023−1030, Copyright (2014), Springer-Verlag Berlin Heidelberg.*

noted that the lowest PDI value is close to the mono-disperse state. Further ultrasonication after 2 h showed that PDI was increased with sonication period. The results of Fig. 3-26 show that the range of the cluster sizes of nanoparticles were further increased after 2 h of ultrasonication. It is known that ultrasonication can break down the cluster, however; further agglomeration could be the result of prolonged ultrasonication (Taurozzi et al., 2012). Moreover, longer ultrasonication could re-agglomerate the nanoparticles again. A similar trend has also been reported in the literature (Kwak & Kim, 2005). However, in Fig. 3-29, the PDI values were within 0.25 for the ultrasonication period of 1−5 h. Sadeghi et al. (2015) stated that a suspension will be mono-disperse if the PDI value is lower than 0.3 and with a single peak in size distribution curve.

The PDI published results of Sadeghi et al. (2015) are portrayed in Fig. 3-30. They found that PDI of Al_2O_3 nanoparticles was decreased with an increase in the sonication period. They reported a rapid decrement of PDI with the start of ultrasonication until 15 min, after which PDI decreased slowly and after 3 h of ultrasonication, the PDI became approximately 0.15. According to Fig. 3-30, PDI equals 0.3 when the ultrasonication period is 30 min. They concluded that to obtain a mono-disperse solution, at least 30 min of ultrasonication is required. Furthermore, it is clear in Fig. 3-30 that the concentrations (1, 2, and 3 vol.%) of nanofluid do not have a remarkable effect on PDI (Sadeghi et al., 2015).

3.2.4 Zeta Potential

Zeta potential was measured for each sample to quantify the stability of the nanofluid. Sadeghi et al. (2015) stated that, in general, zeta potential is the best method to evaluate the dispersion characteristics of nanofluids and nanoparticle behavior, although it is more expensive in comparison to other techniques. The zeta potential of the 0.5 vol.% of Al_2O_3−water nanofluid has been investigated for 1, 2, 3, 4, and 5 h of ultrasonication and

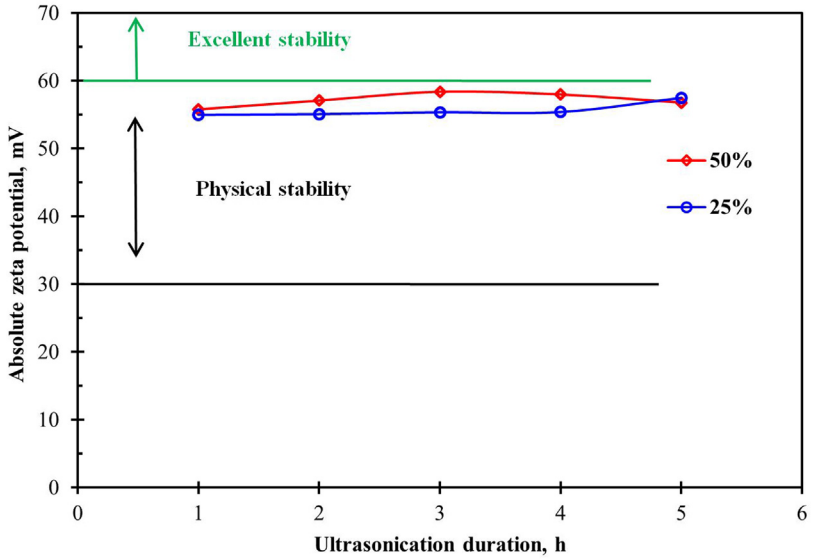

FIGURE 3-31 Absolute zeta potential of Al_2O_3–water nanofluid after varying ultrasonication durations, at 25% and 50% amplitudes. *Reprinted from Mahbubul, I. M., Saidur, R., Amalina, M. A., Elcioglu, E. B., and Okutucu-Ozyurt, T. (2015). Effective ultrasonication process for better colloidal dispersion of nanofluid.* Ultrasonics Sonochemistry 26*, 361–369, copyright (2015), with permission from Elsevier.*

with 25% and 50% sonicator amplitudes. The results are illustrated in Fig. 3-31, together with the limits of the excellent and physical stability (Müller, 1996). As is apparent in Fig. 3-31, the zeta potential of the sample is always lying on the maximum limit of the physical stability and is approaching excellent stability. The highest zeta potential value 58.4 mV was observed for 3 h of ultrasonication with 50% amplitude of power and further sonication until 5 h could not increase the value. In the case of 25% amplitude, the zeta potential value was slowly increased until 5 h of sonication and the highest value was 57.5 mV at this ultrasonication period. The nanoparticles usually tend to agglomerate over time because of interparticle adhesion forces. The ultrasonication techniques affect the surface and structure of nanoparticles (act as repulsive forces) and prevent the agglomeration of particles to achieve stable nanofluids (Ghadimi et al., 2011). At higher ultrasonication, nanoparticles overcome the adhesion forces and higher zeta potential was observed. As a result of the zeta potential analyses, it could be predicted that with 50% amplitude, the nanoparticles received highest ultrasound energy at 3 h of duration. However, in the case of 25% amplitude, the ultrasound energy was effective until the 5 h period. Very similar types of trends were also observed in TEM microstructures of Figs. 3-8–3-12, where nanoparticles ultrasonicated with 25% amplitudes were not properly homogenized due to the lack of sufficient sonication power. Again, the result of average particle size after each ultrasonication reported in Fig. 3-19 shows that particle sizes were not changed after 3 h of ultrasonication (with 50% amplitudes). It can be predicted that for longer ultrasonication durations with 25% amplitudes, the zeta potential

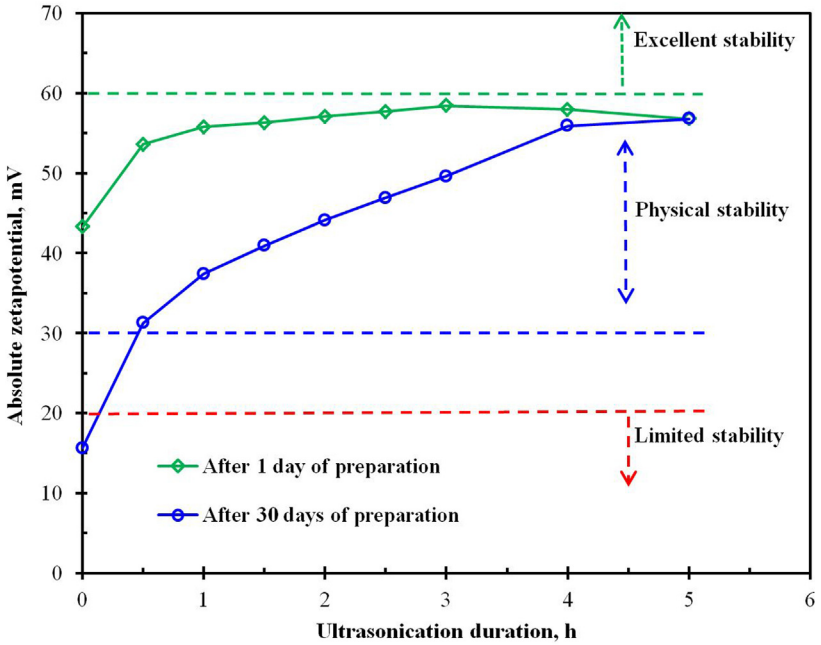

FIGURE 3-32 Absolute zeta potential of Al_2O_3–water nanofluid after varying ultrasonication durations. *Reprinted from Mahbubul I.M., Shahrul I.M., Khaleduzzaman S.S., Saidur R., Amalina M.A. and Turgut A. (2015). Experimental investigation on effect of ultrasonication duration on colloidal dispersion and thermophysical properties of alumina–water nanofluid,* International Journal of Heat and Mass Transfer 88, *73–81, copyright (2015), with permission from Elsevier.*

value can increase and may shift to the excellent stability range. [This paragraph is adapted from Mahbubul et al. (2015a), copyright (2015), with permission from Elsevier.]

As the highest zeta potential was found to be 58.4 mV for 3 h of ultrasonication with 50% amplitude of sonicator power, therefore, a more intermediate duration of under 3 h of ultrasonication was considered for analysis to investigate where the peak value of zeta potential is. The zeta potential values of 0, 0.5, 1, 1.5, 2, 2.5, 3, 4, and 5 h of ultrasonication are shown in Fig. 3-32. Again, the absolute zeta potential value was found to be increased according to the ultrasonication duration up to 3 h, as seen in Fig. 3-32. With the starting of ultrasonication, zeta potential increases to a higher value and with further ultrasonication it rises slowly (Mahbubul et al., 2014). Here, the highest zeta potential value is the same as observed in Fig. 3-31, that is 58.4 mV for 3 h of ultrasonication. Kwak and Kim (2005) found the highest absolute zeta potential value about 50 mV for 9 h of ultrasonication, whereas further ultrasonication until 30 h did not increase the value. Lee et al. (2008) ultrasonicated Al_2O_3 nanoparticles in water for durations of 0, 5, 20, and 30 h. It was found that the ultrasonication duration of $\sim$5 h gave the best result, with about 34.5 mV zeta potential (as shown in Fig. 3-33). They observed that with further ultrasonication over 5 h, the zeta potential was decreased (Mahbubul et al., 2015b).

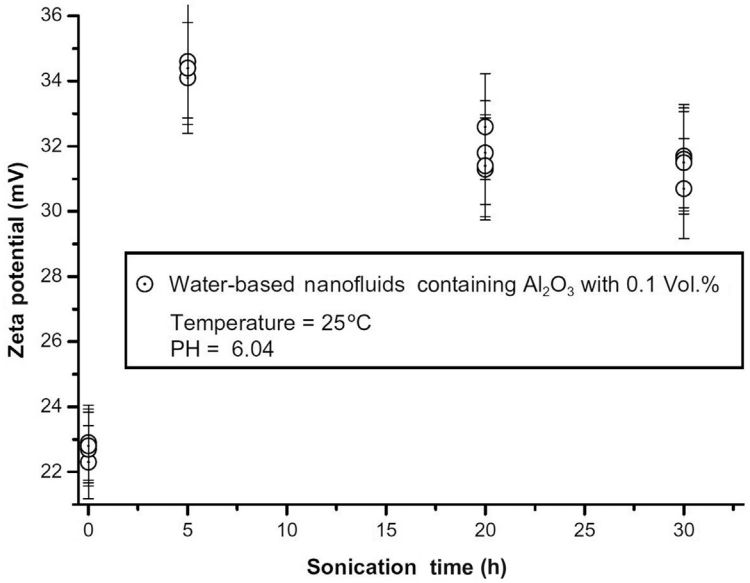

FIGURE 3-33 Effect of sonication time (h) on zeta potential of the Al_2O_3 nanoparticles dispersed in water. *Reprinted from Lee, J., Hwang, K., Jang, S., Lee, B., Kim, J., Choi, S., and Choi, C. (2008). Effective viscosities and thermal conductivities of aqueous nanofluids containing low volume concentrations of Al_2O_3 nanoparticles.* International Journal of Heat and Mass Transfer 51*, 2651–2656, copyright (2007), with permission from Elsevier.*

In Fig. 3-32, a comparison is drawn between the zeta potential values of samples on 1 day and 30 days of preparation. It was found that by 30 days from preparation, the zeta potential values of the nanofluids were decreased based on the used ultrasonication period during preparation. The difference in zeta potential values between 1 day and 30 days were found to be higher for the samples prepared with a lower ultrasonication duration. Thirty days after preparation, the absolute value was found to be 15 mV for the sample prepared without ultrasonication (termed as 0 h), which was 44.3 mV after 1 day of preparation. The zeta potential value was not changed for the nanofluid prepared by 5 h of ultrasonication even after 30 days of preparation. After 30 days of preparation, the absolute zeta potential value was found to be 56.8 mV for the sample prepared with an ultrasonication duration of 5 h, that is the same value observed after 1 day of preparation with this period of sonication. In the case of nanofluid prepared by 4 h of ultrasonication, the zeta potential was changed only a little, about 2.1 mV, in comparison to the values after 1 day and 30 days from preparation. Therefore, longer ultrasonication durations increased the stability of the nanofluid (Mahbubul et al., 2014). It was pronounced that absolute zeta potential values over 60 mV indicate excellent stability, those above 30 mV indicate physical stability, those below 20 mV indicate limited stability, and those lower than 5 mV are evidence of agglomeration (Mahbubul et al., 2014; Müller, 1996). Hence, the electro-dynamic stability of the samples prepared by 4 h and higher ultrasonication durations could be considered as outstanding

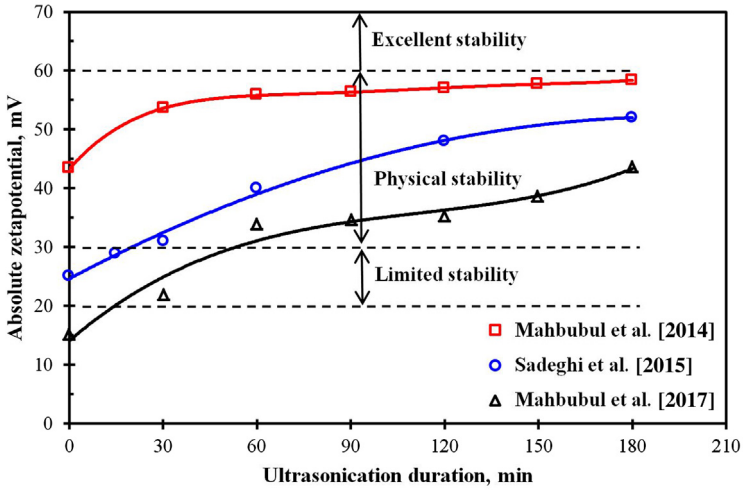

FIGURE 3-34 Absolute zeta potentials of nanofluids after different periods of ultrasound treatment. *Adapted from Mahbubul, I. M., Elcioglu, E. B., Saidur, R., and Amalina, M. A. (2017). Optimization of ultrasonication period for better dispersion and stability of TiO_2–water nanofluid.* Ultrasonics Sonochemistry 37, *360–367, copyright (2017), with permission from Elsevier.*

(Mahbubul et al., 2015b). [This paragraph is adapted with permission from Mahbubul et al. (2014). Copyright (2014) American Chemical Society.]

Furthermore, some experimental published results of absolute zeta potential values for different ultrasonication durations are compared and plotted in Fig. 3-34, along with the limited stability, physical stability, and excellent stability ranges (Müller, 1996). The behavior of the data presented in Fig. 3-34 shows that in comparison to the cases in which the samples were ultrasonicated to some extent, nanoparticles in the sample without ultrasonication were more prone to form agglomerates. This deduction is due to the fact that the larger the absolute value of the zeta potential, the greater the repulsive charges of nanoparticles and suspension stability (Xian-Ju, Hai, Xin-Fang, Zhou-Fei, & Fang, 2011). After 60 min ultrasonication, absolute zeta potentials of all the studies became greater than 30 mV, yielding a stable suspension (Müller, 1996), in a general sense (Turgut, Tavman, Cetin, Chirtoc, & Fudym, 2011). Fig. 3-34 shows that the zeta potential was increasing until 180 min of ultrasonication and can possibly increase further after 180 min of ultrasonication. If the trend in Fig. 3-34 is extrapolated, it can be forecasted that for longer durations of ultrasonication, the zeta potential could reach the excellent stability level. However, further ultrasonication could result in the coalescence of the nanoparticles again, as reported in Kwak and Kim (2005) and Mahbubul et al. (2014). Also, there are chances of erosion of ultrasonication tip for the prolonged ultrasonication, as indicated in Chang and Lin (2007). Comparison of the zeta potential data in Fig. 3-34 shows that zeta potential data of Mahbubul et al. (2014) nearly reaches its highest limit and almost saturates after 60 min of ultrasonication. However, the zeta potential data of Mahbubul et al. (2017) and Sadeghi et al. (2015) were found to be

continuously improved with increasing ultrasonication period. The zeta potential data of Mahbubul et al. (2014) were the highest, and this tendency can be attributed to the comparatively smaller primary particle size of Al_2O_3 nanoparticles (13 nm), which also may affect average cluster sizes (as shown in Fig. 3-28, for comparison). It could be noted that the primary particle size of Sadeghi et al. (2015) was 25 nm and that was 21 nm in Mahbubul et al. (2017). It was mentioned that in Mahbubul et al. (2014) and Sadeghi et al. (2015), zeta potential measurements were performed right after the sample preparation, while in Mahbubul et al. (2017), zeta potential measurements were conducted 6 days after the nanofluid preparation. Zeta potential is a time-dependent property and with time, the colloidal stability of nanofluids generally gets worse, and zeta potential values diminish consequently (as shown in Fig. 3-32). The time-dependent nature of zeta potential may be one reason behind the comparatively low zeta potential values observed in Mahbubul et al. (2017), in comparison to those in Mahbubul et al. (2014) and Sadeghi et al. (2015). The other reason may be the greater hydrophilic nature of Al_2O_3 ceramic when compared to TiO_2 ceramic, as indicated in Santos et al. (2003) since the base fluid was the same (H_2O) in all cases. [This paragraph is adapted from Mahbubul et al. (2017), copyright (2017), with permission from Elsevier.]

Unlike other studies, Asadi, Asadi, Siahmargoi, Asadi, and Gholami Andarati (2017) observed decreasing zeta potential with increasing ultrasonication duration after 7 and 30 days of sample preparation, as shown in Fig. 3-35. They measured zeta potential of 0.8% Mg $(OH)_2$−water nanofluid prepared by using ultrasonication durations of 30, 50, 80, and

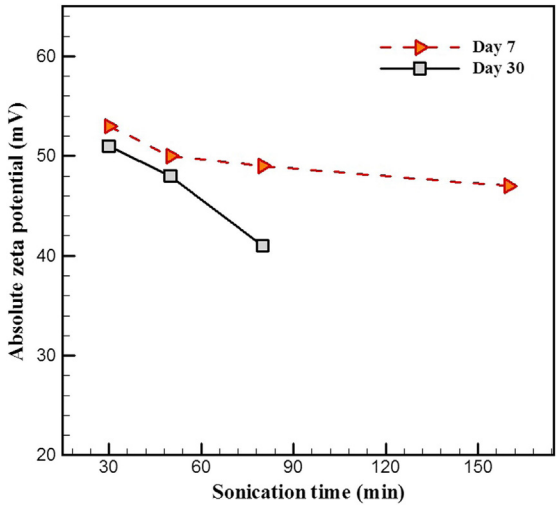

FIGURE 3-35 Zeta potential of $Mg(OH)_2$−water nanofluid versus sonication time and at the solid concentration of 0.8%. *Reprinted from Asadi, A., Asadi, M., Siahmargoi, M., Asadi, T., and Gholami Andarati, M. (2017). The effect of surfactant and sonication time on the stability and thermal conductivity of water-based nanofluid containing $Mg(OH)_2$ nanoparticles: An experimental investigation.* International Journal of Heat and Mass Transfer 108, *191−198, copyright (2016), with permission from Elsevier.*

160 min. It can be seen in Fig. 3-35 that the best zeta potential values are 53 and 51 mV on the 7th and 30th days, respectively for the nanofluid prepared by 30 min of ulltrasonication. It can be summarized from Fig. 3-35 that 30 min of ultrasonication is the optimum duration in the presence of a surfactant and further ultrasonication leads to deteriorating the nanofluid's stability (Asadi et al., 2017).

3.2.5 Other Characterization Techniques

Other than investigating the microstructure, aggregation, polydispersity, and zeta potential; absorption and sedimentation analyses are also used to determine the stability of a dispersion. Ultraviolet-visible (UV-vis) spectroscopy is used for absorption analysis (related to the stability of a suspension) and sedimentation could be determined by sediment photograph capturing method and sedimentation balance method.

3.2.5.1 UV-vis Spectroscopy

Ultraviolet−visible spectrophotometer (UV−Vis) measurements are used to quantitatively characterize the colloidal stability of the dispersions. One of the most striking features of this apparatus is its applicability for all base fluids, whereas zeta potential analysis has restrictions for the viscosity of the host fluid. A UV−vis spectrophotometer exploits the fact that the intensity of light becomes different by absorption and scattering of light passing through a fluid. At 200−900 nm wavelength, the UV−vis spectrophotometer measures the absorption of liquid and is used to analyze various dispersions in the fluid (Lee et al., 2009). Typically, suspension stability is resolved by measuring the sediment volume versus the sediment time. However, this method is unsuitable for nanofluid dispersions with a high concentration, and especially for CNT solutions. These dispersions are too dark to differentiate the sediment visibly. Jiang, Gao, and Sun (2003) were the first investigators who proposed sedimentation estimation using a UV−vis spectrophotometer for nanosuspensions. In this method, the first step is to find the peak absorbance of the dispersed nanoparticles in very dilute suspensions by scanning. As the concentration of suspension has a linear relation with absorbance, preparing a standard to fit a linear relation to at least three different dilute concentrations (0.01%−0.03%) will be the next step in this method. Relative stability measurement will be followed by preparing the desired concentration of nanofluid and putting it aside for a couple of days. Whenever it is needed to check the relative stability, the supernatant concentration will be measured by a UV−vis spectrophotometer and the concentration can be plotted against time. This method was used in Hwang et al. (2007), Kim, Choi, and Kim (2006), and Lee et al. (2009). There also exists a summary from different nanofluid peak absorptions by UV−vis spectrophotometer in Table 3-4. According to Mie's theory (Kreibig & Genzel, 1985), the surface plasmon absorption and the plasmon bandwidth are dependent on the size of metallic particles in the solution. Consequently, the peak value represents the most populated nanoparticle size in the solution. Additionally, by increasing the particle size, especially those smaller than 20 nm, the bandwidth decreases. Contrarily, the bandwidth of the surface plasmon for the particles larger than 20 nm increases with particle size (Kreibig & Vollmer, 1995; Link & El-Sayed, 2003). As the

Table 3-4 Summary of Different Nanofluids Peak Absorption Measured by UV−vis Spectrophotometer

Nanoparticle	Base Fluid	Peak Wavelength (nm)	Investigator
MWCNT and fullerene	Oil	397	Hwang et al. (2007)
Aligned CNT	Distilled water	210	Liu, Ma, and Cui (2008)
CNT	Distilled water	253	Jiang et al. (2003)
TiO_2	Deionized water	280−400	Chang, Jwo, Fan, and Pai (2007)
Cu	Deionized water	270	Chang, Wu, Chen, and Kao (2000)
CuO	Deionized water	268	Chang et al. (2000)
Ag	Water	410	Sato et al. (2011)

Source: Adapted from Ghadimi, A., Saidur, R., and Metselaar, H.S.C. (2011). A review of nanofluid stability properties and characterization in stationary conditions. International Journal of Heat and Mass Transfer 54, 4051−4068, copyright (2011), with permission from Elsevier.

Table 3-5 Volumes of Gold Nanofluid in Different Synthesis Conditions

Condition	Base Fluid	Na_3 Citrate (ml)	Tannic Acid (ml)	$HAuCl_4$ (ml)	Particle Size (nm)	Peak Wavelength (nm)
A	Deionized water	0.2	2.5	3	21.3	528
B	Deionized water	0.2	5	6	43.7	530.5
C	Deionized water	3	0.1	1	8	568.5
E	Deionized water	3	2.5	6	9.3	647
G	Deionized water	3	0.1	3	15.6	721.5

Source: Adapted from Tsai, C.Y., Chien, H.T., Ding, P.P., Chan, B., Luh, T.Y., and Chen, P.H. (2004). Effect of structural character of gold nanoparticles in nanofluid on heat pipe thermal performance. Materials Letters 58, 1461−1465, copyright (2003); and from Ghadimi, A., Saidur, R., and Metselaar, H.S.C. (2011). A review of nanofluid stability properties and characterization in stationary conditions. *International Journal of Heat and Mass Transfer 54*, 4051−4068, copyright (2011), with permission from Elsevier.

particle size increases, the local peak in the UV−vis spectra shifts towards a longer wavelength (Tsai et al., 2004). Tsai et al. (2004) have conducted a series of tests on this theory. The sizes of Au nanoparticles from different preparation methods measured by TEM and peak wavelength are summarized in Table 3-5. [This paragraph is adapted from Ghadimi et al. (2011), copyright (2011), with permission from Elsevier.]

Ghadimi and Metselaar (2013) analyzed stability of nanofluid by using UV-vis spectroscopy. The experiments were conducted using 0.1 wt.% TiO_2−distilled water nanofluid. The samples were prepared in three groups. The groups include samples with surfactant (SDS as an anionic surfactant), sonicated by an ultrasonic horn for 15 min, and sonicated by an ultrasonic bath for 3 h. Fig. 3-36 shows the UV-vis scan (absorbance curve) of the TiO_2−distilled

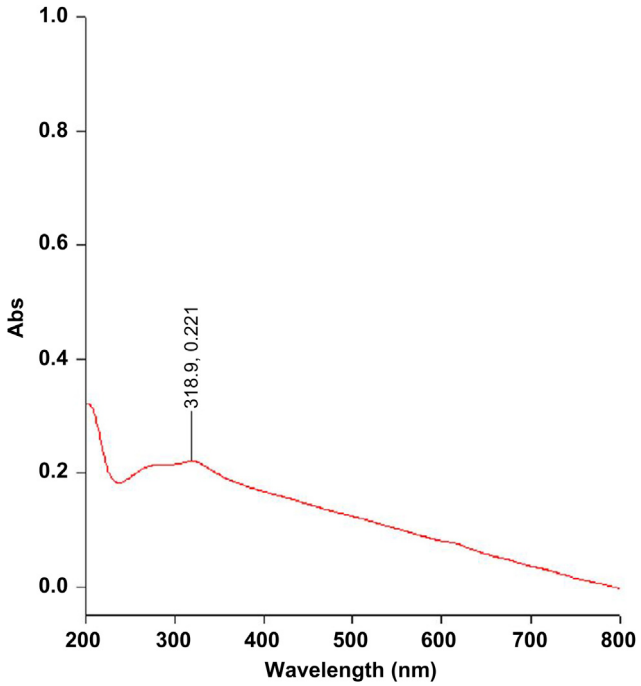

FIGURE 3-36 UV−vis spectrophotometer for TiO_2 nanofluid with 25 nm average diameter directly after preparation. *Reprinted from Ghadimi, A., and Metselaar, I.H. (2013). The influence of surfactant and ultrasonic processing on improvement of stability, thermal conductivity and viscosity of titania nanofluid. Experimental Thermal and Fluid Science 51, 1−9, copyright (2013), with permission from Elsevier.*

water nanofluid. Based on the suggestion of Habibzadeh et al. (2010), a standard preparation method should be a diluted suspension of around (0.01−0.02 wt.%) so that a UV-vis spectrophotometer can detect the wavelengths. Therefore, a diluted concentration of TiO_2−distilled water nanofluid between 0.007−0.012 wt.% was considered in Ghadimi and Metselaar (2013). A linear calibration curve was constructed at a wavelength of 320 nm, as shown in Fig. 3-37, which is also called the concentration (standard) graph. The six prepared samples were monitored by UV sedimentation method as shown in Fig. 3-38. This graph demonstrates the relative concentrations of the six samples (as introduced in Table 3-6) in the elapsed time of 7 days. Nanofluid sample without ultrasonic processing and surfactant would sediment the fastest (T1 and T2). As can be seen in Fig. 3-38, the measurement after 2 days shows very little concentration, which confirms the unstable condition of this simple mixture. Although this method has the lowest rate of precipitation, its low concentration makes it unappealing as a target. Comparing T1, T3, and T5 reveals that (Fig. 3-38) 15 min ultrasonic horn would not have a proper influence on absorbance as it has the lowest concentration rate due to the UV−vis spectrophotometer results. Conversely, suspensions with surfactant had better concentration and relative stability. However, it is evident that the impact of

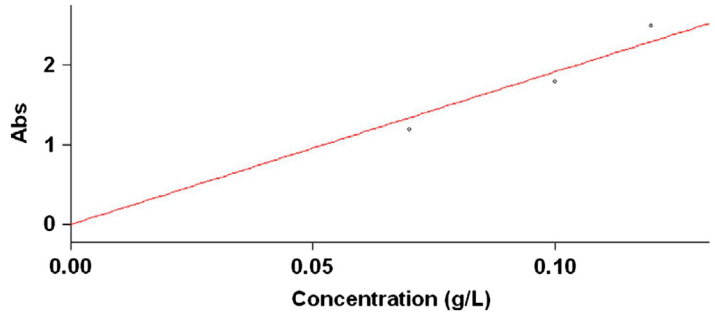

FIGURE 3-37 Standard graph of calibration at wavelength of 320 nm for titanium dioxide nanofluid shortly after preparation. *Reprinted from Ghadimi, A., and Metselaar, I.H. (2013). The influence of surfactant and ultrasonic processing on improvement of stability, thermal conductivity and viscosity of titania nanofluid.* Experimental Thermal and Fluid Science 51, *1–9, copyright (2013), with permission from Elsevier.*

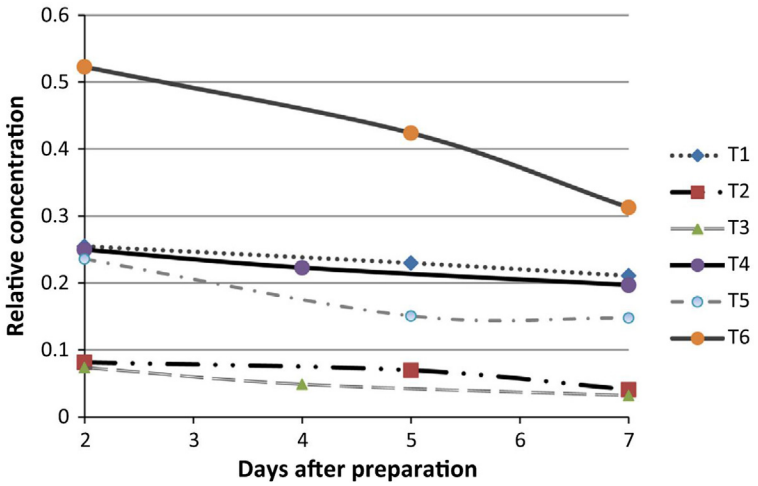

FIGURE 3-38 Sedimentation rate for six prepared samples within 7 days after preparation. Note: the abbreviations in Fig. 3-38 are explained in Table 3-6. *Reprinted from Ghadimi, A., and Metselaar, I.H. (2013). The influence of surfactant and ultrasonic processing on improvement of stability, thermal conductivity and viscosity of titania nanofluid.* Experimental Thermal and Fluid Science 51, *1–9, copyright (2013), with permission from Elsevier.*

15 min ultrasonic horn is more than an unprocessed nanofluid. The best relative concentration of nanofluid comparing with the fresh one is for T6, although the slope of the sedimentation rate is steep and it is possible to have a clear nanofluid after 1 month. As a result, surfactant addition to the nanofluid shows a very effective influence on the stability of nanofluid. The rate of sedimentation is different among these six samples as different techniques are imposed. This rate is changing as the lowest precipitation rate appears from 17% by the first sample (T1) to the highest of 56% by the third one (T3). [This paragraph is adapted from Ghadimi and Metselaar (2013), copyright (2013), with permission from Elsevier.]

Table 3-6 Different Homogenization Methods for Preparing the Samples

Sample	Homogenization Technique
T1	0.1 wt.% TiO_2, a simple mixture
T2	0.1 wt.% SDS and TiO_2, a simple mixture
T3	0.1 wt.% TiO_2 prepared by 15 min ultrasonic horn
T4	0.1 wt.% TiO_2 and SDS prepared by 15 min ultrasonic horn
T5	0.1 wt.% TiO_2 prepared by 3 h ultrasonic bath
T6	0.1 wt.% TiO_2 and SDS prepared by 3 h ultrasonic bath

Source: Reprinted from Ghadimi, A., and Metselaar, I.H. (2013). The influence of surfactant and ultrasonic processing on improvement of stability, thermal conductivity and viscosity of titania nanofluid. *Experimental Thermal and Fluid Science 51*, 1–9, copyright (2013), with permission from Elsevier.

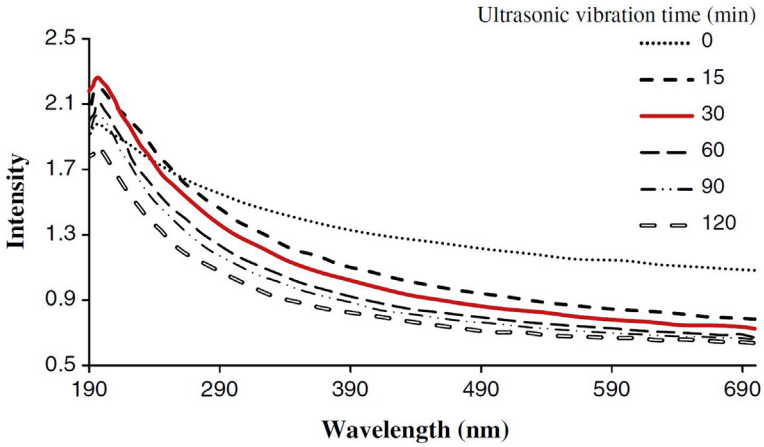

FIGURE 3-39 Effect of ultrasonic time on UV absorbency (concentration of nanofluid is 2%). *Reprinted by permission from Springer Nature, Sadeghi, R., Etemad, S. G., Keshavarzi, E., and Haghshenasfard, M. (2015). Investigation of alumina nanofluid stability by UV–vis spectrum.* Microfluidics and Nanofluidics 18*, 1023–1030, Copyright (2014), Springer-Verlag Berlin Heidelberg.*

Sadeghi et al. (2015) conducted several experiments using 2 vol.% concentration of Al_2O_3–water nanofluid to study the effect of ultrasonic mixing time on UV absorbency. The results are shown in Fig. 3-39, where the UV–vis spectrum is plotted for various ultrasonic mixing times. It is found that maximum absorbency occurs in the wavelength of 195 nm. By increasing the ultrasonic mixing time from 0 to 30 min, the maximum absorbency increases, then for a time longer than 30 min, this value decreases. Also, the wavelength of the maximum absorption (195 nm) is constant. Fig. 3-40 presents maximum absorbency plotted versus ultrasonic mixing times in nanofluids with concentrations of 1%, 2%, and 3% by volume. The trend of absorbency versus mixing time is similar to Fig. 3-39. It shows that for 150 min

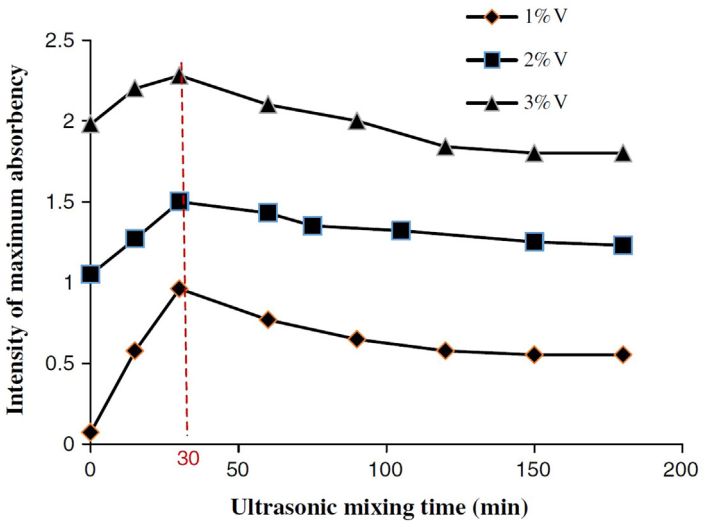

FIGURE 3-40 Effect of ultrasonic mixing on maximum UV absorbency for different volume concentrations. *Reprinted by permission from Springer Nature, Sadeghi, R., Etemad, S. G., Keshavarzi, E., and Haghshenasfard, M. (2015). Investigation of alumina nanofluid stability by UV−vis spectrum.* Microfluidics and Nanofluidics 18, *1023−1030, Copyright (2014), Springer-Verlag Berlin Heidelberg.*

of ultrasonic mixing time, maximum absorbency does not change; therefore, this time is considered as an optimum mixing ultrasonic time. It can be seen that maximum absorbency increases by increasing the nanofluid concentration. The maximum absorbency for 30 min mixing time for nanofluid with 3 vol.% concentration is higher than those of other concentrations. [This paragraph is adapted by permission from Springer Nature (Sadeghi et al., 2015), Copyright (2014), Springer-Verlag Berlin Heidelberg.]

3.2.5.2 Sediment Photograph Capturing

This method (photo analysis) is a qualitative analysis and is considered to be a primary method to get an idea of sedimentation and by this method the exact quantity of sedimentation could not be measured. Some amounts of nanofluid are put into a clear bottle/container immediately after the preparation of the sample and kept aside in a stationary condition. Photos are captured after certain durations of time and photos are compared to analyze sedimentation of the suspension. Although it is a simple method, it has some disadvantages like long waiting time to study nanofluid stability, moreover, particle clustering information cannot be found by this method (Sadeghi et al., 2015).

Mahbubul et al. (2014) applied up to 180 min of ultrasonication duration to prepare Al_2O_3−water nanofluid. Sedimentation of the prepared samples was recorded at 30 days after preparation by a photo-capturing method as shown in Fig. 3-41. A thick layer of sedimentation is formed at the bottom of the nanofluid without ultrasonication (0 min), as shown in Fig. 3-41A. However, for the nanofluids prepared by the ultrasonication process, the amount

FIGURE 3-41 The Al_2O_3—water nanofluids after 30 days of preparation, prepared with ultrasonication durations of (A) 0, (B) 30, (C) 60, (D) 90, (E) 120, (F) 150, and (G) 180 min. *Reprinted with permission from Mahbubul, I. M., Chong, T. H., Khaleduzzaman, S. S., Shahrul, I. M., Saidur, R., Long, B. D., and Amalina, M. A. (2014). Effect of Ultrasonication Duration on Colloidal Structure and Viscosity of Alumina—Water Nanofluid.* Industrial & Engineering Chemistry Research 53, *6677—6684. Copyright (2014) American Chemical Society.*

of sedimentation was found to be negligible, as shown in Fig. 3-41B—G. Supernatant levels are marked in Fig. 3-41, though it is very difficult to find the exact level. The supernatant level was found to be higher in Fig. 3-41A, which proves the higher sedimentation of particles. Fig. 3-41B and C shows a very small amount of supernatant level, whereas in Fig. 3-41D—G, no supernatant has been observed. This indicates that the stability of the nanofluid increased with increasing ultrasonication duration. Therefore, the stability of the nanofluids can be improved by the increase of ultrasonication duration during the preparation of nanofluids. [This paragraph is adapted with permission from Mahbubul et al. (2014). Copyright (2014) American Chemical Society.]

Shahrul, Mahbubul, Saidur, and Sabri (2016) prepared 0.5 vol.% of SiO_2—water nanofluid by 90 min of ultrasonication. Photos of the samples (inside a narrow and small measuring beaker of 10 ml) were captured just after preparation and every week afterwards for a month. The results are shown in Fig. 3-42. It can be seen in Fig. 3-42 that SiO_2—water nanofluid was stable until the second week after the preparation of the nanofluid since there is no supernatant observed. Sedimentation was started from the third week after preparation as the supernatant level was increased, as can be seen in Fig. 3-42C and D.

3.2.5.3 Sedimentation Balance Method

The stability of the nano-suspension can also be measured by another method called sedimentation balance. The tray of a sedimentation balance is immersed in a fresh nano-suspension. The weight of sediment nanoparticles during a certain period of time is measured. The suspension fraction (F_s) of nanoparticles at an acceptable time is calculated by the formula $F_s = (W_o - W)/W_o$ in which W_o is the total weight of all nanoparticles in

FIGURE 3-42 SiO_2—water nanofluid (A) just after preparation, (B) in week 2, (C) in week 3, and (D) in week 4. *Reprinted from Shahrul, I.M., Mahbubul, I.M., Saidur, R., and Sabri, M.F.M. (2016). Experimental investigation on Al_2O_3—W, SiO_2—W and ZnO—W nanofluids and their application in a shell and tube heat exchanger. International Journal of Heat and Mass Transfer 97, 547—558, copyright (2016), with permission from Elsevier.*

the measured space and W is the weight of the sediment nanoparticles at a certain time (Zhu et al., 2007). [This paragraph is adapted from Ghadimi et al. (2011), copyright (2011), with permission from Elsevier.]

Zhu et al. (2007) studied the stability of graphite suspension for the influence of polyvinylpyrrolidone (PVP) concentration by using the above method and the results are portrayed in Fig. 3-43. It can be seen in Fig. 3-43 that when the PVP concentration is less than 0.35 wt.%, the stability of the graphite suspension is improved with the increase in PVP. When the PVP concentration is higher than 0.35 wt.%, the stability does not show further improvement. When the PVP concentration is lower, with the increase of PVP, the surface of the graphite particles is gradually coated by PVP molecules. The increasing steric effect of PVP improves the stability of the graphite suspension. When the PVP concentration is 0.35—0.6 wt.%, probably all the particles were fully coated by PVP, resulting in the highest stability. [This paragraph is adapted from Zhu et al. (2007), copyright (2006), with permission Elsevier.]

3.2.5.4 Sedimentation From Real-Time Density Measurement

Lee, Han, and Koo (2014) introduced a new method to track the temporal changes of the particle volume fraction that will quantitatively analyze the stability of a dispersion. They considered different nanofluid systems (Al_2O_3—water, SiO_2—water, Ag—water, Al_2O_3—EG, ZnO—EG). The stability of the samples was evaluated using a hydrometer to measure the nanoparticle concentration and sedimentation using Eq. (3.1).

$$\varphi = \frac{\rho_n - \rho_f}{\rho_p - \rho_f} \tag{3.1}$$

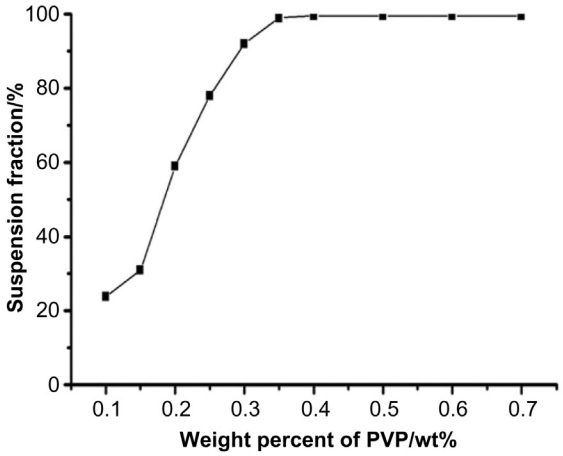

FIGURE 3-43 Stability of graphite suspension at different PVP concentrations (sedimentation for 3 weeks, pH = 9.5). *Reprinted from Zhu, H., Zhang, C., Tang, Y., Wang, J., Ren, B., and Yin, Y. (2007). Preparation and thermal conductivity of suspensions of graphite nanoparticles.* Carbon 45*, 226–228, copyright (2006), with permission from Elsevier.*

where, φ is the volume concentration of the nanofluid, ρ_n is the density of the nanofluid, ρ_f is the density of the base fluid, and ρ_p is the particle density.

The samples were prepared both by one-step (Ag–water and ZnO–EG) and two-step (Al_2O_3–water, SiO_2–water, and Al_2O_3–EG) methods. The researchers measured nanoparticle sedimentation for 31 days and, except for the Ag–water nanofluid (for which a slight decrease was observed), all samples experienced a decrease of nanoparticle fraction due to sedimentation, as shown in Fig. 3-44.

3.2.6 Impact of Prolonged Ultrasonication

From the above analyses, it can be concluded that ultrasonication is necessary for proper dispersion of nanofluids. However, excessive ultrasonication is a waste of time and energy. In most cases, prolonged ultrasonication could not give better performance. However, in some cases, it was observed that the results of prolonged ultrasonication were better; but, the ratio of improvement during the later period of ultrasonication is negligible in comparison to the improvement observed during the initial period of ultrasonication. Moreover, erosion of ultrasonic tip and re-agglomeration of nanoparticles are the consequence of prolonged ultrasonication. One further example and precaution are described here.

The images of fresh Al_2O_3–water nanofluid prepared by different ultrasonication durations are shown in Fig. 3-45. From Fig. 3-45, it is clear that the colors of nanofluids were darker with an increase in the ultrasonication duration. The possible reason could be due to the erosion of the ultrasonication tip along with the effect of particle–particle friction, heat, and many others.

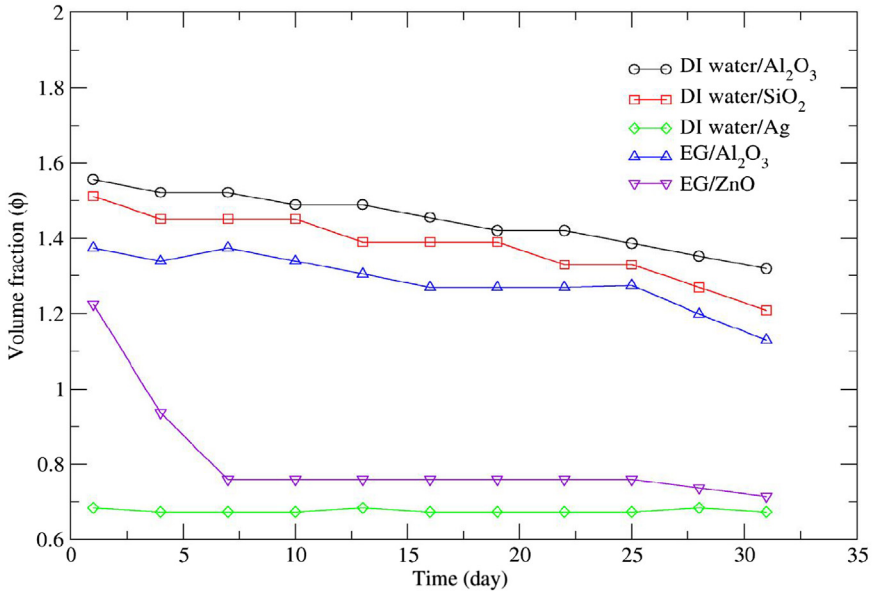

FIGURE 3-44 Volume concentration change of various nanofluids with the elapse of time. *Reprinted from Lee, J., Han, K., and Koo, J. (2014). A novel method to evaluate dispersion stability of nanofluids.* International Journal of Heat and Mass Transfer 70*, 421–429, copyright (2013), with permission from Elsevier.*

FIGURE 3-45 Fresh Al_2O_3–water nanofluid prepared by different ultrasonication durations.

3.3 Surfactant

This is one of the general methods to avoid sedimentation of nanoparticles. The addition of surfactant can improve the stability of nanoparticles in aqueous suspensions. The reason is that the hydrophobic surfaces of nanoparticles/nanotubes are modified to become

hydrophilic and vice versa for nonaqueous liquids. A repulsion force between suspended particles is caused by the zeta potential, which will rise due to the surface charge of the particles suspended in the base fluid (Huang et al., 2009; Hwang et al., 2007). However, care should be taken to apply enough surfactant as inadequate surfactant cannot give sufficient coating to persuade electrostatic repulsion and compensate for van der Waals attraction (Jiang et al., 2003). The effect of surfactant on aggregated particle size distribution can be demonstrated as shown in Fig. 3-46. Popular surfactants that have been used in the literature can be listed as sodium dodecyl sulfate (SDS) (Hwang et al., 2006, 2007, 2008; Jiang et al., 2003; Lee, 2009; Zhang, Gu, & Fujii, 2007), sodium dodecylbenzene sulfonate (SDBS) (Lee, 2009; Li et al., 2008; Wang, Zhu, & Yang, 2009b; Zhu et al., 2009), salt and oleic acid (Ding et al., 2007; Hwang et al., 2008; Yu, Xie, Chen, & Li, 2010), cetyltrimethylammonium bromide (CTAB) (Assael, Metaxa, Arvanitidis, Christofilos, & Lioutas, 2005; Pantzali, Mouza, & Paras, 2009), dodecyl trimethylammonium bromide (DTAB) and sodium octanoate (SOCT) (Madni, Hwang, Park, Choa, & Kim, 2010), hexadecyltrimethylammonium bromide (HCTAB), polyvinylpyrrolidone (PVP) (Shahrul et al., 2016; Zhu et al., 2007), and gum arabic (GA) (Lee, 2009; Rashmi et al., 2011). Choosing the right surfactant is the most important part of the

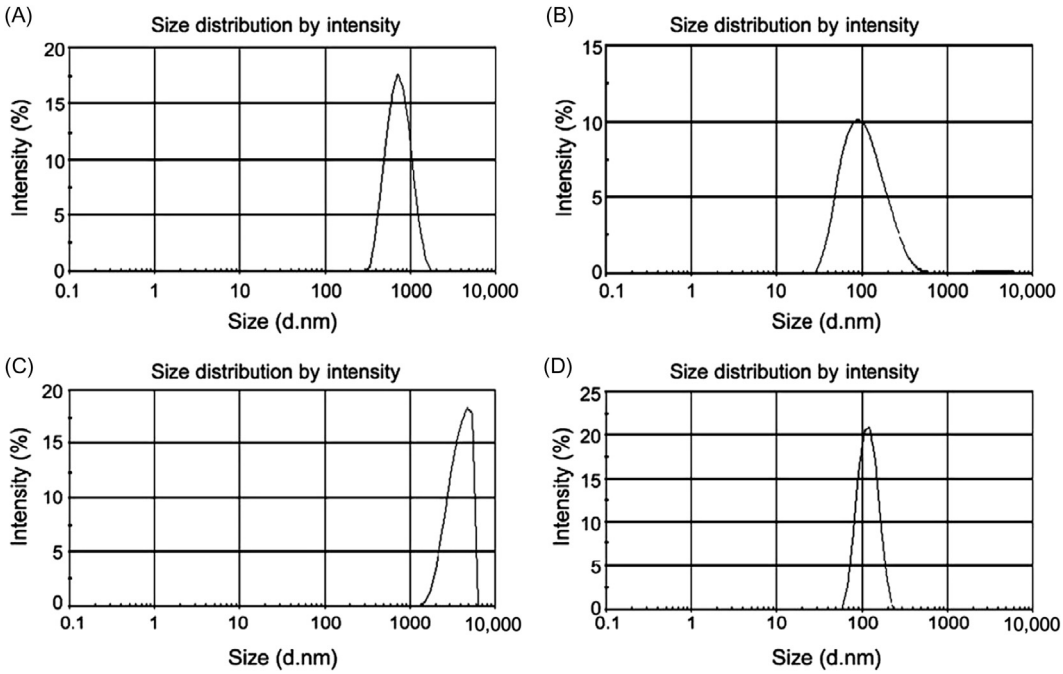

FIGURE 3-46 Particle size distributions of nano-suspensions: (A) $Al_2O_3-H_2O$ without SDBS, (B) $Al_2O_3-H_2O$ with SDBS, (C) $Cu-H_2O$ without SDBS, and (D) $Cu-H_2O$ with SDBS. Concentrations of nanoparticles and SDBS surfactant are 0.05% weight fraction, respectively. *Reprinted from Wang, X.-j., Zhu, D.-s., and yang, S. (2009). Investigation of pH and SDBS on enhancement of thermal conductivity in nanofluids.* Chemical Physics Letters 470, *107–111, copyright (2009), with permission from Elsevier.*

FIGURE 3-47 $ZnO-H_2O$ nanofluid without surfactant: (A) first day of preparation, (B) after 1 week of preparation. *Reprinted from Shahrul, I.M., Mahbubul, I.M., Saidur, R., and Sabri, M.F.M. (2016). Experimental investigation on Al_2O_3-W, SiO_2-W and $ZnO-W$ nanofluids and their application in a shell and tube heat exchanger.* International Journal of Heat and Mass Transfer 97, *547–558, copyright (2016), with permission from Elsevier.*

procedure. It can be anionic, cationic, or nonionic (Zhu, Lin, & Yin, 2004). The disadvantage of surfactant addition is for applications at the high temperatures (Wang & Mujumdar, 2008; Wen, Lin, Vafaei, & Zhang, 2009; Wu, Zhu, Wang, & Liua, 2009) as above 60°C (Assael et al., 2005; Murshed, Leong, & Yang, 2008) the bonding between surfactant and nanoparticles can be damaged. Therefore, the nanofluid will lose its stability and sedimentation of nanoparticles will occur (Wang & Mujumdar, 2007). [This paragraph is adapted from Ghadimi et al. (2011), copyright (2011), with permission from Elsevier.]

Shahrul et al. (2016) studied the effect of surfactant on nanofluid stability and characterized by the sediment photograph capturing method. First, $ZnO-H_2O$ nanofluid was prepared without surfactant and the rapid sedimentation of nanoparticles was observed, as reported in Fig. 3-47. Therefore, different types of surfactants were mixed in the mixture of $ZnO-H_2O$ nanofluids before ultrasonication to obtain the appropriate surfactant. First, HCTAB surfactant was used in $ZnO-H_2O$ nanofluid. It was found to be stabler than without surfactants. Then, SDS surfactant was used in $ZnO-H_2O$ and found to be more stable than the nanofluid prepared with HCTAB. Finally, $ZnO-H_2O$ nanofluids were prepared with PVP surfactant and it was observed that ZnO–water nanofluid with PVP was most stable compared to the other mentioned surfactants. The stability results with PVP surfactant are reported in Fig. 3-48. Very little sedimentation was observed after 2 weeks, as shown in Fig. 3-48. Therefore, the authors (Shahrul et al., 2016) finally used PVP surfactant (1.5 times of the vol.% of ZnO) to prepare $ZnO-H_2O$ nanofluid to use in a heat exchanger. Shahrul et al. (2016) prepared Fe_3O_4–water nanofluids by using 90 min of ultrasonication and found this to be fully unstable. Nanoparticles were sedimented within few minutes after preparation. Therefore,

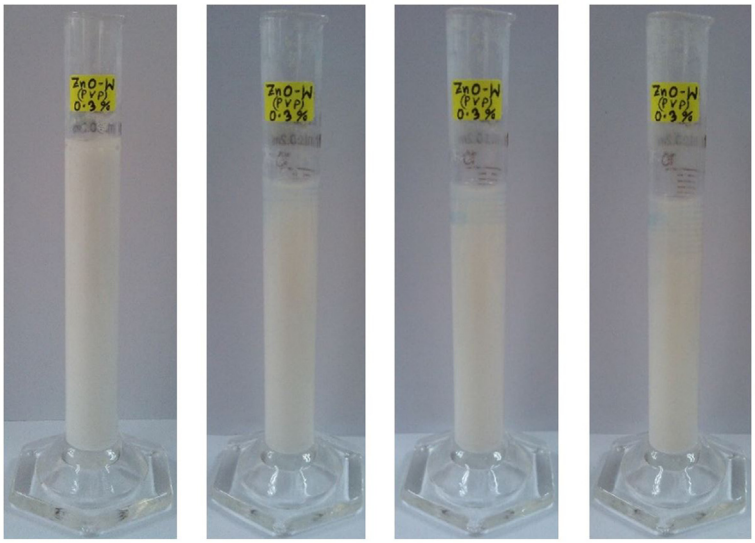

FIGURE 3-48 $ZnO-H_2O$ nanofluid with PVP: (A) first day of preparation, (B) week 1, (C) week 2, and (D) week 3. *Reprinted from Shahrul, I.M., Mahbubul, I.M., Saidur, R., and Sabri, M.F.M. (2016). Experimental investigation on Al_2O_3-W, SiO_2-W and $ZnO-W$ nanofluids and their application in a shell and tube heat exchanger.* International Journal of Heat and Mass Transfer 97, *547–558, copyright (2016), with permission from Elsevier.*

HCTAB, SDS, and PVP surfactants were used separately before ultrasonication of Fe_3O_4–water nanofluid. However, the efforts were unsuccessful in making Fe_3O_4–water nanofluid stable and it was fully sedimented within a few minutes after preparation of the nanofluids even with surfactants, which are shown in Fig. 3-49 (Shahrul et al., 2016). Therefore, the proper surfactant is important to make a suspension stable. [This paragraph is adapted from Shahrul et al. (2016), copyright (2016), with permission from Elsevier.]

Asadi et al. (2017) investigated the effect of surfactant on the stability of nanofluid prepared with different sonication times. The nanofluids were prepared with and without adding a surfactant to the suspensions. Fig. 3-50 shows the studied nanofluids at a solid concentration of 0.8% prepared with different sonication times over a period of 30 days, prepared without using any surfactants. It can be clearly seen that the nanofluid without using any surfactant showed unacceptable stability over the period of 30 days and that they showed good stability only on the first day of the experiment. Furthermore, it can be seen that increasing the sonication time leads to increasing the stability of the nanofluid without any surfactant in the first 7 days of experiments. The results of adding a surfactant to the Mg $(OH)_2$–water nanofluid in different sonication time and over the period of 30 days are illustrated in Fig. 3-51. As can be seen, all the samples showed excellent stability on the first day of experiments. After 7 days, the sample with a sonication time of 10 min showed considerable sedimentation, but the rest of the samples were still had good stability. On the seventh

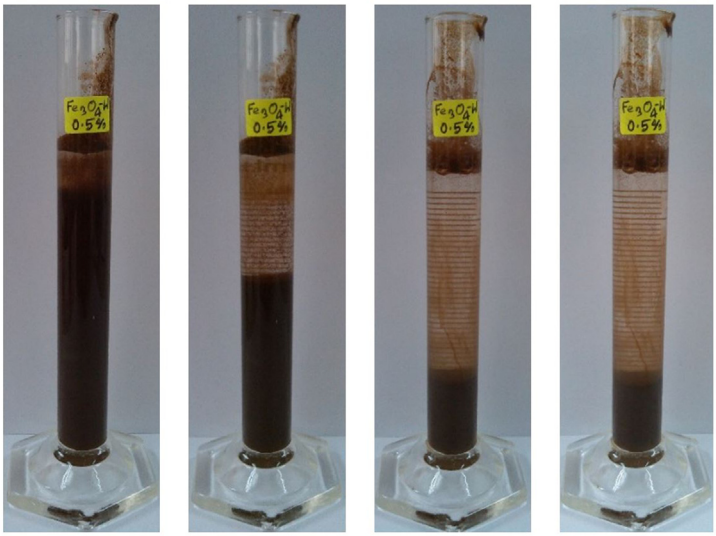

FIGURE 3-49 Fe_3O_4−water nanofluid with PVP: (A) just after preparation, (B) 1 min, (C) 2 min, and (D) 3 min after preparation. *Reprinted from Shahrul, I.M., Mahbubul, I.M., Saidur, R., and Sabri, M.F.M. (2016). Experimental investigation on Al_2O_3−W, SiO_2−W and ZnO−W nanofluids and their application in a shell and tube heat exchanger.* International Journal of Heat and Mass Transfer 97*, 547−558, copyright (2016), with permission from Elsevier.*

day, it was visually observed that the samples prepared with 30, 50, 80, and 160-min sonication showed acceptable stability, while on the 30th day, only the samples prepared with 30 and 50 min of sonication showed better stability in comparison to the rest of the samples. Thus, based on what has been discussed above, it can be inferred that the presence of the surfactant leads to increasing the stability of the studied nanofluid. [This paragraph is adapted from Asadi et al. (2017), copyright (2017), with permission from Elsevier.]

Li et al. (2008) studied the effect of surfactant on particle size distributions of Cu−H_2O nano-suspensions. Fig. 3-52 shows the distributions in the absence (a) and presence (b) of SDBS surfactant. There are significant shift in the particle size distributions of the two samples. The average particle sizes obtained are (a) in the absence of SDBS surfactant: 6770 nm, (b) in the presence of SDBS surfactant: 207 nm. Based on the particle size distribution shown in Fig. 3-52, it is certain that the stabilization of Cu−H_2O suspension with SDBS surfactant is better (Li et al., 2008).

Ghadimi and Metselaar (2013) analyzed the effect of surfactant and/or ultrasonication on TiO_2−water nanofluid. They prepared four samples as (a) with surfactant but without ultrasonic process, (b) with surfactant and 15 min horn ultrasonic, (c) without surfactant but with 15 min horn ultrasonic, and (d) without surfactant and ultrasonic process and captured photos to see the effect after 5 days of preparation. The images are shown in Fig. 3-53. Sedimentation of the nanoparticles is clearly observed in the case of (a) and (d). Better

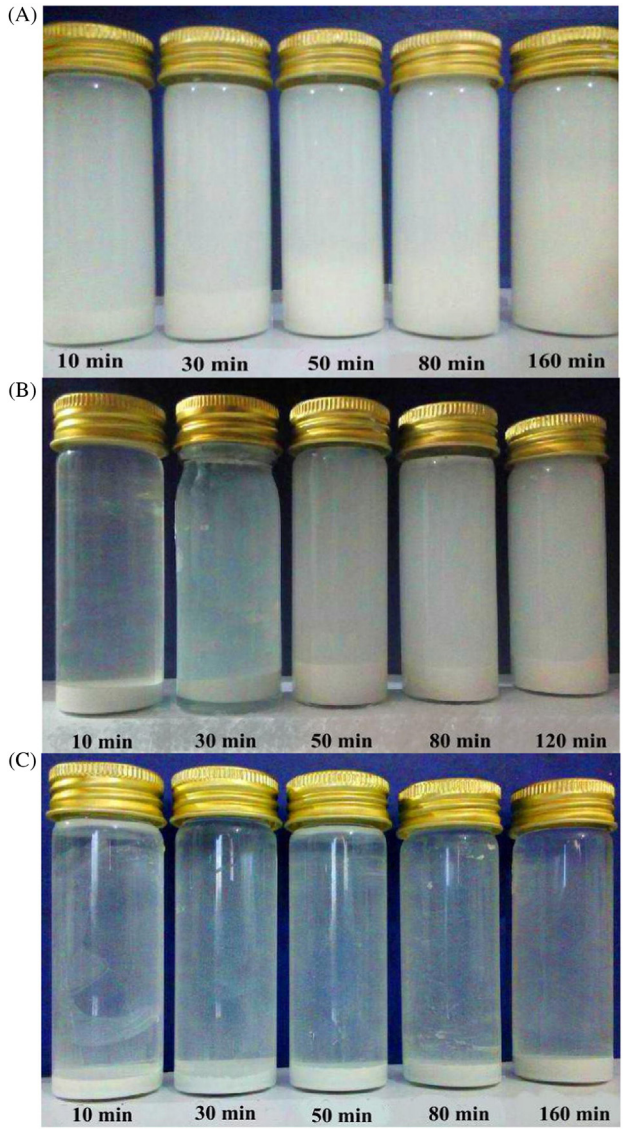

FIGURE 3-50 $Mg(OH)_2$—water nanofluid at a solid concentration of 0.8% without using surfactant in different ultrasonication times after (A) 1 day, (B) 7 days, and (C) 30 days. *Reprinted from Asadi, A., Asadi, M., Siahmargoi, M., Asadi, T., and Gholami Andarati, M. (2017). The effect of surfactant and sonication time on the stability and thermal conductivity of water-based nanofluid containing $Mg(OH)_2$ nanoparticles: An experimental investigation.* International Journal of Heat and Mass Transfer 108*, 191–198, copyright (2016), with permission from Elsevier.*

dispersion of nanoparticle is seen for the case of (b) and (c). The foaming effect of surfactant is observed in (b). Fig. 3-53C looks to be better although it is without the SDS surfactant.

Wang, Li, and Yang (2009a) studied the influence of SDBS surfactant concentration on the stability (zeta potential and absorbency) and dispersion (cluster size) of Al_2O_3—H_2O and

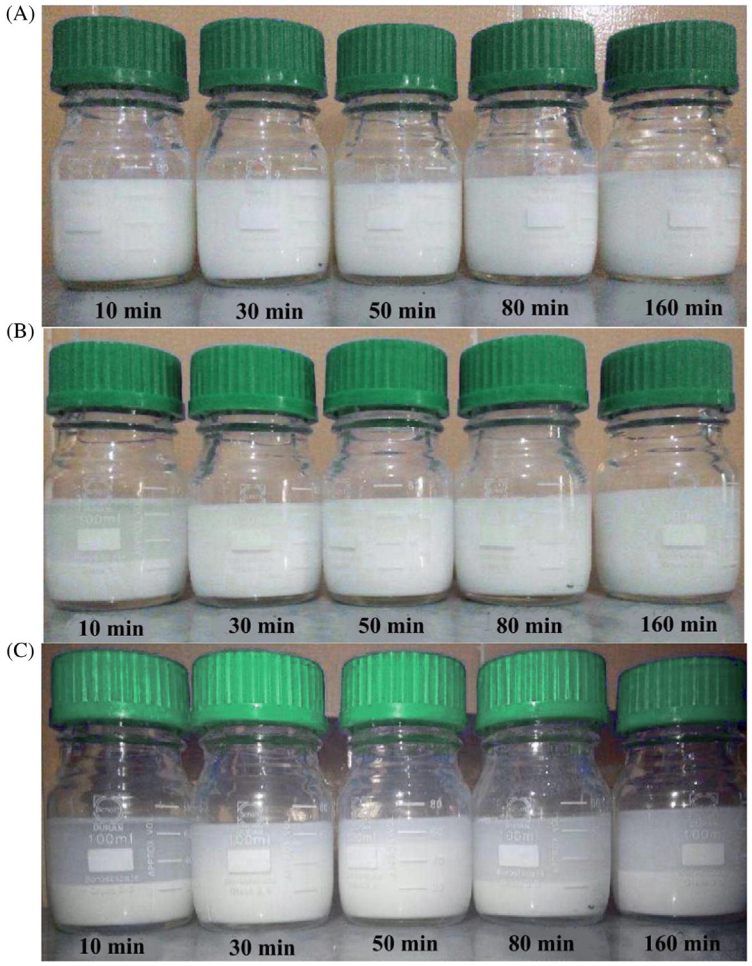

FIGURE 3-51 $Mg(OH)_2$—water nanofluid at a solid concentration of 0.8% using CTAB surfactant in different sonication times after (A) 1 day, (B) 7 days, and (C) 30 days. *Reprinted from Asadi, A., Asadi, M., Siahmargoi, M., Asadi, T., and Gholami Andarati, M. (2017). The effect of surfactant and sonication time on the stability and thermal conductivity of water-based nanofluid containing $Mg(OH)_2$ nanoparticles: An experimental investigation.* International Journal of Heat and Mass Transfer 108*, 191–198, copyright (2016), with permission from Elsevier.*

Cu—H_2O nanofluid, which are illustrated in Figs. 3-54 and 3-55, respectively. It can be seen in Fig. 3-54 that with the increase in SDBS concentration for a certain limit, zeta potential and absorbency of the mentioned two nanofluids are increased to the maximum. The highest zeta potential and absorbency values were observed for SDBS concentrations of 0.10% and 0.07% for Al_2O_3—H_2O and Cu—H_2O nanofluids, respectively. Wang et al. (2009a) discussed the dispersion mechanism in Fig. 3-54 as SDBS can partially ionize in water and give anionic species, whereas alumina and copper nanoparticles carry positive charge in a neutral

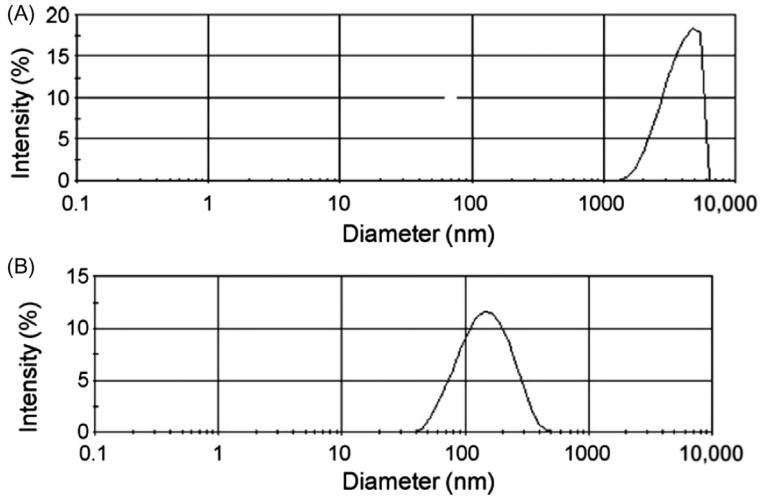

FIGURE 3-52 Particle size distributions of Cu−H_2O suspensions in the absence (A) and presence (B) of SDBS surfactant. Concentration of Cu and SDBS surfactant are 0.05 wt%. *Reprinted from Li, X. F., Zhu, D. S., Wang, X. J., Wang, N., Gao, J. W., and Li, H. (2008). Thermal conductivity enhancement dependent pH and chemical surfactant for Cu-H_2O nanofluids.* Thermochimica Acta 469, *98−103, copyright (2008), with permission from Elsevier.*

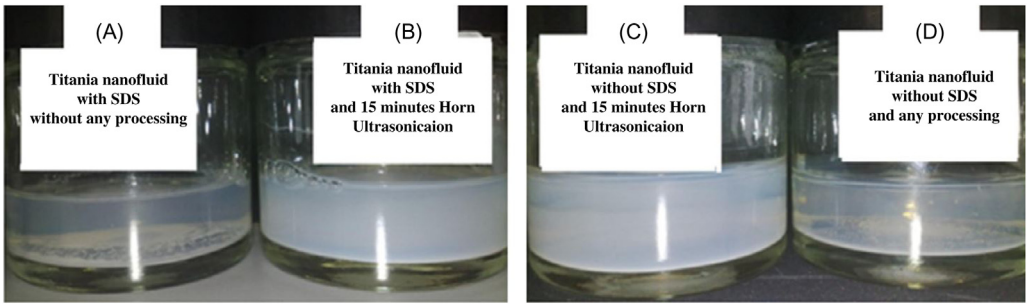

FIGURE 3-53 Photo capturing of the effect of surfactant and horn ultrasonic on TiO_2 nanofluid at 5 days after preparation; (A) with surfactant but without ultrasonic process, (B) with surfactant and 15 min horn ultrasonic, (C) without surfactant but with 15 min horn ultrasonic, and (D) without surfactant and ultrasonic process. *Reprinted from Ghadimi, A., and Metselaar, I.H. (2013). The influence of surfactant and ultrasonic processing on improvement of stability, thermal conductivity and viscosity of titania nanofluid.* Experimental Thermal and Fluid Science 51, *1−9, copyright (2013), with permission from Elsevier.*

aqueous medium, having a strong affinity for anionic groups. When the SDBS concentration is lower, the negatively charged dodecylbenzene sulfonate formed by dissociation of SDBS is adsorbed on the positively charged surfaces of the nanoparticles and, consequently, the surfaces are negatively charged, and this leads to an electrostatic stabilization effect. With the increase in SDBS, on the one hand, the anion groups pushed into the adsorbed layer make the absolute value of zeta potential increase, resulting in increasing the repulsive forces

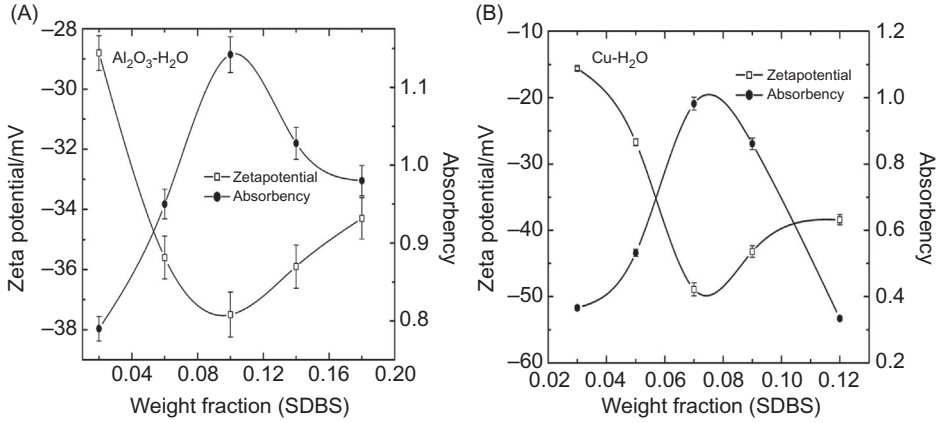

FIGURE 3-54 Effect of SDBS concentration on the stability of nanofluids: (A) zeta potential and absorbency of Al_2O_3–H_2O, pH = 8.0; (B) zeta potential and absorbency of Cu–H_2O, pH = 9.5. Concentration of nanoparticles for the measurement of zeta potential is 0.05 wt.%, and concentration of nanoparticles for the measurement of absorbency is 0.1 wt.%. *Reprinted with permission from Wang, X. J., Li, X., and Yang, S. (2009). Influence of pH and SDBS on the stability and thermal conductivity of nanofluids.* Energy and Fuels 23*, 2684–2689. Copyright (2009) American Chemical Society.*

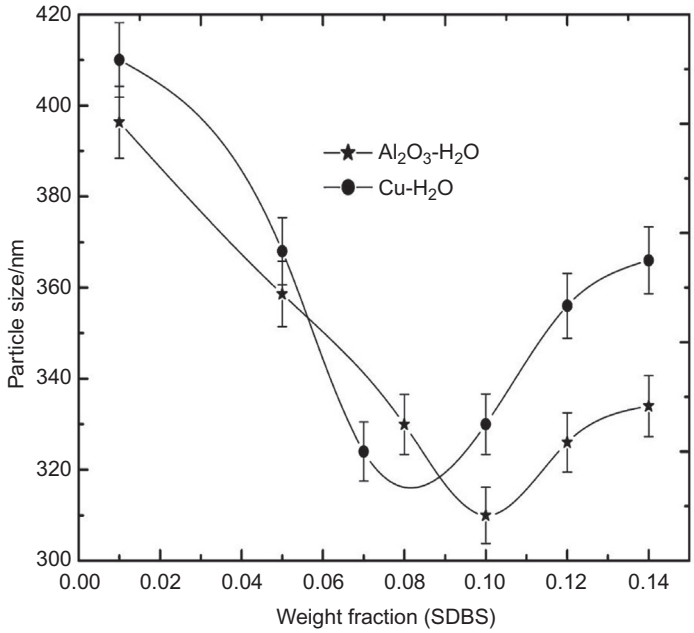

FIGURE 3-55 Effect of SDBS weight fraction on particle size. Concentration of nanoparticles is 0.05 wt.%. *Reprinted with permission from Wang, X. J., Li, X., and Yang, S. (2009). Influence of pH and SDBS on the stability and thermal conductivity of nanofluids.* Energy and Fuels 23*, 2684–2689. Copyright (2009) American Chemical Society.*

between the particles, thereby increasing the thickness of the electrical double layer; on the other hand, large numbers of anion groups in the aqueous suspension hinder the particles from colliding and then reduce the collision probability between the particles. Here, the adsorbed phenyl sulfonic group and a significant electrical double layer were simultaneously presented. When more SDBS is added into the suspension, the concentration of Na^+ increases with SDBS concentration increase, and the Na^+ group entering into the absorbed layer reduces the net charge of powder surface and makes the absolute value of zeta potential decrease, resulting in a weak dispersion system. [This paragraph is adapted with permission from Wang et al. (2009a). Copyright (2009) American Chemical Society.]

Fig. 3-55 shows the influence of SDBS concentration on cluster size of $Al_2O_3-H_2O$ and $Cu-H_2O$ nanofluids. It can be seen in Fig. 3-55 that the cluster sizes were found to be higher at the low SDBS concentrations. Cluster size is in reality a reflection of particle dispersion as it represents the particle aggregate in a dispersion state. Cluster sizes were reduced until a certain limit, with the increase of SDBS concentration. The optimum SDBS concentrations were found to be 0.10% and 0.07% for $Al_2O_3-H_2O$ and $Cu-H_2O$ nanofluids, respectively, at which the cluster sizes were minimum and were 310 and 320 nm, respectively (Wang et al., 2009a).

3.4 pH Control

The stability of an aqueous solution like nanofluid directly links to its electrokinetic properties. Through a high surface charge density, strong repulsive forces can stabilize a well-dispersed suspension (Chang et al., 2000; Chou & Liao, 2005; Fovet, Gal, & Toumelin-Chemla, 2001; Huang et al., 2009; Lee, Kim, & Kim, 2006; Wang et al., 2009b; Wei, Zhu, Kong, & Wang, 2009; Zhu et al., 2009). Xie, Lee, Youn, and Choi (2003) showed that by simple acid treatment a carbon nanotube suspension gained good stability in water. This was caused by a hydrophobic-to-hydrophilic conversion of the surface nature due to the generation of a hydroxyl group. The isoelectric point (IEP) is the concentration of potential controlling ions at which the zeta potential is zero. Thus, at the IEP, the surface charge density equals the charge density, which is the start point of the diffuse layer. Therefore, the charge density in this layer is zero. Critical to nanoparticle nucleation and stabilization in solution is that the repulsive energy is smaller for small particles, so a larger zeta potential is required for suspension stability (Chang et al., 2007). As the pH of the solution departs from the IEP of particles the colloidal particles get more stable and ultimately modify the thermal conductivity of the fluid. The surface charge state is a basic feature which is mainly responsible for increasing the thermal conductivity of the nanofluids (Huang et al., 2009; Lee et al., 2006). Also, in some experiments, particles' shape conversion was related to the pH variation (Hadjov, 2009; Wei et al., 2009).

In the liquid suspension, particles attract or repel each other. This interaction depends on the distance between particles and the total interface energy E_{tot} that is the sum of the van der Waals attraction E_A and the electrostatic repulsion E_{el} between them. The E_{el} between

two charged particles with the surface potentials ψ_{d1} and ψ_{d2} is approximated by the DLVO theory:

$$E_{el} = \frac{\varepsilon_0 \varepsilon_1 r_1 r_2}{r_1 + r_2} \left\{ 2\psi_{d1}\psi_{d2} \ln\left[\frac{1+\exp(-kx)}{1-\exp(-kx)}\right] + (\psi_{d1}^2 + \psi_{d2}^2)\ln[1-\exp(-2kx)] \right\} \tag{3.2}$$

where r is the radius of particles, x is an interparticle surface-to-surface distance, and the other symbols have their conventional meanings.

It is notable that higher potentials (ψ_d or ζ) lead to a larger potential barrier for agglomeration. In aqueous nanofluid of CuO with 0.3 vol.% and point of zero charge (PZC) of about 8.5−9.5, the interparticle distance is about 100 nm for mobility-equivalent spherical particles. At this condition, the second term in the bracket of the above equation is negligible compared to the first. Thus, the repulsion energy of the same-sized particles goes up approximately in proportion to ζ^2.

The attraction energy between the same particles is given by the Hamaker equation: $E_A = -A_{132}r/(12x)$. The Hamaker constant A_{132} of metal oxide is typically on the order of 10^{-20} J. Using the above equation, the Hamaker equation, and the estimated ψ_d, E_{tot} is calculated as a function of x at different pHs, as shown in Fig. 3-56. In this condition, the repulsion barrier gets bigger than the attraction as pH goes from the PZC, which makes the colloids more stable. At pH 8 or 10 when ψ is small, however, the repulsion barrier disappears, and particles are only subjected to the attractions. Strong particle agglomeration is expected in that situation. Here, we need to quantify the suspension stability in terms of collision efficiency, α, which is responsible for colloidal particle growth. The α, a reciprocal value of stability coefficient W, is related to the rate constant of aggregation, $k = \alpha k_{diff} = k_{diff}/W$.

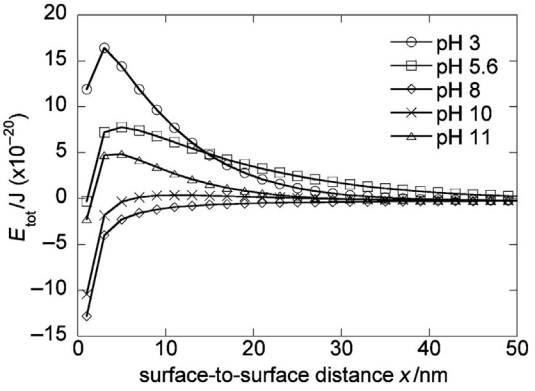

FIGURE 3-56 The interaction potentials at various pHs as a function of interparticle distance. *Reprinted with permission from Lee, D., Kim, J.-W., and Kim, B. G. (2006). A new parameter to control heat transport in nanofluids: Surface charge state of the particle in suspension.* The Journal of Physical Chemistry B 110, *4323−4328. Copyright (2006) American Chemical Society.*

The k_{diff} represents the rate constant of the coagulation between uncharged particles. Then a general relation of stability coefficient W to total interaction energy E_{tot} can be derived (Lee et al., 2006).

$$W = 2r\int_0^{\infty} \exp\left(\frac{E_{tot}}{K_b T}\right)\frac{dx}{(2r+x)^2} \tag{3.3}$$

For example, as the pH of the nanofluid goes far from the isoelectric point, the surface charge increases by applying SDBS surfactant in Cu−H_2O nanofluid. Since more frequent attacks occur to the surface hydroxyl and phenyl sulfonic group by potential-determining ions (H^+, OH^-, and phenyl sulfonic group), zeta potential and the colloidal particles increase. So the suspension gets more stable and eventually changes the thermal conductivity of the fluid (Li et al., 2008).

Lee et al. (2009) worked on different pH of Al_2O_3 nanofluids. The experiments indicated that when the nanofluid had a pH of 1.7, the agglomerated particle size was reduced by 18% and when the nanofluid had a pH of 7.66, the agglomeration size was increased by 51%. More particles aggregated in pH of 7.66 because of the reduction in electric repulsion force. When Al_2O_3 particles are immersed in water, hydroxyl groups (−OH) are produced at the surface of the Al_2O_3 particle. The relevant reactions depend on the solution pH. When the pH of the solution is lower than the PZC, the hydroxyl groups react with H^+ from water, which leads to a positively charged surface. Alternatively, when the pH of the solution is higher than the PZC, the hydroxyl groups react with OH^- from water and create a negatively charged surface (Peterson & Li, 2006). The optimized pH is different for different nanoparticles. For example, the proper pH for alumina is around 8, meanwhile for copper and graphite nanoparticles it is 9.5 (Wang & Li, 2009) and about 2.0, respectively. The pH for the point of zero charge also changes by temperature variation as shown in Table 3-7 (Chou & Liao, 2005).

Table 3-7 Actual Values of pH_{PZC} of the TiO_2 Between 5 and 55°C

Temperature (°C)	pH_{PZC}
5	6.62
15	6.39
25	6.17
35	5.97
45	5.78
55	5.61

Source: Adapted from Chou, J.-C., and Liao, L.P. (2005). Study on pH at the point of zero charge of TiO_2 pH ion-sensitive field effect transistor made by the sputtering method. Thin Solid Films 476, 157−161, copyright (2004), with permission from Elsevier.

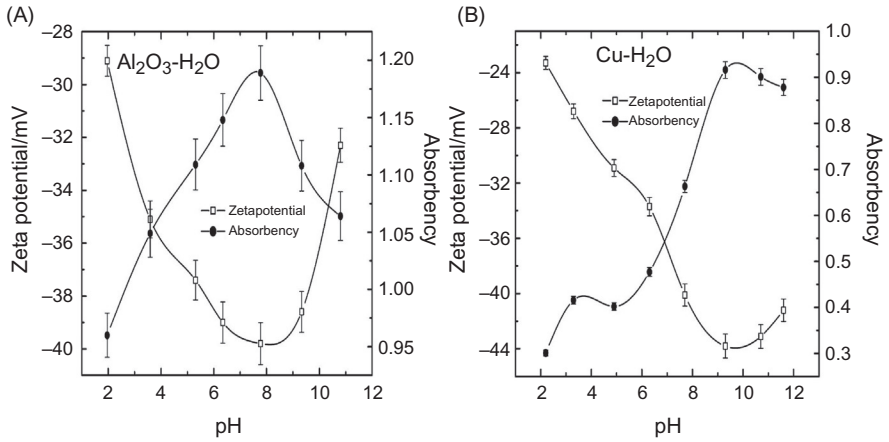

FIGURE 3-57 Effect of pH on zeta potential and absorbency of nanosuspensions with SDBS dispersants. Concentration of nanoparticles and dispersants for the measurement of zeta potential is 0.05 wt.%, and concentration of nanoparticles and SDBS for the measurement of absorbency is 0.1 wt.%. (A) $Al_2O_3-H_2O$, (B) $Cu-H_2O$. *Reprinted with permission from Wang, X. J., Li, X., and Yang, S. (2009). Influence of pH and SDBS on the stability and thermal conductivity of nanofluids.* Energy and Fuels 23, *2684–2689. Copyright (2009) American Chemical Society.*

[The above paragraphs of this section (3.4 pH control) are adapted from Ghadimi et al. (2011), copyright (2011), with permission from Elsevier.]

Wang et al. (2009a) studied the influence of pH on the stability and dispersion of $Al_2O_3-H_2O$ and $Cu-H_2O$ nanofluids (prepared with the addition of SDBS surfactant), which are presented here in Figs. 3-57 and 3-58, respectively. The effect of pH changes on zeta potential and absorbency of the mentioned two nanofluids are depicted in Fig. 3-57. The lowest zeta potential and absorbency were observed at pH of 2 for both nanofluids. This could be because, at that point, the electrostatic repulsion force between particles is not sufficient to overcome the attraction force between particles. Therefore, poor dispersion stability was observed. With the increase of pH, the electrostatic repulsion force between particles increases and prevents the attraction of particles. Moreover, a collision between particles is caused by Brownian motion. The larger the electrostatic force the more free particles and the particle–particle distance increases to exceed the hydrogen bonding range between particles and further reduces the probability of particle coagulation and settling, hence improving the dispersion stability of nanoparticles. The highest zeta potential and absorbency values were observed at pHs of 8.0 and 9.5 for $Al_2O_3-H_2O$ and $Cu-H_2O$ nanofluids, respectively. However, further increasing pH value causes the compression of an electrical double layer, which continues further because of the reagent (NaOH) in the system increasing, which minimizes the absolute zeta potential of the particle surface and electrostatic repulsion force. Therefore, further increasing pH results in poorer dispersion and stability. Fig. 3-58 shows the influence of pH on cluster size of $Al_2O_3-H_2O$ and $Cu-H_2O$ nanofluids. It can be seen in Fig. 3-58 that the cluster sizes were found to be higher at the low pH value of the nanofluids.

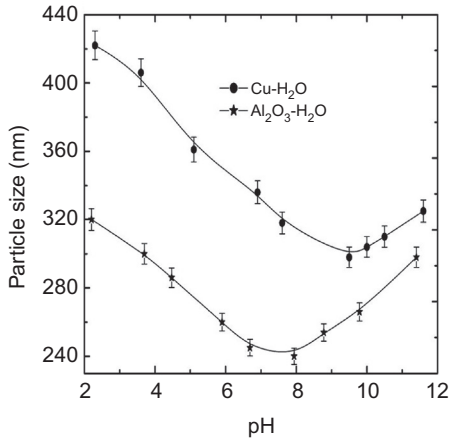

FIGURE 3-58 Effect of pH on particle cluster size. Concentration of nanoparticles is 0.05 wt.%. *Reprinted with permission from Wang, X. J., Li, X., and Yang, S. (2009). Influence of pH and SDBS on the stability and thermal conductivity of nanofluids.* Energy and Fuels 23, *2684–2689. Copyright (2009) American Chemical Society.*

Cluster size is in reality a reflection of particle dispersion as it represents the particle aggregate in a dispersion state. Cluster sizes were reduced for a certain limit with an increase in pH value. The optimum pH values were found to be 8.0 and 9.5 for $Al_2O_3-H_2O$ and $Cu-H_2O$ nanofluids, respectively, at which the cluster sizes were minimum and 240 and 320 nm, respectively. By comparing Figs. 3-57 and 3-58, it can be concluded that the optimum pH values were fixed for zeta potential, absorbency, and cluster size. According to the trends in Figs. 3-57 and 3-58, in the region, $2 < pH < 8$, stability and dispersion of $Al_2O_3-H_2O$ nanofluid was better than $Cu-H_2O$ nanofluid. However, in the region, $pH > 8.0$, the stability and dispersion of $Cu-H_2O$ nanofluid was found to be better than $Al_2O_3-H_2O$ nanofluid (Wang & Li, 2009; Wang et al., 2009a).

Hwang et al. (2008) studied the effect of pH on the zeta potential of carbon black (CB)–water nanofluid with and without SDS surfactant. Fig. 3-59 shows the outcome from Hwang et al. (2008) as zeta potentials of the CB suspensions as a function of pH (a) without SDS and (b) with SDS (1 wt.%). These suspensions were prepared by using a high-pressure homogenizer. It can be seen in Fig. 3-59, without SDS addition, the zeta potential of the CB suspension was significantly decreased with increasing pH value. However, with the controlled-amount addition of SDS (1 wt.%), the zeta potential of the CB suspension remained at relatively low negative charge range regardless of pH value, indicating that the hydrophilic segment of the SDS added was presumably negatively ionized in the broad pH ranges (Jiang et al., 2003). It can be seen in Fig. 3-59 that the highest zeta potential is observed at the lowest pH value and without surfactant. [This paragraph is adapted from Hwang et al. (2008), copyright (2007), with permission from Elsevier.]

The effect of varying ultrasonication on pH value was studied. The pH of the Al_2O_3–water nanofluids (prepared by ultrasonication durations of 0–5 h) were measured at

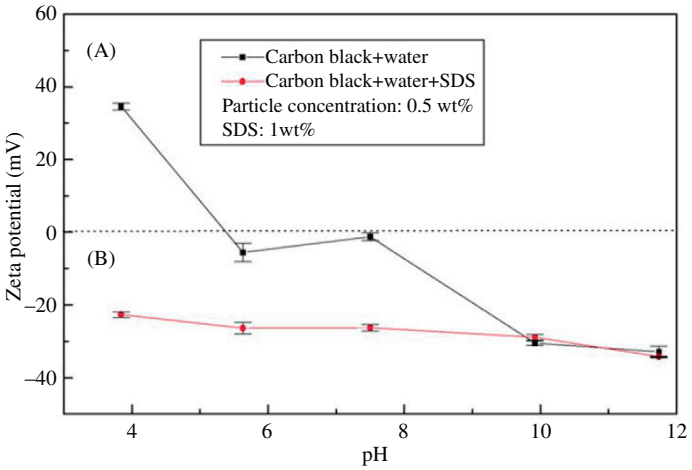

FIGURE 3-59 The evolution of zeta potentials of the water-based carbon black nanofluids as a function of pH: (A) without SDS and (B) with SDS (1 wt.%). *Reprinted from Hwang, Y., Lee, J.-K., Lee, J.-K., Jeong, Y.-M., Cheong, S.-I., Ahn, Y.-C., and Kim, S.H. (2008). Production and dispersion stability of nanoparticles in nanofluids. Powder Technology 186, 145–153, copyright (2007), with permission from Elsevier.*

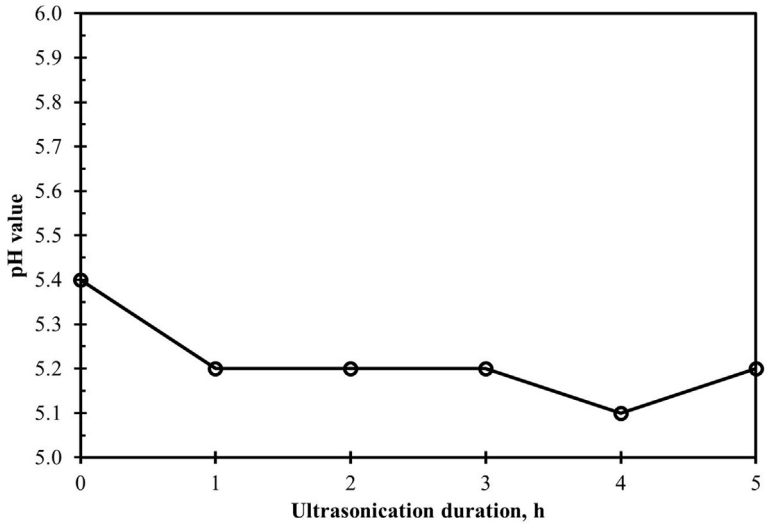

FIGURE 3-60 pH value of Al_2O_3–water nanofluid after different durations of ultrasonication at 50% amplitude.

25°C and are reported in Fig. 3-60. The pH of the samples was found to be 5.1 ± 0.1 for the nanofluids prepared by different durations of ultrasonication. However, the pH of nanofluid prepared without ultrasonication (0 h) was found to be 5.6 ± 0.2. Lee et al. (2008) reported a pH of 6.04 and Chandrasekar, Suresh, and Chandra Bose (2010) found it to be around

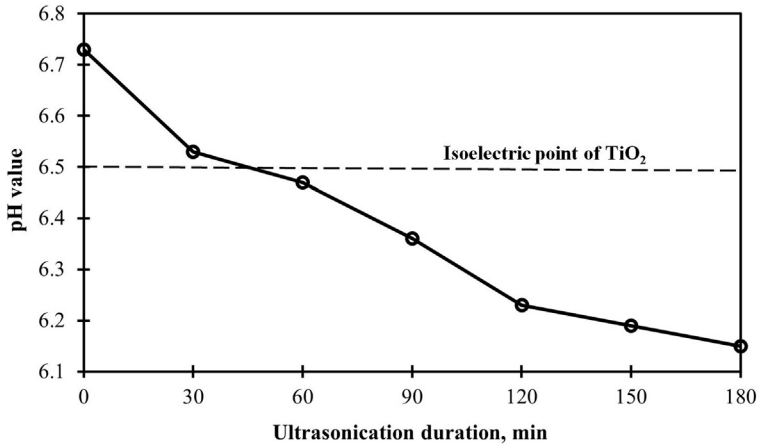

FIGURE 3-61 Change in pH value of TiO_2−H_2O nanofluid with varying ultrasonication durations with the isoelectric point of TiO_2. *Adapted from Mahbubul, I. M., Elcioglu, E. B., Saidur, R., and Amalina, M. A. (2017). Optimization of ultrasonication period for better dispersion and stability of TiO_2−water nanofluid.* Ultrasonics Sonochemistry 37, *360−367, copyright (2017), with permission from Elsevier.*

5 for Al_2O_3−water nanofluid at 25ºC. This minor difference of the pH values reported in different studies (Chandrasekar et al., 2010; Lee et al., 2008) may be because of the variation of particle concentration and source of the nanoparticle, which is related to the percentage of the composition. Xie, Chen, and Wu (2008) measured the isoelectric point of Al_2O_3 nanoparticles and found it to be 9.2. The authors urged that if the pH of a suspension is far from this isoelectric point, then the nanoparticles are expected to be well dispersed, as the repulsive forces of nanoparticles are increased. On the other hand, if the pH value is near to 9.2, then the repulsive forces among nanoparticles are decreased and lead to coagulation and aggregation of nanoparticles. As there is an extreme distance between the obtained pH of Fig. 3-60 with the isoelectric point, therefore, the nanofluid could be considered as stable.

Mahbubul et al. (2017) measured the effect of changing ultrasonication duration on pH values. The variation of sample pH value with the ultrasonication duration is illustrated here in Fig. 3-61. The pH values of the samples were observed to be 6.73, 6.53, 6.47, 6.36, 6.23, 6.19, and 6.15, respectively, for ultrasonication durations of 0, 30, 60, 90, 120, 150, and 180 min. It can be concluded from Fig. 3-61 that the pH values are inversely proportional to the ultrasonication duration. The isoelectric point of TiO_2 was reported by Haddad, Abid, Oztop, and Mataoui (2014) as 6.5, and moving away from the isoelectric point with increasing ultrasonication duration, mainly after 60 min, is an indicator of improved colloidal stability. [This paragraph is adapted from Mahbubul et al. (2017), copyright (2017), with permission from Elsevier.]

References

Amrollahi, A., Hamidi, A., & Rashidi, A. (2008). The effects of temperature, volume fraction and vibration time on the thermo-physical properties of a carbon nanotube suspension (carbon nanofluid). *Nanotechnology, 19,* 315701.

Asadi, A., Asadi, M., Siahmargoi, M., Asadi, T., & Gholami Andarati, M. (2017). The effect of surfactant and sonication time on the stability and thermal conductivity of water-based nanofluid containing $Mg(OH)_2$ nanoparticles: An experimental investigation. *International Journal of Heat and Mass Transfer*, *108*, 191−198.

Assael, M. J., Metaxa, I. N., Arvanitidis, J., Christofilos, D., & Lioutas, C. (2005). Thermal conductivity enhancement in aqueous suspensions of carbon multi-walled and double-walled nanotubes in the presence of two different dispersants. *International Journal of Thermophysics*, *26*, 647−664.

Chakraborty, S., Mukherjee, J., Manna, M., Ghosh, P., Das, S., & Denys, M. B. (2012). Effect of Ag nanoparticle addition and ultrasonic treatment on a stable TiO_2 nanofluid. *Ultrasonics Sonochemistry*, *19*, 1044−1050.

Chandrasekar, M., Suresh, S., & Chandra Bose, A. (2010). Experimental investigations and theoretical determination of thermal conductivity and viscosity of Al_2O_3/water nanofluid. *Experimental Thermal and Fluid Science*, *34*, 210−216.

Chang, H., Jwo, C. S., Fan, P. S., & Pai, S. H. (2007). Process optimization and material properties for nanofluid manufacturing. *The International Journal of Advanced Manufacturing Technology*, *34*, 300−306.

Chang, H., & Lin, S.-C. (2007). Fabrication method for a TiO_2 nanofluid with high roundness and superior dispersion properties. *Materials transactions*, *48*, 836−841.

Chang, H., Wu, Y., Chen, X., & Kao, M. (2000). Fabrication of Cu based nanofluid with superior dispersion. *National Taipei University of Technology Journal*, *5*, 201−208.

Chen, H., Ding, Y., & Tan, C. (2007). Rheological behaviour of nanofluids. *New Journal of Physics*, *9*, 367.

Chou, J.-C., & Liao, L. P. (2005). Study on pH at the point of zero charge of TiO_2 pH ion-sensitive field effect transistor made by the sputtering method. *Thin Solid Films*, *476*, 157−161.

Chung, S. J., Leonard, J. P., Nettleship, I., Lee, J. K., Soong, Y., Martello, D. V., & Chyu, M. K. (2009). Characterization of ZnO nanoparticle suspension in water: Effectiveness of ultrasonic dispersion. *Powder Technology*, *194*, 75−80.

Ding, Y., Chen, H., He, Y., Lapkin, A., Yeganeh, M., Šiller, L., & Butenko, Y. V. (2007). Forced convective heat transfer of nanofluids. *Advanced Powder Technology*, *18*, 813−824.

Duangthongsuk, W., & Wongwises, S. (2009). Measurement of temperature-dependent thermal conductivity and viscosity of TiO_2-water nanofluids. *Experimental Thermal and Fluid Science*, *33*, 706−714.

Elcioglu, E.B., and Okutucu-Ozyurt, T. (2014). An experimental study on the dispersion stability of alumina-water nanofluids via particle size distribution and zeta potential measurements. In International Conference on Thermophysical and Mechanical Properties of Advanced Materials, Cesme - Izmir, Turkey.

Everett, D. H. (1988). *Basic principles of colloid science*. London: Royal Society of Chemistry.

Fovet, Y., Gal, J.-Y., & Toumelin-Chemla, F. (2001). Influence of pH and fluoride concentration on titanium passivating layer: Stability of titanium dioxide. *Talanta*, *53*, 1053−1063.

Garg, P., Alvarado, J. L., Marsh, C., Carlson, T. A., Kessler, D. A., & Annamalai, K. (2009). An experimental study on the effect of ultrasonication on viscosity and heat transfer performance of multi-wall carbon nanotube-based aqueous nanofluids. *International Journal of Heat and Mass Transfer*, *52*, 5090−5101.

Ghadimi, A., & Metselaar, I. H. (2013). The influence of surfactant and ultrasonic processing on improvement of stability, thermal conductivity and viscosity of titania nanofluid. *Experimental Thermal and Fluid Science*, *51*, 1−9.

Ghadimi, A., Saidur, R., & Metselaar, H. S. C. (2011). A review of nanofluid stability properties and characterization in stationary conditions. *International Journal of Heat and Mass Transfer*, *54*, 4051−4068.

Habibzadeh, S., Kazemi-Beydokhti, A., Khodadadi, A. A., Mortazavi, Y., Omanovic, S., & Shariat-Niassar, M. (2010). Stability and thermal conductivity of nanofluids of tin dioxide synthesized via microwave-induced combustion route. *Chemical Engineering Journal*, *156*, 471−478.

Haddad, Z., Abid, C., Oztop, H. F., & Mataoui, A. (2014). A review on how the researchers prepare their nanofluids. *International Journal of Thermal Sciences*, *76*, 168−189.

Hadjov, K. B. (2009). Modified self-consisted scheme to predict the thermal conductivity of nanofluids. *International Journal of Thermal Sciences*, *48*, 2249−2254.

Huang, J., Wang, X., Long, Q., Wen, X., Zhou, Y., and Li, L. (2009). Influence of pH on the stability characteristics of nanofluids. In Proceedings of the Symposium on Photonics and Optoelectronics (SOPO'09).

Hwang, Y., Ahn, Y., Shin, H., Lee, C., Kim, G., Park, H., & Lee, J. (2006). Investigation on characteristics of thermal conductivity enhancement of nanofluids. *Current Applied Physics*, *6*, 1068−1071.

Hwang, Y., Lee, J. K., Lee, C. H., Jung, Y. M., Cheong, S. I., Lee, C. G., . . . Jang, S. P. (2007). Stability and thermal conductivity characteristics of nanofluids. *Thermochimica Acta*, *455*, 70−74.

Hwang, Y., Lee, J.-K., Lee, J.-K., Jeong, Y.-M., Cheong, S.-I., Ahn, Y.-C., & Kim, S. H. (2008). Production and dispersion stability of nanoparticles in nanofluids. *Powder Technology*, *186*, 145−153.

Jiang, L., Gao, L., & Sun, J. (2003). Production of aqueous colloidal dispersions of carbon nanotubes. *Journal of Colloid and Interface Science*, *260*, 89−94.

Kabir, M. E., Saha, M. C., & Jeelani, S. (2007). Effect of ultrasound sonication in carbon nanofibers/polyurethane foam composite. *Materials Science and Engineering: A*, *459*, 111−116.

Kim, S. H., Choi, S. R., & Kim, D. (2006). Thermal conductivity of metal-oxide nanofluids: Particle size dependence and effect of laser irradiation. *Journal of Heat Transfer*, *129*, 298−307.

Kole, M., & Dey, T. K. (2012). Effect of prolonged ultrasonication on the thermal conductivity of ZnO−ethylene glycol nanofluids. *Thermochimica Acta*, *535*, 58−65.

Kreibig, U., & Genzel, L. (1985). Optical absorption of small metallic particles. *Surface Science*, *156*, 678−700.

Kreibig, U., & Vollmer, M. (1995). *Optical properties of metal clusters*. Springer.

Kwak, K., & Kim, C. (2005). Viscosity and thermal conductivity of copper oxide nanofluid dispersed in ethylene glycol. *Korea-Australia Rheology Journal*, *17*, 35−40.

Lam, C.-K., Lau, K.-T., Cheung, H.-Y., & Ling, H.-Y. (2005). Effect of ultrasound sonication in nanoclay clusters of nanoclay/epoxy composites. *Materials Letters*, *59*, 1369−1372.

Lee, D., Kim, J.-W., & Kim, B. G. (2006). A new parameter to control heat transport in nanofluids: surface charge state of the particle in suspension. *The Journal of Physical Chemistry B*, *110*, 4323−4328.

Lee, J., Han, K., & Koo, J. (2014). A novel method to evaluate dispersion stability of nanofluids. *International Journal of Heat and Mass Transfer*, *70*, 421−429.

Lee, J., Hwang, K., Jang, S., Lee, B., Kim, J., Choi, S., & Choi, C. (2008). Effective viscosities and thermal conductivities of aqueous nanofluids containing low volume concentrations of Al_2O_3 nanoparticles. *International Journal of Heat and Mass Transfer*, *51*, 2651−2656.

Lee, J. H. (2009). *Convection performance of nanofluids for electronics cooling*. *Department of Mechanical Engineering*. Stanford University.

Lee, K., Hwang, Y., Cheong, S., Kwon, L., Kim, S., & Lee, J. (2009). Performance evaluation of nano-lubricants of fullerene nanoparticles in refrigeration mineral oil. *Current Applied Physics*, *9*, e128−e131.

Li, X. F., Zhu, D. S., Wang, X. J., Wang, N., Gao, J. W., & Li, H. (2008). Thermal conductivity enhancement dependent pH and chemical surfactant for Cu-H_2O nanofluids. *Thermochimica Acta*, *469*, 98−103.

Link, S., & El-Sayed, M. A. (2003). Optical properties and ultrafast dynamics of metallic nanocrystals. *Annual Review of Physical Chemistry*, *54*, 331−366.

Liu, Z.-Q., Ma, J., & Cui, Y.-H. (2008). Carbon nanotube supported platinum catalysts for the ozonation of oxalic acid in aqueous solutions. *Carbon*, *46*, 890−897.

LotfizadehDehkordi, B., Ghadimi, A., & Metselaar, H. S. (2013). Box–Behnken experimental design for investigation of stability and thermal conductivity of TiO_2 nanofluids. *Journal of Nanoparticle Research*, *15*, 1369.

Madni, I., Hwang, C.-Y., Park, S.-D., Choa, Y.-H., & Kim, H.-T. (2010). Mixed surfactant system for stable suspension of multiwalled carbon nanotubes. *Colloids and Surfaces A: Physicochemical and Engineering Aspects*, *358*, 101–107.

Mahbubul, I. M. (2015). *Investigation of fundamental properties of nanorefrigerants*. Saarbrücken: LAP Lambert Academic Publishing.

Mahbubul, I. M., Chong, T. H., Khaleduzzaman, S. S., Shahrul, I. M., Saidur, R., Long, B. D., & Amalina, M. A. (2014). Effect of ultrasonication duration on colloidal structure and viscosity of alumina–water nanofluid. *Industrial & Engineering Chemistry Research*, *53*, 6677–6684.

Mahbubul, I. M., Elcioglu, E. B., Saidur, R., & Amalina, M. A. (2017). Optimization of ultrasonication period for better dispersion and stability of TiO_2–water nanofluid. *Ultrasonics Sonochemistry*, *37*, 360–367.

Mahbubul, I. M., Saidur, R., Amalina, M. A., Elcioglu, E. B., & Okutucu-Ozyurt, T. (2015a). Effective ultrasonication process for better colloidal dispersion of nanofluid. *Ultrasonics Sonochemistry*, *26*, 361–369.

Mahbubul, I. M., Saidur, R., Amalina, M. A., & Niza, M. E. (2016). Influence of ultrasonication duration on rheological properties of nanofluid: An experimental study with alumina–water nanofluid. *International Communications in Heat and Mass Transfer*, *76*, 33–40.

Mahbubul, I. M., Saidur, R., Hepbasli, A., & Amalina, M. A. (2016). Experimental investigation of the relation between yield stress and ultrasonication period of nanofluid. *International Journal of Heat and Mass Transfer*, *93*, 1169–1174.

Mahbubul, I. M., Shahrul, I. M., Khaleduzzaman, S. S., Saidur, R., Amalina, M. A., & Turgut, A. (2015b). Experimental investigation on effect of ultrasonication duration on colloidal dispersion and thermophysical properties of alumina–water nanofluid. *International Journal of Heat and Mass Transfer*, *88*, 73–81.

Mandzy, N., Grulke, E., & Druffel, T. (2005). Breakage of TiO_2 agglomerates in electrostatically stabilized aqueous dispersions. *Powder Technology*, *160*, 121–126.

Müller, R. H. (1996). *Zetapotential und Partikelladung in der Laborpraxis*. Stuttgart, Germany: Wissenschaftliche Verlagsgesellschaft.

Murshed, S., Leong, K., & Yang, C. (2008). Investigations of thermal conductivity and viscosity of nanofluids. *International Journal of Thermal Sciences*, *47*, 560–568.

Nguyen, V. S., Rouxel, D., Hadji, R., Vincent, B., & Fort, Y. (2011). Effect of ultrasonication and dispersion stability on the cluster size of alumina nanoscale particles in aqueous solutions. *Ultrasonics Sonochemistry*, *18*, 382–388.

Özcan-Taşkin, N. G., Padron, G., & Voelkel, A. (2009). Effect of particle type on the mechanisms of break up of nanoscale particle clusters. *Chemical Engineering Research and Design*, *87*, 468–473.

Pantzali, M., Mouza, A., & Paras, S. (2009). Investigating the efficacy of nanofluids as coolants in plate heat exchangers (PHE). *Chemical Engineering Science*, *64*, 3290–3300.

Peterson, G. P., & Li, C. H. (2006). Heat and mass transfer in fluids with nanoparticle suspensions. In A. George, J. P. H. A. B.-C. Greene, & I. C. Young (Eds.), *Advances in heat transfer* (39, pp. 257–376). Elsevier.

Rashmi, W., Ismail, A., Sopyan, I., Jameel, A., Yusof, F., Khalid, M., & Mubarak, N. (2011). Stability and thermal conductivity enhancement of carbon nanotube nanofluid using gum arabic. *Journal of Experimental Nanoscience*, *6*, 567–579.

Rice, S. B., Chan, C., Brown, S. C., Eschbach, P., Han, L., Ensor, D. S., . . . Zheng, J. (2013). Particle size distributions by transmission electron microscopy: An interlaboratory comparison case study. *Metrologia*, *50*, 663–678.

Ruan, B., & Jacobi, A. M. (2012). Ultrasonication effects on thermal and rheological properties of carbon nanotube suspensions. *Nanoscale Research Letters*, *7*, 127.

Sadeghi, R., Etemad, S. G., Keshavarzi, E., & Haghshenasfard, M. (2015). Investigation of alumina nanofluid stability by UV−vis spectrum. *Microfluidics and Nanofluidics*, *18*, 1023−1030.

Santos, F. D. P., Campos, E. D., Costa, M., Melo, F. C. L., Honda, R. Y., & Mota, R. P. (2003). Superficial modifications in TiO_2 and Al_2O_3 ceramics. *Materials Research*, *6*, 353−357.

Sato, M., Abe, Y., Urita, Y., Di Paola, R., Cecere, A., & Savino, R. (2011). Thermal performance of self-rewetting fluid heat pipe containing dilute solutions of polymer-capped silver nanoparticles synthesized by microwave-polyol process. *International Journal of Transport Phenomena*, *12*, 339−345.

Shahrul, I. M., Mahbubul, I. M., Saidur, R., & Sabri, M. F. M. (2016). Experimental investigation on Al_2O_3−W, SiO_2−W and ZnO−W nanofluids and their application in a shell and tube heat exchanger. *International Journal of Heat and Mass Transfer*, *97*, 547−558.

Taurozzi, J., Hackley, V., & Wiesner, M. (2012). *Preparation of nanoparticle dispersions from powdered material using ultrasonic disruption*. *NanoEHS Protocols*. Gaithersburg, MD: National Institute of Standards and Technology.

Tsai, C. Y., Chien, H. T., Ding, P. P., Chan, B., Luh, T. Y., & Chen, P. H. (2004). Effect of structural character of gold nanoparticles in nanofluid on heat pipe thermal performance. *Materials Letters*, *58*, 1461−1465.

Turgut, A., Tavman, I., Cetin, L., Chirtoc, M., & Fudym, O. (2011). *Preparation and characterization of nanofluids containing alumina particles*. *ICHMT Digital Library Online*. Begel House Inc.

Wang, X.-J., & Li, X.-F. (2009). Influence of pH on nanofluids' viscosity and thermal conductivity. *Chinese Physics Letters*, *26*, 056601.

Wang, X. J., Li, X., & Yang, S. (2009a). Influence of pH and SDBS on the stability and thermal conductivity of nanofluids. *Energy and Fuels*, *23*, 2684−2689.

Wang, X.-J., Zhu, D.-S., & Yang, S. (2009b). Investigation of pH and SDBS on enhancement of thermal conductivity in nanofluids. *Chemical Physics Letters*, *470*, 107−111.

Wang, X. Q., & Mujumdar, A. S. (2007). Heat transfer characteristics of nanofluids: A review. *International Journal of Thermal Sciences*, *46*, 1−19.

Wang, X. Q., & Mujumdar, A. S. (2008). A review on nanofluids - Part II: Experiments and applications. *Brazilian Journal of Chemical Engineering*, *25*, 631−648.

Wei, X., Zhu, H., Kong, T., & Wang, L. (2009). Synthesis and thermal conductivity of Cu2O nanofluids. *International Journal of Heat and Mass Transfer*, *52*, 4371−4374.

Wen, D., Lin, G., Vafaei, S., & Zhang, K. (2009). Review of nanofluids for heat transfer applications. *Particuology*, *7*, 141−150.

Wen, D. S., & Ding, Y. L. (2005). Formulation of nanofluids for natural convective heat transfer applications. *International Journal of Heat and Fluid Flow*, *26*, 855−864.

Wu, D., Zhu, H., Wang, L., & Liua, L. (2009). Critical issues in nanofluids preparation, characterization and thermal conductivity. *Current Nanoscience*, *5*, 103−112.

Xian-Ju, W., Hai, L., Xin-Fang, L., Zhou-Fei, W., & Fang, L. (2011). Stability of TiO_2 and Al_2O_3 nanofluids. *Chinese Physics Letters*, *28*, 086601.

Xie, H., Chen, L., & Wu, Q. (2008). Measurements of the viscosity of suspensions (nanofluids) containing nanosized Al_2O_3 particles. *High Temperatures High pressures*, *37*, 127−135.

Xie, H., Lee, H., Youn, W., & Choi, M. (2003). Nanofluids containing multiwalled carbon nanotubes and their enhanced thermal properties. *Journal of Applied Physics*, *94*, 4967−4971.

Yang, Y., Grulke, E. A., Zhang, Z. G., & Wu, G. (2006). Thermal and rheological properties of carbon nanotube-in-oil dispersions. *Journal of Applied Physics*, *99*, 114307.

Yu, H., Hermann, S., Schulz, S. E., Gessner, T., Dong, Z., & Li, W. J. (2012). Optimizing sonication parameters for dispersion of single-walled carbon nanotubes. *Chemical Physics*, *408*, 11–16.

Yu, J., Grossiord, N., Koning, C. E., & Loos, J. (2007). Controlling the dispersion of multi-wall carbon nanotubes in aqueous surfactant solution. *Carbon*, *45*, 618–623.

Yu, W., Xie, H., Chen, L., & Li, Y. (2010). Enhancement of thermal conductivity of kerosene-based Fe_3O_4 nanofluids prepared via phase-transfer method. *Colloids and Surfaces A: Physicochemical and Engineering Aspects*, *355*, 109–113.

Zhang, X., Gu, H., & Fujii, M. (2007). Effective thermal conductivity and thermal diffusivity of nanofluids containing spherical and cylindrical nanoparticles. *Experimental Thermal and Fluid Science*, *31*, 593–599.

Zhu, D., Li, X., Wang, N., Wang, X., Gao, J., & Li, H. (2009). Dispersion behavior and thermal conductivity characteristics of Al_2O_3-H_2O nanofluids. *Current Applied Physics*, *9*, 131–139.

Zhu, H., Li, C., Wu, D., Zhang, C., & Yin, Y. (2010). Preparation, characterization, viscosity and thermal conductivity of $CaCO_3$ aqueous nanofluids. *Science China Technological Sciences*, *53*, 360–368.

Zhu, H., Zhang, C., Tang, Y., Wang, J., Ren, B., & Yin, Y. (2007). Preparation and thermal conductivity of suspensions of graphite nanoparticles. *Carbon*, *45*, 226–228.

Zhu, H.-T., Lin, Y.-S., & Yin, Y.-S. (2004). A novel one-step chemical method for preparation of copper nanofluids. *Journal of Colloid and Interface Science*, *277*, 100–103.